# Investigating the Toxicity and Mechanisms of Non-Protein Amino Acids

Kate Samardzic

BMedSc (Hons)

Submitted in fulfilment of the requirements for the degree of

Doctor of Philosophy (Science) from:

School of Life Sciences,

University of Technology Sydney

June 2020

# DECLARATION

I, Kate Samardzic, certify that this thesis is submitted in fulfilment of the requirements for the award of Doctor of Philosophy, in the School of Life Sciences at the University of Technology Sydney.

This thesis is wholly my own work unless otherwise referenced or acknowledged. In addition, I certify that all information sources and literature used are indicated in the thesis.

This document has not been submitted for qualifications at any other academic institution.

This research is supported by an Australian Government Research Training Program.

Signature of candidate

Production Note:
Signature removed prior to publication.

Date
  16/6/2020

## ACKNOWLEDGEMENTS

The journey toward a successful PhD is not an easy one and, thankfully, one that I didn't walk alone. I will be forever grateful to those who have supported me through the highs and lows of this journey, and it's only fitting that they are recognised in this section.

First and foremost, I'd like to thank my family. Your support transcends my PhD; you have been there all my life, but, you have been especially wonderful over the past decade. Mum and Dad's initial confusion when I graduated from my undergraduate degree and told them that no, I wouldn't be getting a job yet turned to mild suspicion when after Honours graduation I admitted it would still be a few more years before I had a real job. Well, finally the time has come, and it wouldn't have been possible without you. You've provided a roof over my head and kept me fed while I was working late in the lab or deep in writing mode. You provided the essentials so I could focus on doing what I love. You printed out each paper I wrote and read them enthusiastically, even though you admitted later to not entirely understanding all of it. Most importantly, though, you taught me not to stress and worry as much as I otherwise might have. Your voices saying "don't stress", "take it easy," and "take your time" gave me the strength to finish this.

Michelle, my sister. You are also my confidant, proofreader, cheerleader, motivational speaker, stylist and inspiration. Even though you have lived overseas for the past four years, I never felt your absence. You were with me every step of this journey, and I think you know more about my research than anyone else.

My friends, both in and out of UTS, made the whole process bearable. Some of my favourite times over the past four years were spent with you. You listened to me complain about my experiments, took me out dancing to take my mind off things and very sincerely enquired about the health of my cells. Special mentions to my long-distance best friend Maddy, who helped me practice every single presentation I had to do during this PhD, and Vince, who, as own personal guru, provided me with endless

emotional support, advice and love. To my lab members, Brendan, Joel, Jake, Carly (and honorary member Nat) thank you so much for the support and friendship over the years.

Finally, no one knows the naïve and inexperienced scientist I started as like my two supervisors; Ken Rodgers and Matt Padula. Ken, thank you for the opportunity to join your lab and work on this project. It has continued to excite me over the years and my time in your lab has nurtured my love of research. Matt, thank you for your omnipresence in the lab. It was always so helpful to be able to find you at any time and talk to you about anything (even though you often wished I didn't).

Thank you to all those I've listed here and the many others who know who they are. This has been one of the most challenging yet rewarding tasks I've ever undertaken.

# LIST OF PUBLICATIONS

Rodgers, K.J., **Samardzic, K.**, and Main, B.J. (2015) Toxic Nonprotein Amino Acids, in *Plant Toxins*. Springer. p. 1-20.

**Samardzic, K.,** and Rodgers, K.J. (2017). Oxidised protein metabolism: recent insights. Biol Chem, 398: p. 1165-1175.

Rodgers, K.J., Main, B.J., and **Samardzic, K.** (2017). Cyanobacterial Neurotoxins: Their Occurrence and Mechanisms of Toxicity. Neurotox Res, 33: p. 168-177.

**Samardzic, K**. and K.J. Rodgers. (2019). Cytotoxicity and mitochondrial dysfunction caused by the dietary supplement L-norvaline. Toxicol in Vitro, 56: p. 163-171.

**Samardzic, K.** and K. J. Rodgers (2019), Cell death and mitochondrial dysfunction induced by the dietary non-proteinogenic amino acid L-azetidine-2-carboxylic acid (Aze). Amino Acids, 8: p. 1221-1232.

Giannopoulos, S., **Samardzic, K.**, Raymond, B.A., Djordjevic, S.P., and Rodgers, K.J. (2019) L-DOPA causes mitochondrial dysfunction in vitro: a novel mechanism of L-DOPA toxicity uncovered. Int J Biochem Cell Biol, 117.

## CONFERENCE PROCEEDINGS

Algal Research Symposium, Sydney, NSW, Australia          2015

Oral Presentation

"Phytotoxic Activity of Non-Protein Amino Acids Synthesised by Cyanobacteria"


Society of Environmental Toxicology and Chemistry, Hobart, TAS, Australia      2016

Oral Presentation

"Phytotoxic Activity of Non-Protein Amino Acids Synthesised by Cyanobacteria"


FameLab, Sydney, NSW, Australia          2018

Oral presentation

"Mitochondria: Cellular Superheroes and their Kryptonite"


Multifaceted Mitochondria, San Diego, CA, USA          2018

Poster Presentation

"Mitochondrial Dysfunction caused by Non-Protein Amino Acid Dietary Supplements"


AMP Amplify PhD Pitch Competition, Sydney, NSW, Australia          2018

Oral Presentation

"Supplement Dos and Don'ts"


AussieMit, Melbourne, VIC, Australia          2018

Poster Presentation

"Mitochondrial Dysfunction caused by Non-Protein Amino Acid Dietary Supplements"

# ABSTRACT

Non-protein amino acids (NPAAs) are amino acids not normally used in protein synthesis. However, a small subset of this type of amino acid, known as amino acid analogues, can be mistakenly utilised in protein synthesis due to their structural similarity to a canonical protein amino acid. This process has been implicated in the development of neurodegenerative disease. This research set out to investigate the toxicity and mechanisms of two lesser studied NPAAs which enter the human food chain and have the potential to contribute to the development of disease. These were L-norvaline (Nva), an analogue of the branched chain amino acids that is usually found in dietary supplements consumed by bodybuilders, and L-azetidine-2-carboxylic acid (Aze), an analogue of L-proline that is produced by sugar beets and enters the human food as a dietary supplement and as fodder for livestock.

Initial experiments sought to identify whether either Nva or Aze induced cell death using metabolic and imaging assays. Both NPAAs were cytotoxic to human neuroblastoma cells, confirming the rationale behind the present investigation and providing the impetus for further research. Cell death pathways were also investigated, and death was determined to be necrotic following Nva exposure, and both necrotic and apoptotic following treatment with Aze. The toxicity of these NPAAs to mitochondria was then characterised using immunofluorescence microscopy and bioenergetic flux assays. These revealed, for the first time, that Nva and Aze cause mitochondrial dysfunction. Distinct morphological changes and bioenergetic failure were common to both conditions, however, for Nva bioenergetic failure was only observed in the presence of a nitric oxide synthase inhibitor due to Nva's secondary action as an arginase inhibitor.

Finally, a proteomic characterisation of cells exposed to both NPAAs was performed to further elucidate the molecular mechanisms involved in their toxicity. This was the first study to perform this analysis in human cells treated with either NPAA and revealed disruptions to processes that precede protein translation. Changes to proteins involved in the processing of DNA and RNA during cell cycle progression indicate, for the first

time, that NPAA exposure exerts toxic effects upstream of protein translation. These results identify Nva and Aze as NPAAs with significant potential for toxicity that should, therefore, be consumed with caution. Furthermore, these results add to the existing knowledge of the mechanisms of both these individual NPAAs, and amino acid analogues in general.

# CONTENTS

## LIST OF TABLES AND FIGURES

**\*Please note that the Tables and Figures listed above include those in chapters one, two and five only.**

# LIST OF ABBREVIATIONS

| | |
|---|---|
| ATP | adenosine triphosphate |
| AD | Alzheimer's disease |
| ALS | Amyotrophic Lateral Sclerosis |
| ALS-PDC | Amyotrophic Lateral Sclerosis-Parkinsonism-Dementia Complex |
| aaRS | aminoacyl transfer ribonucleic acid synthetase |
| BCA | bicinchoninic acid |
| BP | Biological Process |
| CC | Cellular Compartment |
| DNA | deoxyribonucleic acid |
| DTT | dithiothreitol |
| DMEM | Dulbecco's Modified Eagle's Medium |
| EMEM | Eagle's Minimum Essential Medium |
| EF-Tu | elongation factor Tu |
| ER | endoplasmic reticulum |
| *E. coli* | *Escherichia coli* |
| FDR | false discovery rate |
| fALS | familial Amyotrophic Lateral Sclerosis |
| FBS | foetal bovine serum |
| GO | Gene Ontology |
| HSP | heat shock protein |
| HD | Huntington's disease |
| IRES | internal ribosome entry site |

| | |
|---|---|
| DAB | L-2, 4-diaminobutanoic acid |
| L-DOPA | L-3,4- dihydroxyphenylalanine |
| Aze | L-azetidine-2-carboxylic acid |
| Nva | L-norvaline |
| BMAA | L-β-*N*-methylaminoalanine |
| BOAA | L-β-*N*-oxalylamino-L-alanine |
| LFQ | label free quantification |
| LeuRS | leucyl-transfer ribonucleic acid synthetase |
| LC-MS | liquid chromatography-mass spectrometry |
| mRNA | messenger ribonucleic acid |
| MS | Multiple Sclerosis |
| NO | nitric oxide |
| NPAA | non-protein amino acid |
| OXPHOS | oxidative phosphorylation |
| PD | Parkinson's disease |
| PBS | phosphate buffered saline |
| PI | Propidium Iodide |
| ROS | reactive oxygen species |
| RFC | replication factor C |
| RNA | ribonucleic acid |
| sALS | sporadic  Amyotrophic Lateral Sclerosis |
| SOD1 | superoxide dismutase 1 |
| SLE | Systemic Lupus Erythematosus |

| | |
|---|---|
| THOC | THO complex |
| tRNA | transfer ribonucleic acid |
| TCEP | tris(2-carboxyethyl)phosphine |
| UPR | unfolded protein response |
| VCP | valosin containing protein |
| ZnF | zinc finger |

**\*Please note that the abbreviations listed above include those in chapters one, two, five and six only**

# Chapter One:

An overview of the thesis

# CHAPTER ONE: OVERVIEW OF THE THESIS

## 1.1 Introduction

Neurodegenerative disorders are a subset of diseases that are characterised by the progressive loss of neurons in the brain [1]. Pathologically united by this common feature, diagnosis of a particular neurodegenerative disease is dependent on the neurological symptoms that manifest, which correspond to the loss of neuronal function in a particular subset of neurons. Neurodegenerative diseases are one of the leading causes of death and disability worldwide, and with onset typically occurring later in life, the disease burden is set to increase as the global population ages [2]. Some examples of common neurodegenerative diseases include Alzheimer's disease, Parkinson's disease, and motor neuron disease, characterised by loss of function in neurons of the cerebral cortex, substantia nigra and motor cortex respectively [2]. In addition to their progressive nature, an incomplete understanding of their pathogenesis and, consequently, the lack of effective treatments are major contributors to the disease burden of neurodegenerative diseases.

In addition to the loss of neuronal function, molecular hallmarks that correspond with each neurodegenerative disease exist. These include senile plaques, neurofibrillary tangles and inclusion bodies, which are all forms of aggregated protein [3]. While there is conclusive evidence linking protein aggregation to the development of neurodegenerative disease, the molecular mechanisms behind the initial formation of insoluble protein aggregates are far reaching. As a result, neurodegenerative diseases are often classified into two subtypes, familial and sporadic [4]. Familial cases of neurodegenerative diseases are characterised by a family history of the disease and the aetiology is primarily attributed to a genetic mutation. Sporadic diseases are not characterised by a family history and environmental triggers, or a combination of environmental and genetic factors, may play a causal role [4]. Although approximately 90% of cases are sporadic, due to the long latency of neurodegenerative diseases and the complex interaction between environmental and genetic factors, there is immense difficulty identifying environmental causes [5-7]. In light of the rising disease burden of

neurodegenerative diseases and the absence of a cure, significant emphasis must be placed on understanding the genetic, lifestyle and environmental factors whereby these diseases occur.

One compound, a non-protein amino acid (NPAA) called L-β-*N*-methylaminoalanine (BMAA), has been identified as a potential environmental factor based on its structural similarity to a protein amino acid and ability to enter the human food chain [8]. This NPAA, and several others, have been extensively studied and found to elicit toxic effects both *in vitro* and *in vivo*. Of the hundreds of NPAAs readily available in nature, this work sought to identify and investigate lesser-known NPAAs that, like BMAA, are analogues of protein amino acids and are known to enter the human food chain. Using these criteria, L-norvaline (Nva) and L-azetidine-2-carboxylic acid (Aze) were identified as potential environmental factors due to their presence in human dietary supplements. Thus, this thesis is an investigation into the toxicity and mechanisms of Nva and Aze on human neuronal cells.

## 1.2 Aims of the Thesis

The previous section identifies the two NPAAs that are the subjects of this dissertation. The overarching aims of this thesis were to investigate the potential toxicity of these two NPAAs and where toxicity was detected, identify the mechanisms whereby toxicity was elicited. In order to address these overarching aims, a series of sub-aims were created and they are as follows:

- Aim One: Determine whether either of the two NPAAs induce cell death in SH-SY5Y neuroblastoma cells
- Aim Two: Investigate the effects of Nva and Aze on mitochondrial function
- Aim Three: Determine whether necrotic, apoptotic or autophagic cell death pathways are activated
- Aim Four: Perform a holistic proteomic investigation of cells exposed to both NPAAs

This thesis will present the first in-depth toxicological studies of Nva and Aze in a human cell line. In addition, it describes the first proteomic and subsequent pathway analysis studies of human cells exposed to these NPAAs.

## 1.3 Dissertation Organisation

Following this chapter, this dissertation is organised in the following manner:

- Chapter two: Critical review of research into NPAAs. It aims to provide background information on the scope of previous research into NPAAs, mechanisms of human exposure to NPAAs and the associated cellular responses they may induce.

- Chapter three: This chapter describes, for the first time, the toxicity of Nva and aims to, in part; address aims one, two and three of this dissertation. This chapter is published in *Toxicology In Vitro* in a manuscript entitled 'Cytotoxicity and mitochondrial dysfunction caused by the dietary supplement l-norvaline.'

- Chapter four: This chapter describes the toxicity of Aze and completes aims one, two and three of this dissertation. It is published in *Amino Acids* under the heading 'Cell death and mitochondrial dysfunction induced by the dietary non-proteinogenic amino acid l-azetidine-2-carboxylic acid (Aze).'

- Chapter five: This chapter provides the first proteomic investigation of the effects of Nva and Aze on human cells and addresses aim four.

- Chapter six: This is the final chapter of this dissertation and contains concluding remarks and future directions.

# Chapter Two:

Critical Review

# CHAPTER TWO: CRITICAL REVIEW

## 2.1 Amino Acids

Since the discovery of the first amino acid in the nineteenth century, the study of these unique compounds has been essential to our understanding of the human body [9,10]. French vegetable chemists Louis-Nicolas Vauquelin and Pierre Jean Robiquet identified L-asparagine from asparagus and though unsure of the exact chemical nature of the substance, guessed that it contained carbon, hydrogen, oxygen and nitrogen [11]. It wasn't until later that an amino acid was defined as a molecule consisting of an amino ($-NH_2$) group, a carboxylic acid (-COOH) group and a unique side chain known as an R group (Figure 1.) [12]. The unique R side chain is responsible for the variability amongst amino acids in nature and enables them to perform the essential function of making up proteins from the translation of genetic information [13].
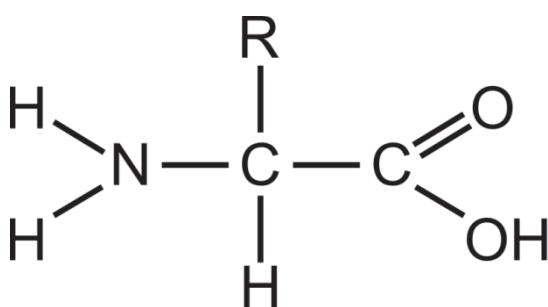


**Figure 1. Structural representation of an amino acid molecule.** The molecule consists of an amino ($-NH_2$) group, a carboxylic acid (-COOH) and an R side chain.

In the following century, it was hypothesised that proteins originated from the bonding of the amino group of one amino acid to the carboxyl group of another, forming a peptide bond and allowing for the formation of polypeptide chains [13,14]. This hypothesis was eventually proven and earned Fred Sanger a Nobel Prize in Chemistry for his identification of the amino acid sequence of the protein insulin, solidifying the role of amino acids as one of the chemical foundations of life [15].

The 20 amino acids (Table 1.) that are involved in protein synthesis are known as protein, proteinogenic, natural or canonical amino acids [16]. However, there are over a thousand naturally occurring amino acids and the protein amino acids only represent a small fraction (~2%) of them [17]. In addition to protein synthesis, the protein amino acids are also responsible for a range of functions including energy supply as oxidative substrates, precursors of cell signaling molecules [18], gluconeogenesis and lipogenesis [19]. All protein amino acids have a distinctive side chain bonded to the carbon atom adjacent to the carboxylic acid group, the $\alpha$-carbon [12]. The variety of the protein amino acids with their different R side chains provides a set of building blocks with diverse structural and chemical properties that allow for the large functional capacity of proteins [12].

Nine of the protein amino acids are classified as nutritionally essential amino acids because the human body inadequately produces them. They must be obtained through diet either as the free amino acids or as components of an ingested protein which are then released by enzymatic hydrolysis during digestion [20]. Non-essential amino acids are adequately produced in the human body, while conditionally essential amino acids are normally produced in sufficient amounts but may not be effectively produced in certain groups (e.g. children) or during stress (e.g. reproduction, disease) [20,21].

**Table 1. Classification of protein amino acids**

| Protein Amino Acids | Essential to Humans |
|---|---|
| Alanine | No |
| Glutamic Acid | Conditionally |
| Cysteine | Conditionally |
| Aspartic Acid | No |
| Phenylalanine | Yes |
| Glycine | Conditionally |
| Histidine | Yes |
| Isoleucine | Yes |
| Lysine | Yes |

| | |
|---|---|
| **Leucine** | Yes |
| **Methionine** | Yes |
| **Asparagine** | No |
| **Glutamine** | No |
| **Arginine** | Conditionally |
| **Serine** | No |
| **Threonine** | Yes |
| **Tryptophan** | Yes |
| **Tyrosine** | Conditionally |
| **Valine** | Yes |
| **Proline** | No |

## 2.2 Non Protein Amino Acids

While protein amino acids are more widely recognised and have been extensively studied, non-protein amino acids (NPAAs) account for the hundreds of other naturally occurring amino acids [17]. Though not used in protein synthesis, NPAAs play an important role in cellular metabolism. Some NPAAs are converted to protein amino acids while others serve as metabolic intermediates in the production of other compounds [22]. For example L-3,4- dihydroxyphenylalanine (L-DOPA) is a precursor of the neurotransmitter dopamine [23]. It is for these reasons that some NPAAs are used in medicines and nutritional supplements. L-DOPA has been used therapeutically for over 45 years to increase dopamine concentrations during treatment of Parkinson's disease (PD) [24] and recently, the use of supplements containing NPAAs to promote amino acid and hence, protein synthesis has increased [25,26]. NPAAs also occur naturally in plants that are consumed by humans and animals such as the legumes, jack bean and lentils [17] and also play a role in protecting plants from predators [27].

Despite their many positive uses, a small subset of NPAAs called amino acid analogues (Table 2.) are known to inhibit biological processes. This arises from their structural similarity to protein amino acids [16]. These NPAAs have a similar shape, size and charge

to their corresponding 'parent' amino acid [28]. For example, the similarity between the parent protein amino acid tyrosine and its analogue L-DOPA is shown in Figure 2.

**Table 2. Table listing amino acids, their analogues and origins in nature.** *Indicates an isomer of the analogue of interest.

| Amino Acid | Analogue | Origin |
|---|---|---|
| **Serine** | L-β-*N*-methylaminoalanine (BMAA), L-2, 4-diaminobutanoic acid (DAB)* | Derived from cyanobacteria and diatoms [29] |
| **Phenylalanine** | L-m-Tyrosine | Plant derived: Fescue grasses (*Fescue* spp.) [30] |
| **Proline** | L-azetidine-2-carboxylic acid (Aze) | Plant derived: Lily of the Valley (*Convallaria majali*s) Mushroom (*Clavaria miyabeana)* [31] Sugar Beets & Garden/Table Beets (*Beta vulgaris*) [32] |
| **Glutamate** | L-β-*N*-oxalylamino-L-alanine (BOAA) | Derived from leguminous plants: Grass pea *(Lathyrus sativus)* [33] |
| **Arginine** | L-2-amino-4 (guandinooxy) butyric acid (L-Canavanine) | Derived from leguminous plants: Jack beans (*Canavalia* spp.)[34] Wild Potato *(Hedysarum alpinum)* [35] |
| **Tyrosine** | L-3,4-Dihydroxyphenylalanine (L-DOPA) | Derived from leguminous plants: Velvet bean (*Mucuna pruriens)* [36] |
| **Valine or Leucine or Isoleucine** | L-2-Aminopentanoic acid (L-norvaline) | Synthesised as a by-product of amino acid biosynthesis in bacteria or synthetically [37] |
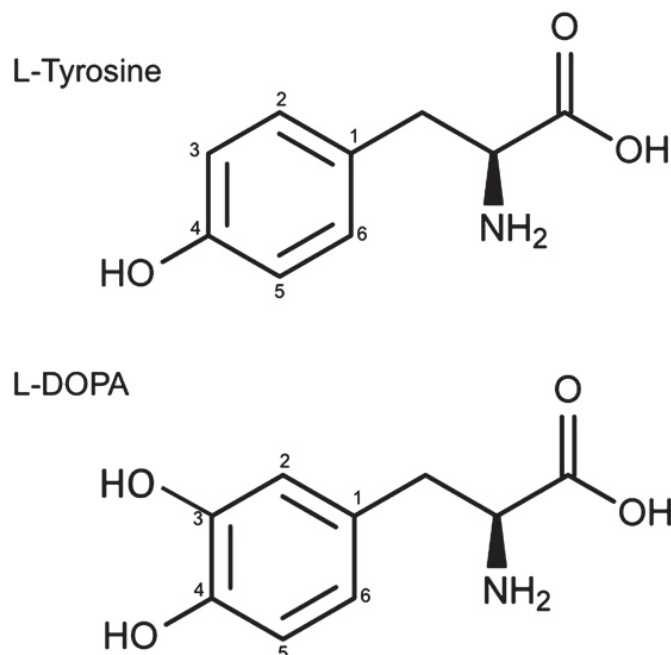
**Figure 2. Structural representation of the protein amino acid L-tyrosine and L-DOPA.**
L-DOPA has an identical chemical structure to the protein amino acid L-tyrosine except for the extra hydroxyl group (OH) on carbon 3 of the aromatic ring [24].

## 2.3 Toxicity of NPAAs

The earliest systematic studies into the toxicity of NPAAs took place in plants during the 1960s [38,39]. Amino acid analogues synthesised by plants were found incorporated into the cellular proteins of competing plants and predators [34]. As a consequence of this process, dubbed misincorporation, herbicidal and insecticidal properties were observed in what is thought to be an evolutionary trait [40,41]. At the heart of this toxicity lies the ability of an NPAA to replace its corresponding parent protein amino acid during protein synthesis. This ability is dependent upon the similarity of an NPAA to a protein amino acid in regard to the following characteristics:

1) Molecular size
2) Molecular shape and stereochemistry
3) The ability to form the same hydrogen bonds as the protein amino acid [38]

Even if these criteria are met, the toxicity of NPAAs can be prevented by the presence of high concentrations of a protein amino acid. Therefore, in order to be toxic an NPAA must be present at a concentration capable of outcompeting the parent protein amino acid in a biological process. The toxic effects of analogues can be induced by disrupting protein synthesis and therefore decreasing the abundance of normal proteins produced and resulting in a loss of function, or by increasing the abundance of abnormal proteins produced that then deviate from their normal functions or become insoluble [28].

## 2.3.1 NPAAs and Bacteria

The discovery of the antimetabolite action of NPAAs prompted investigations into their effect on the growth of microorganisms and provided the earliest evidence for bacterial misincorporation [28]. Overall, amino acid analogues were found to inhibit the growth of bacteria [28]. The NPAAs L-norleucine and L-p-fluorophenylalanine, L-leucine and L-phenylalanine analogues respectively, were found to incorporate into the proteins of *Escherichia coli* (*E. coli*) and reduce enzymatic function [42]. The L-proline analogue Aze has demonstrated growth inhibitory activity in *E. coli* and was detected in hydrolysed protein fractions [43]. More recently, diminished growth rates at concentrations as low as 250 µM were accompanied by misincorporation into recombinant myelin basic protein in *E. coli* [44]. In addition, the relatively low substitution of 3 out of 11 L-proline sites was shown to cause configurational changes to the protein in the form of severe bends and partial uncoiling in the polypeptide chain [44]. This sheds light in regard to the ratio of misincorporation of NPAAs to protein amino acids and provides evidence for the macromolecular changes caused by NPAAs. Interestingly, growth inhibition was not observed when a media containing L-proline was used, suggesting preferential incorporation and the possibly protective role of protein amino acids in the presence of their analogue [43,44].

Though synthesised by several strains of bacteria [45,46], Nva inhibited the growth of mutant strains of *E. coli* [47]. In a more mechanistic study, Cvetesic et al. found Nva binds to bacterial elongation factor Tu (EF-Tu), which facilitates transport of aminoacylated-tRNA synthetases to the ribosome during protein synthesis [48]. The unique role of

aminoacyl-tRNA synthetases in NPAA's mechanism of action is discussed further in section 2.6.1. Nva was found to incorporate into recombinant human hemoglobin expressed in *E. coli* in the place of L-leucine in a study that confirmed the presence of Nva using several analytical methods including mass spectrometry, peptide mapping and Edman protein sequencing [49]. Nva substitution of L-leucine was also analysed using a kinetic assay and although hemoglobin was detected almost immediately, Nva misincorporation was not detected until 6 h had passed [49]. A potential explanation for this difference may be the 'speed-accuracy trade-off' outlined by Johansson et al. in relation to bacterial protein synthesis whereby proteins utilising non/near-cognate ternary complexes, such as EF-Tu/Nva, proceed at a slower rate than those utilising complexes containing cognate amino acids [50].

## 2.3.2 Plant Defence

While plant NPAAs have roles in signalling and nitrogen storage [17], they are also implemented by plants as a survival strategy. For instance, plants can release certain chemicals called allelochemicals into the environment that have a negative impact on the growth of other surrounding plants. This form of plant biological warfare is known as allelopathy [51].

The use of NPAAs as allelochemicals has been documented in many plants. These include fine-leaf fescue grasses, *Festuca rubra* and *Festuca arizonica*, which deposit L-m-tyrosine into surrounding soil to prevent the growth of competing plants. This defence mechanism has enabled fescue grasses to flourish on roadsides with little competition for space [30]. In studies by Bertin et al. the phytotoxic activity of L-m-tyrosine on lettuce (*Lactuca sativa*) roots and shoots was observed and the detection of L-m-tyrosine in hydrolysed root proteins of inhibited plants suggests misincorporation [30]. L-DOPA is also a potent allelochemical, with actions on cucumber (*Cucumis sativus*), soybean (*Glycine max*), maize (*Zea mays*), barnyardgrass (*Echinochloa crus-galli*) and lettuce [52-54]. In addition, Nva inhibits chrysanthemum *(Chrysanthemum indicum)* growth when applied to the flowering plant [41] while Aze inhibits the growth of barley *(Hordeum vulgare)* [55], wheat (*Triticum aestivum*) seedlings [56], pea (*Pisum sativum*) root segments

[57] and thale cress (*Arabidopsis thaliana*) [58]. In thale cress it was found that the substrate specificity of the prolyl-tRNA synthetase isoform AtPro-RS-Cyt was nearly identical for L-proline and Aze, suggesting misincorporation as the mechanism of growth inhibition [58]. Though inhibitory effects on plants have not been investigated, the cyanotoxin BMAA has also been shown to accumulate in wheat seedlings [59]. The effects of multiple analogous NPAAs on plants suggest a fundamental biological process, such as protein synthesis, as the mechanism of their allelopathy.

### 2.3.3 NPAA Exposure in Mammals

*2.3.3.1 In Vitro*

Since mammals may be exposed to many of the NPAAs that have exhibited antimetabolite activity in bacteria and plants, further investigation into the toxicity to mammals has been warranted. Unsurprisingly, in most cases where antibacterial and herbicidal activity was observed, cytotoxicity has also been observed. As early as 1959, it was found that the L-arginine analogue L-canavanine inhibits the growth of Walker 256 rat carcinosarcoma cells in L-arginine deficient media [60]. Furthermore, L-canavanine was detected in protein lysates via chromatography following hydrolysis. A more recent study using primary rat neurons and astrocytes found both L-canavanine and Aze induced dose-dependent increases in toxicity [61], while Aze exposure has also led to dose-dependent increases in protein degradation in rat reticulocytes [62].

BMAA toxicity has been investigated in several cell culture models. In human SH-SY5Y neuroblastoma cells, BMAA binds to intracellular proteins and induces cytotoxicity at concentrations of 1 and 2 mM [63]. Another study that utilised the same cell line but lower concentrations (0.5 mM) of BMAA and a shorter treatment time found that BMAA exposure led to proteotoxic stress in the form of endoplasmic reticulum (ER) stress, caspase activation and increased lysosomal enzyme activity [64]. This proteotoxic stress was either completely or partially restored by co-incubation with L-serine at the ratio of 10:1 BMAA: L-serine, suggesting misincorporation as a potential mechanism [64]. Indeed, in a subsequent study the authors detected an increase in radiolabeled BMAA binding

to SH-SH5Y proteins in a time dependent manner [65]. Studies using primary rat glial cells and human neurons also detected cytotoxicity via lactate dehydrogenase release [66,67].

Nva has also been the subject of several *in vitro* studies however, in contrast to other analogous NPAAs, the primary objective of these studies has been to investigate any potential therapeutic effects stemming from Nva's action as an arginase inhibitor and the potential for misincorporation has been ubiquitously overlooked [68]. In human tumour cells that underwent nutrient starvation to induce apoptosis, Nva demonstrated antiapoptotic activity in a manner that almost doubled in response to a 4-fold increase in Nva concentration (1 mM to 4 mM) [69]. In rat PC12h pheochromocytoma cells, Nva significantly increased neurite outgrowth at concentrations ranging from $1 - 20$ mM [70]. In both cases, the effects of Nva were attributed to the suppression of arginase and subsequent increases in nitric oxide (NO). Ming et al. discovered an alternative mechanism when studying Nva in a primary human endothelial model of inflammation. Nva inhibited the induction of inflammatory adhesion molecules in an arginase and NO independent manner. Instead, the study concluded that the anti-inflammatory properties of Nva were at least partially due to the inhibition of the ribosomal protein S6 kinase β-1 signalling pathway [71]. To date, there has been no investigation into the potential for Nva toxicity as a result of misincorporation.

### 2.3.3.2 In Vivo

Numerous reviews have documented the toxic effects of human and animal exposure to NPAAs [38,72-74]. Among these toxic NPAAs is L-canavanine which has been shown to cause Systemic Lupus Erythematosus (SLE), an autoimmune disease, in primates when L-canavanine-containing alfalfa seeds were ingested [75]. Furthermore, L-canavanine was linked to the death of the American wilderness explorer Chris McCandless in 1992 when wild potato (*Hedysarum alpinum*) seeds that made up his diet were found to contain the NPAA [35]. One of his final diary entries described himself as, 'extremely weak and unable to move', and blamed the potato seeds for his condition [35]. Cattle allowed to forage on the L-canavanine-containing jack bean also experienced progressive weakness and stiffness of their hindquarters [76]. Also in livestock, the NPAA mimosine (β-[N-(3-hydroxy-

4-pyridone)]-L-2-aminopropanoic acid) led to hair loss and growth retardation in animals ingesting mimosine containing seeds or leaves of *Leucaena* plants as their main dietary source [77,78]. Teratogenic effects, including decreased fetal growth and external skeletal abnormalities, have been observed in hamster fetuses treated with Aze [79]. These effects were attributed to Aze's mimicry of L-proline and the authors suggested the skeletal abnormalities observed were due to Aze incorporation into collagen, which normally consists of ~23% L-proline and its derivative L-hydroxyproline [80].

In a similar vein to *in vitro* studies conducted using Nva, the primary objective of *in vivo* studies has been to use Nva's arginase inhibition to restore dysfunction in various disease models. Nva promoted vasodilation in a rat model of endothelial dysfunction caused by NO deficiency [81], and this can also lead to disturbances in osteogenesis [82]. Sobolev et al. treated osteoporotic mice with 10 mg/kg/day Nva in combination with the cholesterol lowering drug rosusvastatin for 4-weeks and observed both a decrease in endothelial dysfunction and a protective effect on bone tissue formation [83]. Changes to the vascular endothelium has also been implicated in hypotension during metabolic syndrome and 50 mg/kg/day Nva administration over a 6-week period was found to ameliorate fructose-induced hypotension in male rats while preventing impaired NO generation [84]. Since metabolic syndrome increases the risk of diabetes and subsequent arginase overexpression [85], De et al. investigated Nva as a treatment for erectile dysfunction due to decreased NO levels. After 30 days, they found that diabetes-induced sexual dysfunction was significantly improved following Nva treatment at 10 mg/ kg/day [86].

Metabolic dysfunction has also been hypothesised to contribute to the development of Alzheimer's disease (AD) [87] and consequently, Nva treatment has been studied in a mouse model of AD. A 6-week treatment of 40-50 mg/kg/day Nva significantly improved memory deficits in 3xTransgenic mice and decreased aggregate formation in the cortex with no reported negative side effects [88]. This study is especially pertinent as recent epidemiological studies using spatial clustering have suggested that NPAAs are an environmental trigger for the development of sporadic neurodegenerative diseases [89,90].

These conditions are classified as neurodegenerative diseases because they are associated with neuronal death in different regions of the brain [91]. The results of Polis et al.'s study of Nva in an AD model contrasts greatly with *in vivo* results for studies investigating BMAA neurotoxicity, which will be explored in more detail in the following section [88].

## 2.4 Neurodegenerative Disease

One of the earliest documented neurodegenerative diseases, neurolathyrism, is caused by an NPAA and was described by Hippocrates in around 400 BC. Throughout history, this disease has been associated with the consumption of the grass pea *Lathyrus sativus,* a BOAA containing legume [72,74,92]. The main symptom of the disease is lower limb paralysis caused by upper motor neuron damage [33]. Unlike other neurodegenerative disorders, onset of lathyrism symptoms have been observed in as little as 30 days after ingestion [72]. Exposure to BOAA, a close analogue of glutamate, in prolonged periods of famine, when the grass pea is a dietary staple, leads to the development of neurolathyrism. BOAA has been identified as the cause of neurolathyrism hotspots in developing countries [56,93-95]. Studies of modern day cases of lathyrism show the incidence rate of the disease is declining due to reduced grass pea consumption as it is no longer used as a dietary staple [96,97]. Furthermore, efforts have been made to detoxify the grass pea via food processing techniques, decreasing the BOAA content, yet preserving the nutritional value of the pea [98].

While the association between BOAA and lathyrism is historically far-reaching and well documented, in recent times another NPAA has been linked to neurodegenerative disease and has proven to be a more controversial candidate for toxicity. The NPAA BMAA has been linked to the Amyotrophic Lateral Sclerosis-Parkinsonism-Dementia Complex (ALS-PDC), which is characterised by the appearance of traits of one or more of the diseases [99], and Amyotrophic Lateral Sclerosis (ALS) in Guam, Japan and the United States [89]. In the 1960s presentations of ALS-PDC reached unprecedented levels on the West Pacific island of Guam [100]. This prompted intense scrutiny into the genetic

background and habits of the indigenous Chamorro population. When at its peak the incidence of these disorders was 50 to 100 times greater than those estimated for the United States and other developed countries [101]. ALS-PDC also affected immigrants from the Philippines and Japan who had adopted the Chamorro lifestyle [102] suggesting that environmental factors were involved. Studies found that cycad seeds containing BMAA as a result of a symbiotic relationship with cyanobacteria formed a considerable portion of the Chamorro diet [100].

Following on from this discovery, Spencer et al. [101] performed an *in vivo* study on macaques, in which macaques were given BMAA by gavage for periods up to 13-weeks. During this period, it was noted that repeated oral administration of BMAA caused ALS-like symptoms such as stooped posture, tremor and weakness in the extremities. Macaques treated with BMAA for the full 13-weeks experienced episodes of immobility. Further evidence of neurotoxicity was provided when motor neuron damage developed in mouse cortical cells treated with BMAA [103]. BMAA treated rats have experienced locomotor deficiencies, motor coordination difficulties, myoclonus, convulsions and neuropathology consistent with neurodegenerative diseases [104-106]. This research led to disparity amidst the scientific community as the acute symptoms observed are inconsistent with the long-term progressive nature of neurodegenerative diseases [91]. Additionally, the high doses used in studies that observed neurotoxicity were strongly criticised and have led to uncertainty about a possible link to disease [107].

Although *in vivo* studies using Nva have been approximately half the length of BMAA toxicity studies, the lack of reported negative side effects adds to the disparity. Since Fowden's landmark findings that some NPAAs are antimetabolites, it has been assumed that all analogous NPAAs would have a similar mechanism, misincorporation, and thereby exert similarly toxic effects [38]. This was disproven when van Onselen et al. performed a side-by-side investigation of BMAA and the proven misincorporation candidate L-m-tyrosine into metabolic activity, apoptosis, necrosis and amino acid composition in human cells [108]. BMAA treatment did not result in significant changes when compared to vehicle-treated controls and was not detected in purified protein

extracts, unlike L-m-tyrosine [108]. The authors concluded that BMAA is not incorporated into human proteins, a conclusion which is in direct conflict with previous studies and questions the mechanisms whereby the observed *in vivo* toxicity is exerted. To further complicate the matter, post mortem studies have found BMAA in brains from Chamorro people who had died from ALS-PDC and in the brain tissue of two Canadian AD patients [109].

Though less established than the BMAA hypothesis, it has been hypothesised that Aze exposure may contribute to the development of the neurodegenerative demyelinating disorder multiple sclerosis (MS) [110]. Like BMAA, spatial clustering linking worldwide MS prevalence and the geographical distribution of Aze-containing sugar beet production, specifically in Japan, Finland, the Middle East, Canada and Scotland's Orkney Islands supports this hypothesis [110]. However, a causal link has not been established, and there have been no publications in the past five years linking Aze exposure to MS in humans. The theory was initially supported by the observation that lambs born to ewes fed Aze-containing sugar beet silage developed an MS-like phenotype, and is further bolstered by the observation that Aze incorporates into myelin basic protein, potentially disrupting myelination [111,112].

While NPAAs and neurodegenerative disease are strongly associated, there is still uncertainty about whether there is a causal link and more research is needed to understand their potential for adverse effects. Some, like BMAA, have been studied extensively, while others such as Nva and Aze have been studied to a much lesser extent and warrant further investigation. Toxicity has been cited in numerous results but the inconsistency of the data and a lack of understanding into the mechanisms involved mean that the potential toxic effects of NPAAs are not yet fully understood.

### 2.4.1 Mitochondria and Neurodegenerative Disease

Several factors contribute to development of neurodegenerative disease including genetics, ageing, metabolic dysfunction and environmental factors. Recently, mitochondrial dysfunction has been implicated and there have been many lines of

evidence implicating mitochondrial dysfunction in the development of neurodegenerative diseases including ALS, AD and PD [113-116]. Mitochondria are dynamic organelles at the centre of a number of complex cellular functions. The normal functioning of mitochondria is paramount to cellular survival and their roles include, but are not limited to, adenosine triphosphate (ATP) production, metabolite synthesis, apoptotic regulation and synthesis of reactive oxygen species (ROS) [117]. With many essential roles, it comes as no surprise that dysfunctional mitochondria have been linked to a number of disease pathophysiologies. Neurodegenerative diseases are among these as neurons are particularly sensitive to changes in mitochondrial function. This is because they are extremely energy dependent and, as post mitotic cells, are especially sensitive to ROS. A balance between mitochondrial fusion, where long elongated networks are formed, and fission, where mitochondria divide into two or more independent structures, must be maintained. These processes are rapid, highly regulated and control mitochondrial morphology, length, size, number, function and distribution [117]. Disruptions to these processes manifest as mitochondrial dysfunction in the facets they control [118,119]. Mutations in this fusion/fission machinery have been linked to rare neurodegenerative diseases [120] and increasingly, mitochondrial abnormalities are becoming a feature of more common neurodegenerative disorders.

A small number of recent studies have discovered an emerging pattern of mitochondrial abnormalities following NPAA treatment. These include SH-SY5Y neuroblastoma cells exposed to L-canavanine, which developed aberrant mitochondrial proteins resulting in the loss of respiratory chain complexes [121]. In addition, mitochondrial swelling, vacuolisation and fragmentation have been observed in both the Purkinje cells and spinal motor neurons of BMAA treated rats [104,122]. These finding were complemented when Tian et al. reported BMAA induced changes in mitochondrial morphology accompanied by motor neuron death [123]. However, the studies are far from extensive and mitochondrial function following either Nva or Aze exposure has never been studied. Additionally, such studies should be performed given that mitochondrial proteins are also susceptible to misincorporation due to the absence of the previously mentioned tRNA proofreading steps that ensure the fidelity of protein synthesis [124]. The

increased likelihood of misincorporation in mitochondria, along with new associations between mitochondrial dysfunction and neurodegenerative disease, suggest that mitochondria may be a target of NPAA toxicity and requires further exploration.

## 2.5 Routes of Exposure to NPAAs

### 2.5.1 Biomagnification

Since BMAA was discovered in cycad seeds, research interest into NPAAs has fluctuated over time. This was in part due to uncertainty about the mechanism of toxicity and how the Chamorro initially came into contact with concentrations of BMAA high enough to cause the disease complex [99]. As additional research came to light sixteen years after the initial ALS-PDC observations on Guam that identified BMAA biomagnification through the Guamian food chain (Figure 3.), the idea of NPAAs as an environmental factor in the etiology of neurodegenerative diseases gained popularity once again.
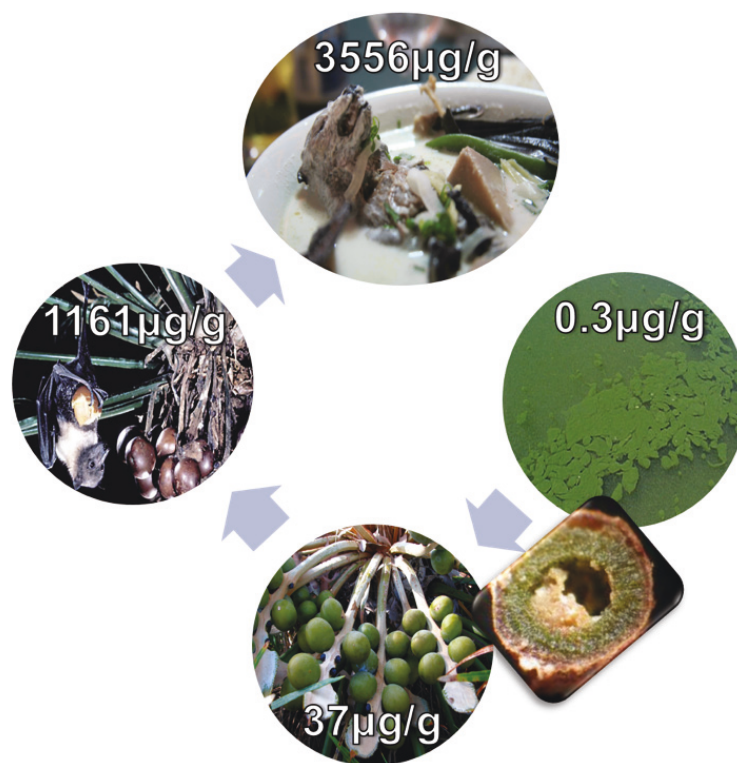


**Figure 3. BMAA bioaccumulation through the Guamian food chain.** BMAA was detected in cyanobacteria at a concentration of 0.3 µg/g, increasing to 37 µg/g in cyanobacteria symbiotic cycad roots, 1161 µg/g in cycad seeds consumed by flying foxes and finally 3556 µg/g in flying foxes served as a traditional Chamorro feast [8].

Biomagnification of NPAAs may increase the concentration of certain NPAAs sufficiently enough to allow for the analogue to occasionally outcompete the parent amino acid. Since Guam, BMAA has been shown to biomagnify in numerous aquatic species. In the last decade BMAA has been isolated in carp from New Hampshire [125], sharks and shellfish from Florida [126,127], sharks from the Atlantic and Pacific Oceans [128], shellfish and molluscs from France [129,130] and most recently in dolphins [131]. BMAA has also been found in the food chain in the Peruvian stew ingredient *Nostoc commune* [132]. Ingestion of the BOAA-containing grass pea (*Lathyrus sativus)* has been linked to neurolathyrism [33] but to date there have been no studies providing evidence for the biomagnification of *Lathyrus* species seeds [133].

Aze also plays a role in human nutrition, since Aze is produced by garden or table beets [134]. While humans are unlikely to consume large enough quantities of beets to induce a deleterious effect, Aze-containing by-products of the sugar beet industry are used as a dietary supplement in meat and dairy livestock and this may serve as a secondary source of Aze to humans [135].    Rubenstein et al. reported the presence of Aze in three commercial by-products fed to farm animals: sugar beet molasses, shredded sugar beet pulp and pelleted sugar beet pulp [32]. Like BMAA, it has been hypothesised that Aze biomagnifies in meat and dairy products consumed by humans [110], though no studies have currently been published confirming this hypothesis.
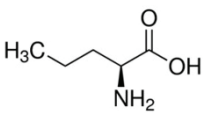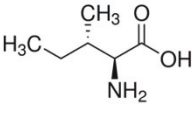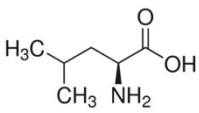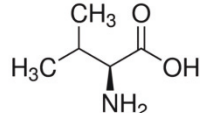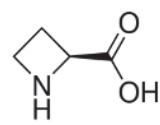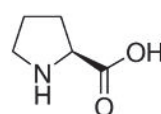
## 2.5.2 Dietary Supplements

Increasingly, NPAAs and plants containing NPAAs are becoming available for purchase online and in supplement and health food stores. Examples of those available online in Australia and their purported benefits are outlined in Table 3. While Aze is most likely present in supplements in small amounts, the prevalence of powdered Nva supplements is concerning. Additionally, Nva is increasingly appearing in patents filed by supplement companies with the intention of using Nva in amino acid compositions to "increase athletic performance" [136-139].

**Table 3. Table listing NPAA containing dietary supplements and their purported benefits.**

| NPAA | Purported Benefit | Product & Brand Name |
|---|---|---|
| **L-DOPA** | Dopamine precursor & cognitive enhancer | Dopa Mucuna, Now Foods [140] |
| | | Dopa-Mind, Life Extension [141] |
| | | Mucuna Dopa, Biovea [142] |
| | | DopaBean, Solaray [143] |
| **L-canavanine** | Improve immune system, anti-cancer & antiviral activity | Sutherlandia Frutescens Cancer Bush, Medico Herbs [144] |
| **L-norvaline** | Improve blood flow, vasodilation, muscle swelling & boosts workout | L-Norvaline Powder, Cyos [145] |
| | | Mega Pre Black, Primeval Labs [146] |
| | | Pump, Ghost [147] |
| **L-azetidine-2-carboxylic acid** | Improve digestive health & circulation | Nat-Lax TNT, Specialist Supplements [148] |
| | | Dietary Fibre Blast, Belle [149] |
| | | Whole Beets Powder, Nature's Answer [150] |

**Table 4. Structural representations of the dietary supplement NPAAs Nva and Aze and their corresponding protein amino acids.**



| | | | |
|---|---|---|---|
| **L-norvaline** $C_5H_{11}NO_2$ MW: 117.1 g/mol | **L-isoleucine** $C_6H_{13}NO_2$ MW: 131.2 g/mol | **L-leucine** $C_6H_{13}NO_2$ MW: 131.2 g/mol | **L-valine** $C_5H_{11}NO_2$ MW: 117.1 g/mol |
| **L-Aze** | **L-proline** | | |

## 2.6 Mechanisms of NPAA Toxicity

At present, the mechanisms whereby NPAAs elicit their toxic effects remain the largest gap in knowledge in NPAA research. Multiple biological pathways have been suggested as possible mechanisms but the theory of misincorporation is currently the most popular. However, it is possible that there is more than one mechanism of action. As analogues of protein amino acids, an understanding of protein synthesis is first required to comprehensively examine the proposed mechanism of NPAA toxicity.

### 2.6.1 Fidelity of Protein Synthesis

The synthesis of proteins involves the transfer of genetic information from deoxyribonucleic acid (DNA) and ribonucleic acid (RNA) to a completed polypeptide chain [151]. Genetic information is encoded in messenger RNA (mRNA) in the form of a degenerate triplet code and an adaptor is required to decode the information in mRNA into the amino acid sequence of proteins [13]. Transfer RNA (tRNA) acts as this adaptor in protein translation [13] and can be aminoacylated (or chemically bonded) to its specific cognate amino acid by an aminoacyl tRNA synthetase (aaRS), forming aminoacyl-tRNA (Figure 4.) [152]. Since multiple tRNAs exist for each amino acid (called isoacceptors), each aaRS has high specificity for a single encoded amino acid and for an isoacceptor set of tRNAs [153]. The ability of aaRS to select the correct protein amino acids is crucial to

preventing errors in protein synthesis and is further supported by the induced-fit mechanism between the amino acid, aaRS and tRNA [154]. The fidelity of protein synthesis is maintained through two proofreading steps that can either occur before (pre-transfer editing) or after (post-transfer editing) the mis-aminoacylation of an amino acid [155].

In post-transfer editing, when an amino acid is mistakenly aminoacylated, the tRNA can dissociate from the ribosome and the non-cognate amino acid is eliminated through hydrolysis [152]. As mentioned previously, this editing mechanism is absent in mitochondria and may leave this organelle more susceptible to errors in protein synthesis [152,156].

Following translation, the linear, nascent polypeptide chain must undergo folding into its native 3D structure to correctly function [157]. The shape of a folded protein is determined by the physicochemical properties of its amino acid sequence, and correct folding assumes a minimal-energy configuration, thus ensuring protein stability [158]. Misfolded proteins are proteins that incorrectly fold into non-native conformations and, if bypassed by protein degradation machinery, tend to form insoluble aggregates that can lead to disease (discussed below) [159].
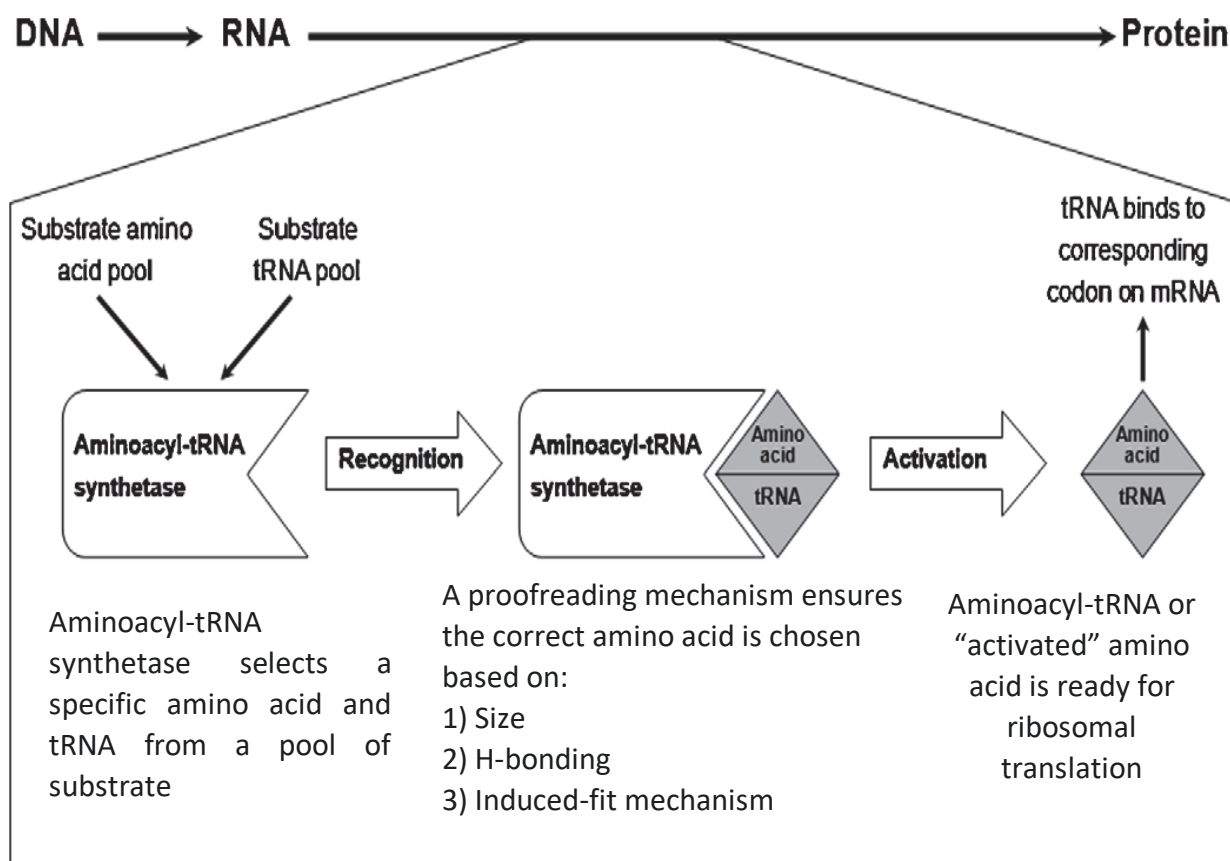
**Figure 4. Fidelity of protein synthesis, adapted from Rodgers and Shiozawa [160].**

## 2.6.2 NPAA Misincorporation and Aggregation

When the proofreading mechanisms are bypassed by an amino acid analogue with similar size and shape to a cognate amino acid, a hydrogen bond with the aaRS forms. The analogue is then incorrectly bonded to tRNA and wrongly inserted into a growing polypeptide chain, which grows by the removal of a water molecule and formation of a peptide bond between two amino acids, following which the tRNA molecule is released [38,161]. This incorrect insertion could potentially interrupt both protein folding and function [154]. Analogues of larger amino acids bind more readily to tRNA synthetases than smaller ones because the larger structure and additional molecular components increase the chances of a part of the molecule matching the structure of the protein amino acid. This allows for tRNA binding [28]. The level of incorporation of these NPAAs into proteins varies and the ratio of replacement is not known [60]. Furthermore, the activation or binding of the analogue by aaRS does not guarantee protein incorporation

[13]. Whether or not this aaRS misactivation and subsequent misincorporation is the cause of toxicity is still debated for some NPAAs, such as BMAA, but is more widely accepted for others such as L-canavanine, where binding to arginyl-tRNA synthetase and misincorporation are responsible for the toxicity that has been observed [162]. Despite the debate, a direct link between BMAA misincorporation and toxicity has been shown. Dunlop et al. found that radiolabeled BMAA incorporated into two mammalian cell lines in a protein synthesis dependent manner [163]. The same study found that upon protein hydrolysis, BMAA was released, and that co-incubation with L-serine inhibited misincorporation [163]. Such definite evidence of misincorporation was accompanied by an increase in apoptotic cell death and protein aggregation [163].

Aze is among the NPAAs that are widely accepted to misincorporate and the earliest evidence of Aze misincorporation was in 1970 when, as previously mentioned, Aze was found to be incorporated into the collagen of chick embryos [164]. A further study on the effect of Aze on hamster fetuses found it was teratogenic and hypothesised that this was due to Aze misincorporation into multiple proteins [79]. When Dasuri et al. observed neuronal Aze toxicity, increased levels of ubiquitinated proteins were also observed [61]. Ubiquitin is a protein that attaches to the protein substrate during the degradation of misfolded or naturally short-lived proteins [165]. The presence of ubiquitinated proteins after Aze treatment suggests that the NPAA is interfering with either protein synthesis or degradation in neuronal cells. Similar increased levels of ubiquitinated proteins have also been detected in BMAA treated rat brains [104]. These increases may correspond to proteins that have had an NPAA misincorporated and can no longer be efficiently degraded. Neurons are particularly vulnerable to damaged proteins as cell division does not take place [166].

Recent research into the editing domain of leucyl-tRNA synthetase (LeuRS) has discovered an evolutionary specificity for Nva, which is readily mischarged to leucine tRNA by LeuRS [47,48,167]. As mentioned previously, Nva binds to EF-Tu and does so at a rate that is similar to L-leucine [48]. The inability of EF-Tu to discriminate against Nva may have acted as the positive selection pressure for the evolution of highly specific LeuRS

editing. This research identifies Nva as a candidate for misincorporation and highlights the importance of Nva toxicity tests due to its increased presence in dietary supplements.

While there is substantial evidence for the misincorporation of NPAAs during protein synthesis, there is still debate about the mechanism by which these non-native proteins could cause neurotoxicity in proteopathies. A study by Ozawa et al. investigated the mechanism of L-DOPA toxicity and found that the incorporation of L-DOPA into proteins synthesised by *E. coli* led to the formation of protein aggregates [168]. This was dependent on which amino acid residue was replaced in the proteins. When solvent-exposed L-tyrosine residues were replaced by L-DOPA the protein retained its solubility. However, replacement of internal L-tyrosine residues with L-DOPA resulted in a loss of solubility [168]. The existing link between many neurodegenerative diseases and protein aggregates strongly supports this as a mode of NPAA toxicity (Table 5.). *In vitro* studies with L-DOPA and SH-SY5Y neuroblastoma cells have shown NPAA substitution, protein misfolding, aggregation and neurotoxicity [24]. In a more recent study, vervet monkey's fed BMAA for 140 days developed β-amyloid plaques and neurofibrillary tangles [169]. The similarity between this behaviour and the pathogenesis of neurodegenerative disorders is further evidence of the potential involvement of NPAAs.

This misincorporation-protein aggregation theory could explain the long period between first exposure to BMAA and the development of neurological symptoms on Guam, estimated to be about 20 years [170]. After the generation of non-native proteins by incorporation, the NPAA aggregates could slowly accumulate in cells and eventually reach a level that causes a decline in cell function. Another related theory is that the aggregates initially formed can cause further protein aggregation through a prion-like action [163]. This theory is based upon the mechanism observed in prion diseases such as Kuru and Creutzfeldt-Jakob disease, however, it has not been the subject of recent research [171]. In prion diseases, prions cause misfolding and aggregation of proteins after their formation. However, their hallmark is the ability of small aggregates or "seeds" to spread the properties of the abnormal diseased proteins to a normal protein [172]. It has

been theorised that seeding is also involved in the progression of neurodegenerative disorders such as PD and AD, which involve the accumulation of the proteins α-synuclein, β-amyloid and tau [173].

Similarly, protein misfolding and aggregation have been proposed in the etiology of ALS [174] . While abnormal proteins and aggregation are implicated in both sporadic and familial cases of ALS, the misfolded proteins superoxide dismutase 1 (SOD1), transactive response DNA binding protein (TDP-43) and valosin containing protein (VCP) have been associated with familial ALS (fALS) [175]. Since fALS only accounts for 10-15% of cases, further research into factors that may contribute to the development of sporadic ALS (sALS) is essential [5]. If misfolded NPAAs exhibited prion-like behavior, the resulting aggregation could theoretically lead to neuronal cell death and the development of neurodegenerative disease.

**Table 5. Characteristics of proteopathies.**

Adapted from [175-177].
* Two of many genes identified for fALS

| Disease | Protein | Region Most Affected | Characterised By |
|---|---|---|---|
| **Alzheimer's disease (AD)** | β-amyloid peptide/ tau | Cortex, hippocampus, basal forebrain, brain stem | Amyloid plaques, neurofibrillary tangles |
| **Parkinson's disease (PD)** | α-synuclein | Substansia nigra, cortex, locus ceruleus, raphe nuclei | Lewy bodies and lewy neurites |
| **Amyotrophic Lateral Sclerosis (ALS)** | Superoxide dismutase 1 (SOD1)* Valosin containing protein (VCP) * | Cortex, spinal cord | Motor neuron degeneration |

| Huntington's disease (HD) | Huntingtin | Striatum | Inclusion bodies |
|---|---|---|---|

## 2.7 Cellular Responses to Stress

When cells experience stress, a wide array of responses can occur, including the activation of survival pathways or 'stress responses' and the initiation of various cell death pathways. In most cases, there is an interplay between these two actions that is dependent on the type of stressor and the severity of the stress [178]. Cellular stress triggers can be chemotherapeutic agents, irradiation, oxidation, environmental toxins, starvation and unfolded or misfolded proteins [178,179]. In the case of misfolded proteins, the heat shock response and the unfolded protein response (UPR) can be utilised to increase the activity of chaperone proteins and enhance protein folding, ultimately reducing the severity of the stressor and allowing continued cell survival [180,181]. A separate response can also occur following DNA damage and consists of both DNA damage and DNA repair signaling pathways [179]. Failure of these responses to successfully resolve the cellular stress leads to the initiation of cell death pathways. Investigating which cell death pathway is activated, whether it be apoptosis, necrosis, or autophagic cell death, can yield useful information about the type of stress present and response induced. For example, following the heat shock response and UPR, programmed cell death or apoptosis typically occurs [182,183]. Furthermore, each death pathway has characteristic morphological features which can be observed experimentally and different families of proteins and enzymes are associated with each cell death pathway (Table 6). Additional pathways, such as pyroptosis, an inflammatory cell death pathway most commonly associated with intracellular pathogen infections, are not included given there is little evidence of their involvement in the response to NPAAs [184].

**Table 6. Cellular morphologies and proteins associated with cell death pathways (relevant to the mechanisms of NPAAs).**

| Cell Death Pathway | Cellular Morphology | Associated Proteins or Enzymes |
|---|---|---|
| **Apoptosis** | Cellular shrinkage and blebbing, nuclear and mitochondrial fragmentation [185,186] | Bcl-2 family of proteins, heat shock proteins, caspase activation, mitochondrial cytochrome c release [182,186,187] |
| **Autophagy** | Formation of acidic autophagic vacuoles, fusion with lysosomes and organelle digestion [188] | Atg proteins, Beclin 1, mTOR, PINK1 [189] |
| **Necrosis** | Cellular swelling, mitochondrial swelling, cell lysis/ membrane rupture [190,191] | Serine/threonine kinase RIP1 [192] |

To date, both the heat shock response and UPR have been investigated following NPAA exposure, with misfolded proteins being the stress inducer. The UPR is activated in the lumen of the ER following ER stress, a well-studied cellular phenomenon that includes, but is not limited to, misfolded proteins. ER stress leading to apoptosis has been observed following treatment with low concentrations of BMAA (0.5 mM) and high concentrations of Aze (10 mM) in cell culture models [63,193-195]. Increases in heat shock response chaperones, termed heat shock proteins (HSPs), have been observed following L-canavanine (0.6mM) and Aze (2.5-10 mM) treatment in primary cells [61,196,197]. HSPs 70 and 80 were also upregulated following Nva (0.5 mM) exposure in yeast [198]. Though both stress responses are often induced following NPAA exposure, Dasuri et al. concluded that HSP levels are not the principle modulators of cell death when, despite observing similar HSP increases in both neuron and astrocytes, neurons experienced preferential cell death [61]. L-DOPA exposure (0.1-1 mM) has resulted in caspase-mediated apoptosis and the formation of autophagic vacuoles while BMAA treatment has also led to increases in the lysosomal cysteine proteases cathepsins B and L [24,64,199,200]. While the activation of cellular stress responses has previously been demonstrated for both Aze

and Nva treated cells, an in depth study of the cell death pathways subsequently activated has not yet been performed.

## 2.8 Methods of Assessing Cellular Stress

Cellular stress caused by NPAAs can initially be assessed using *in vitro* cytotoxicity assays that determine whether an NPAA is toxic to mammalian cells in culture. The basis of such tests is usually the quantification of viable cells following treatment using metabolic activity assays. The MTT assay is named for the water-soluble yellow dye 3-[4,5-dimethylthiazol-2-yl]-2,5-diphenyl tetrazolium bromide and relies on its conversion to insoluble purple formazan. The reduction reaction occurs in the presence of metabolically active cells and is commonly used to measure cell viability [201]. The MTT assay has previously been used to study NPAA-induced cytotoxicity [61,63,202], and one such study investigated BMAA-induced cytotoxicity in the SH-SY5Y cell line that has been selected for the present research [63]. However, the popular assay has shortcomings in that the formation of insoluble formazan crystals is in itself cytotoxic, and a comparative study of the MTT assay and the Alamar Blue viability assay found that the Alamar Blue was more sensitive [201]. In contrast to the MTT assay, the Alamar Blue assay is a more sensitive, non-toxic assay that measures the fluorescence induced by resazurin when reduced by cellular metabolic activity [201,203]. This assay has been used in recent publications investigating BMAA and L-DOPA induced cytotoxicity and will be utilised in this thesis to study Nva and Aze toxicity [193,204].

Once a reduction in cell viability has been identified, additional techniques can detect various cell death pathways. As highlighted in section 2.7, necrosis, apoptosis, and autophagy have distinctive characteristics that can be explored experimentally. Fluorescence microscopy is a useful tool that enables the visualisation of innate cellular events during stress [205]. This is enhanced through the use of live cell imaging techniques that allow stress responses to be measured in real-time [206]. In addition, these observations can be quantified using readily available open-sourced software such as FIJI [207]. The stains used in fluorescence microscopy for cell death assessment are well

characterised, and the stains Annexin V and Propidium Iodide (PI) will be used to visualise early apoptosis and necrotic cell death, respectively. Annexin V binds to phosphatidylserine molecules on the cell membrane that are exposed during early apoptosis, while PI is a cell-impermeable dye that binds to DNA in the nucleus when the cell membrane is compromised during late-apoptosis and necrosis [208,209]. In live cells, the LysoTracker stain will be used to visualise autophagy in real-time, although it is important to note the stain is not selective for lysosomes as suggested by its name [210]. Instead, Lysotracker is selective for acidic organelles, and this distinction will be made during the discussion of relevant results.

Finally, as mitochondria have been identified in section 2.4.1 as an organelle susceptible to NPAA damage, mitochondrial function will also be assessed. During stress, mitochondria may become dysfunctional when their ability to respond to cellular energy demands and produce ATP via respiration is compromised [211]. An analysis of mitochondrial bioenergetics using mitochondrial respiration, or oxygen consumption rate, as a parameter is considered the best general measure of mitochondrial function in intact cells [211]. The Agilent Seahorse Extracellular Flux (XF) Analyser is a relatively new instrument that allows for reliable real-time measurements of mitochondrial respiration in live cells [212]. Using a series of injections during the course of the bioenergetic assay, the XF Analyser allows for the measurement of changes to basal respiration, maximal respiration, ATP production and non-mitochondrial respiration [212]. Together, these measurements provide a clear indication of mitochondrial function and, of all NPAAs, only L-DOPA has been investigated using this technique in a study that found L-DOPA induced mitochondrial dysfunction [204].

# Chapter Three:

Investigation into L-norvaline toxicity

# CHAPTER THREE: INVESTIGATION INTO L-NORVALINE TOXICITY

**Compound Abstract**

The previous chapter revealed numerous examples of NPAA toxicity and their potential for harm to humans. It also showed that NPAAs may also target mitochondria and outlined the association between mitochondrial dysfunction and neurodegenerative disease. It identified that the NPAA L-norvaline is commonly consumed by humans and its toxicity to human cells and effect on mitochondria warrant further investigation. These were investigated in this chapter and the chapter was published in *Toxicology In Vitro*.

**Certificate of Authorship and Originality**

This paper was published in *Toxicology In Vitro*. The following is a copy reprinted with permission from Elsevier Ltd, Copyright ©2019. I certify that the work present in chapter three of this thesis has not been previously submitted as part of the requirements for a degree. I also certify that I carried out all the experimental work, analysis and interpretation of the data presented in this paper.

The remaining author listed on this manuscript contributed in the following way:

- Kenneth Rodgers: Assisted in experimental design, manuscript direction and proofreading

| Principal Supervisor | Student |
|---|---|
| Kenneth Rodgers | Kate Samardzic |
| Production Note: Signature removed prior to publication. | Production Note: Signature removed prior to publication. |
| Signature | Signature |
| 11/12/2019 | 16/06/2020 |
| Date | Date |

# Cytotoxicity and mitochondrial dysfunction caused by the dietary supplement l-norvaline

Kate Samardzic, Kenneth J. Rodgers[*]

*School of Life Sciences, University of Technology Sydney, Harris Street, Sydney, NSW 2007, Australia*

## ARTICLE INFO

## ABSTRACT

In addition to the 20 protein amino acids that are encoded for protein synthesis, hundreds of other naturally occurring amino acids, known as non-proteinogenic amino acids (NPAAs) exist. It is well known that some NPAAs are toxic through their ability to mimic protein amino acids, either in protein synthesis or in other metabolic pathways, and this property is utilised by some plants to inhibit the growth of other plants or kill herbivores. L-norvaline is an NPAA readily available for purchase as a dietary supplement. In light of previous evidence of l-norvaline's antifungal, antimicrobial and herbicidal activity, we examined the toxicity of l-norvaline to mammalian cells *in vitro* and showed that l-norvaline decreased cell viability at concentrations as low as 125 μM, caused necrotic cell death and significant changes to mitochondrial morphology and function. Furthermore, toxicity was reduced in the presence of structurally similar 'protein' amino acids, suggesting l-norvaline's cytotoxicity could be attributed to protein amino acid mimicry.

## 1. Introduction

Protein is an essential component of the human diet and is composed of chains of peptide bonded 'protein' or canonical amino acids. Proteolysis of dietary proteins releases these constituent amino acids for use in *de novo* protein synthesis. The dietary importance of some of the 20 canonical protein amino acids has long been documented, in fact the first amino acid discovered, asparagine, was identified from the vegetable asparagus (Vickery and Schmidt, 1931; Häusler et al., 2014). However, the importance of amino acids extends beyond protein synthesis, and they are involved in diverse cellular processes including energy supply as oxidative substrates, precursors of cell signalling molecules and substrates for gluconeogenesis and lipogenesis (Häusler et al., 2014; Crick et al., 1961; Cynober, 2013). Of the 20 protein amino acids, nine are considered nutritionally essential because they are inadequately produced by the human body and must be obtained through diet. A further five are considered conditionally essential as they may not be effectively produced in certain groups (*e.g.* children) or during stress (*e.g.* reproduction or disease) (Hambræus, 2014; Wu, 2009). These amino acids are available as components of an ingested protein, which are then released by enzymatic hydrolysis during digestion, and as free amino acids in food. Nevertheless, over time free amino acids have also become easily available as dietary supplements in supermarkets, pharmacies and healthfood stores. While dietary supplementation with amino acids in general has been steadily increasing since the 1970s, the highest consumption of amino acids is among athletes and bodybuilders since protein requirements are higher in very active individuals and are considered to increase performance (Bailey et al., 2011; Sharp and Pearson, 2010; Lemon, 2000). Such is the demand for amino acids that supplements have expanded from free 'protein' amino acids to include compounds that act as precursors to the protein amino acids. These compounds belong to an amino acid subcategory called non-proteinogenic amino acids (NPAAs).

NPAAs account for hundreds of naturally occurring, mainly plant-derived, amino acids that are not directly used in protein synthesis by humans (Bell, 2003). In the body, some NPAAs are converted to protein amino acids while others serve as metabolic intermediates in the production of other compounds such as neurotransmitters and NPAA supplement use is prevalent for both these reasons (Osowska et al., 2004; Monte-Silva et al., 2010). For example, in the body the NPAA l-citrulline is converted into l-arginine, a desirable amino acid due to its role in increasing production of the signalling molecule nitric oxide (NO) (Ming et al., 2004). Increased NO levels are associated with increased muscle growth, vasodilation, increased blood flow and ATP synthesis (Ming et al., 2004; Nisoli et al., 2004). A less well known NPAA that has recently been utilised as a dietary supplement among athletes due to its NO stimulating effects is l-norvaline. L-norvaline is an inhibitor of the enzyme arginase, indirectly increasing levels of l-

---

arginine in the body and increasing NO production (Hunter and Downs, 1945).

While NPAAs do have biological benefits, some are known to inhibit biological processes. This arises from their structural similarity to 'protein' amino acids and as such, they are termed amino acid analogues (Thompson et al., 1969) and are capable of 'protein' amino acid mimicry (Song et al., 2017). In plants, these toxic NPAAs have been shown to have an evolutionary significance. Fescue grasses produce the l-tyrosine analogue l-*m*-tyrosine, an herbicidal NPAA that inhibits the growth of other plants competing for space and nutrients (Bertin et al., 2007). In addition, the l-arginine analogue l-canavanine accumulates in the seeds of the jack bean *Canavalia ensiformis*. L-canavanine is insecticidal and protects the plant from insect predation (Rosenthal, 2001). The similarity of these NPAAs to their corresponding 'protein' amino acids has been attributed to their toxicity through a process referred to as 'misincorporation' (Rodgers and Shiozawa, 2008). Due to their structural similarity to protein amino acids, the NPAAs l-*m*-tyrosine and l-canavanine are mistakenly utilised in protein synthesis, in the places of l-tyrosine and l-arginine respectively, with the error in protein synthesis resulting in deleterious effects for the organism.

The dietary supplement l-norvaline is a structural analogue of the branched chain amino acids (BCAAs) l-isoleucine, l-leucine and l-valine (Table 1) and as such, investigation into its safety and potential for causing adverse effects is warranted. L-norvaline is sold as a powder or capsule and is found either individually or in multi-ingredient 'stacked' supplements. According to labelling, the dosage varies between 100 and 400 mg and it is recommended to be consumed daily before exercise dissolved in 250 mL water. According to these instructions l-norvaline, with a molecular weight of 117.15, is consumed at concentrations ranging from 3.4–13.6 mM.

L-norvaline has already been the subject of several *in vitro* studies however, in contrast to other analogous NPAAs, the primary objective of these studies has been to investigate any potential therapeutic effects arising from l-norvaline's action as an arginase inhibitor. The potential for misincorporation into proteins or other mechanisms of toxicity have been overlooked. In human tumour cells that underwent nutrient starvation to induce apoptosis, l-norvaline exhibited antiapoptotic activity that almost doubled in response to a 4-fold increase in l-norvaline concentration (1 mM to 4 mM) (Franek et al., 2002). In rat PC12h pheochromocytoma cells l-norvaline significantly increased neurite outgrowth at concentrations ranging from 1 to 20 mM (Yamazaki and Chiba, 2006). In both cases, the effects were attributed to the suppression of arginase and subsequent increases in NO. Ming et al. discovered an alternative mechanism when studying l-norvaline in a primary human endothelial model of inflammation. L-norvaline inhibited the induction of inflammatory adhesion molecules in an arginase and NO independent manner. Instead, the study concluded that the anti-inflammatory properties of l-norvaline were at least partially due to the inhibition of the ribosomal protein S6 kinase β-1 (S6K1) signalling pathway (Ming et al., 2009).

In a similar vein to *in vitro* studies conducted using l-norvaline, the primary objective of *in vivo* studies has been to use l-norvaline's

arginase inhibition to restore dysfunction in various disease models. Osteoporotic and hypotensive rodent models experienced symptom amelioration following 4 and 6-week l-norvaline administration respectively (Sobolev et al., 2018; El-Bassossy et al., 2013). Additionally, De et al. investigated l-norvaline as a treatment for erectile dysfunction due to decreased NO levels in diabetes and observed significant improvements using 10 mg/kg/day (De et al., 2016). To date, there has been no investigation into the cytotoxicity of l-norvaline and in the present study we examine the effect of l-norvaline on the viability and function of neuroblastoma cells through its ability to mimic structurally similar protein amino acids.

## 2. Experimental materials and methods

### 2.1. Reagents

Dulbecco's Modified Eagle's Medium (DMEM) and Eagle's Minimal Essential Medium (EMEM, deficient in l-isoleucine, l-leucine and l-valine), l-norvaline, l-isoleucine, l-leucine, l-valine and l-serine were from Sigma Chemical Co., St Louis, MO. All aqueous solutions and buffers were prepared using 18 mU water. All other chemicals and solvents were of cell-culture grade.

### 2.2. Cell culture

SH-SY5Y human neuroblastoma cells (American Tissue Culture Collection, catalogue number CRL-2266) were cultured as follows; DMEM was supplemented with 10% heat-inactivated Foetal Bovine Serum (FBS) (US origin, Gibco Carlsbad, CA, USA), and 100 X GlutaMAX (Thermo Fisher Scientific, Waltham, MA, USA). Cells were maintained at 37 °C with 5% $CO_2$ in 175 $cm^2$ flasks until they were plated for specific experiments. During treatment, DMEM culture medium was substituted with l-isoleucine, l-leucine and l-valine deficient EMEM. Experiments were performed between passages 16 and 28.
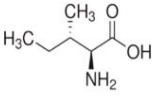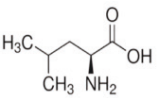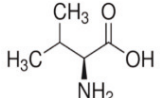
### 2.3. Cell viability

Cells were plated in 96 well plates at 30,000 cells/well, allowed to adhere overnight, then treated in triplicate with the following concentrations of l-norvaline in EMEM; 125 μM, 250 μM, 500 μM, 1000 μM and 2000 μM. Cells were treated for 24 h and then incubated with 10% Alamar Blue cell viability reagent (Thermo Fisher) for 2 h. Fluorescence was read at ex 570/em 585. Protein concentration was determined with the BCA assay (Smith et al., 1985) and fluorescence was normalised to protein concentration. For all experiments, n refers to the number of independent experiments performed.

### 2.4. Amino acid competition

Cell viability was also measured in the presence of l-norvaline in conjunction with l-isoleucine, l-leucine, l-valine and l-serine. Each amino acid was added, separately, to EMEM amino acid deficient media

**Table 1**
Structural representation of l-norvaline and its potential analogue protein amino acids.



| L-norvaline | L-isoleucine | L-leucine | L-valine |
|---|---|---|---|
| $C_5H_{11}NO_2$ | $C_6H_{13}NO_2$ | $C_6H_{13}NO_2$ | $C_5H_{11}NO_2$ |
| MW: 117.1 g/mol | MW: 131.2 g/mol | MW: 131.2 g/mol | MW: 117.1 g/mol |

51

to increase the concentration to 1000 μM. Adhered cells were co-incubated with the amino acid supplemented EMEM and 500 μM l-norvaline for 24 h. Cell viability was measured using the Alamar Blue assay and normalised to protein concentration using the BCA assay.

### 2.5. Cell viability time course

Cells were plated into 24 well plates at 60,000 cells/well, allowed to adhere overnight, then stained with Hoechst 33258 nuclei stain for 15 min and treated in duplicate with l-norvaline at 500 μM and 2000 μM in EMEM containing propidium iodide (PI) and placed in a microscope heated chamber warmed to 37 °C with 5% $CO_2$. Images were captured with a high-speed charge-coupled device (CCD) camera using the NIS-Elements acquisition software mounted on a Nikon Ti inverted fluorescence microscope equipped with 20× objective lens (Plan Apo NA 1.4 aperture) and the Perfect Focus System™ for continuous maintenance of focus. Hoechst was monitored with a bandpass 470 emission filter and propidium iodide was monitored at emission 636. Time-lapse images were collected every 30 min over a 24 h period with 2 fields of view from each well imaged. Exposure time and brightness/contrast setting were kept constant for each using the NIS-Elements acquisition software. Images were analysed in FIJI (Schindelin et al., 2012) following background subtraction with a rolling ball radius. Propidium iodide staining was measured using the mean grey value and fluorescence was normalised to the number of Hoechst positive nuclei.
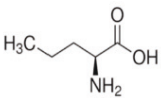
### 2.6. Lysosome activity

Cells were plated into 24 well plates at 60,000 cells/well, allowed to adhere overnight, and then stained with Hoechst 33258 nuclei stain as above. The acidotropic dye LysoTracker Red DND-99 was then diluted in EMEM containing l-norvaline at 500 μM and 2000 μM and added to wells in triplicate. A 10 μM $H_2O_2$ positive control was also included. The plate was then placed in a microscope heated chamber warmed to 37 °C with 5% $CO_2$ and images were then captured using the Nikon Ti and NIS-Elements at emission 470 for Hoechst 33258 and emission 636 for LysoTracker Red DND-99. Time-lapse images were collected every 30 min over a 24 h period with 2 fields of view from each well imaged. Exposure time and brightness/contrast setting were kept constant for each using the NIS-Elements acquisition software. Images were analysed in FIJI following background subtraction with a rolling ball radius. Lysosome activity was measured using the mean grey value of LysoTracker uptake and fluorescence was normalised to the number of Hoechst positive nuclei.

### 2.7. Apoptotic activity

The apoptotic activity of cells was determined using the Annexin V-FITC Apoptosis Detection Kit (Abcam, Cambridge, UK) as recommended by the manufacturer. Cells were plated into 24 well plates at 60,000 cells/well, allowed to adhere overnight, and then stained with Hoechst 33258 nuclei stain as above. The Annexin V-FITC was then diluted in EMEM containing l-norvaline at 500 μM and 2000 μM and added to wells in duplicate. The plate was then placed in a microscope heated chamber warmed to 37 °C with 5% $CO_2$ and images were then captured as above.

### 2.8. Glutamate content

Cellular glutamate content was measured using the Glutamate Assay Kit (Fluorometric) (Abcam) according to the manufactors instructions. Cells were plated into 96 well plates in triplicate at 30,000 cells/well, allowed to adhere overnight and then treated with 2000 μM l-norvaline for 24 h prior to the assay. Fluoresence was normalised to protein concentration using the BCA assay and cellular glutamate concentration

was calculated against a standard curve.

### 2.9. Intracellular $Ca^{2+}$ measurement

The $Ca^{2+}$-sensitive fluorescent indicator Fluo-8 acetoxymethyl ester (Fluo-8/AM) (Abcam) was used to detect intracellular $Ca^{2+}$ using the Nikon Ti inverted microscope. Cells were plated into 12 well plates at 100,000 cells/well, allowed to adhere overnight and treated with 2000 μM l-norvaline for 24 h prior to the assay. Cells were then loaded with 4 μM Fluo-8/AM in Hank's Balanced Salt Solution with Hepes (HHBS) for 20 min at room temperature, washed twice in HHBS and then imaged using the FITC channel every 15 s for 5 min. Fluoresence intensity was then analysed in FIJI and calculated using the eq. $F/F_0$ where F is mean fluorescence intensity and $F_0$ is baseline fluorescence.

### 2.10. Mitochondrial morphology

To examine mitochondrial morphology, cells were seeded on sterile glass coverslips that were placed in 12 well plates. The next day, the cells were treated with 2000 μM l-norvaline. At 24 h post treatment, the cells were fixed with 2% paraformaldehyde for 20 min, quenched in 100 mM glycine for 5 min, blocked in 2% bovine serum albumin (BSA) in phosphate buffered saline (PBS) for 1 h, permeabilised in 0.5% Triton X-100 for 5 min and incubated with mitochondrial mouse monoclonal antibody (Abcam) overnight at 4 °C. Next, the cells were incubated with a mouse secondary antibody conjugated to CF488A for 1 h at RT in the dark, followed by 4′,6-diamidino-2-phenylindole (DAPI) nucleic acid stain (Thermo Fisher) for 5 min. Slides were then prepared with one drop of VECTASHIELD ® and sealed using nail varnish. Images were obtained at 60× using an Olympus BX50 microscope. Images were analysed in FIJI using the macro Mito-Morphology (Dagda et al., 2009).

### 2.11. Mitochondrial bioenergetics

A mitochondrial bioenergetics analysis was performed by measuring the oxygen consumption rate (OCR) of cultured cells using the Seahorse XFe24 Extracellular Flux analyser (Agilent, Santa Clara, CA, USA). Cells were plated at 30,000 cells/well and left overnight to adhere. Cells were then treated with l-norvaline at 500 μM and 2000 μM for 24 h in the presence and absence of the nitric oxide synthase inhibitor $N^{ω}$-Nitro-L-arginine methyl ester (l-NAME) (Abcam). The Mito Stress Test (Agilent) was then performed according to manufacturer's instructions. Cells were then washed in Seahorse assay media and prepared using the manufacturer's protocol and kit reagents (oligomycin (1 μM), FCCP (1 μM) and antimycin A/rotenone (0.5 μM)). OCR values were normalised to protein concentration using the BCA assay. Basal respiration, maximal respiration, ATP production and non-mitochondrial respiration were then calculated using the Seahorse XF Cell Mito Stress Test Report Generator.

### 2.12. Statistics

Statistical analyses were evaluated using GraphPad software (CA, USA) Prism 7 version 7.03 using either one or two-way ANOVA with Dunnett's multiple comparison post-tests to compare replicate means between different treatments across the samples. Normality was tested using the D'Agostino-Pearson normality test and homogeneity corrected using the Geisser-Greenhouse correction. Where data was not normally distributed the Mann-Whitney test was applied. Differences were considered significant at $p < .05$.
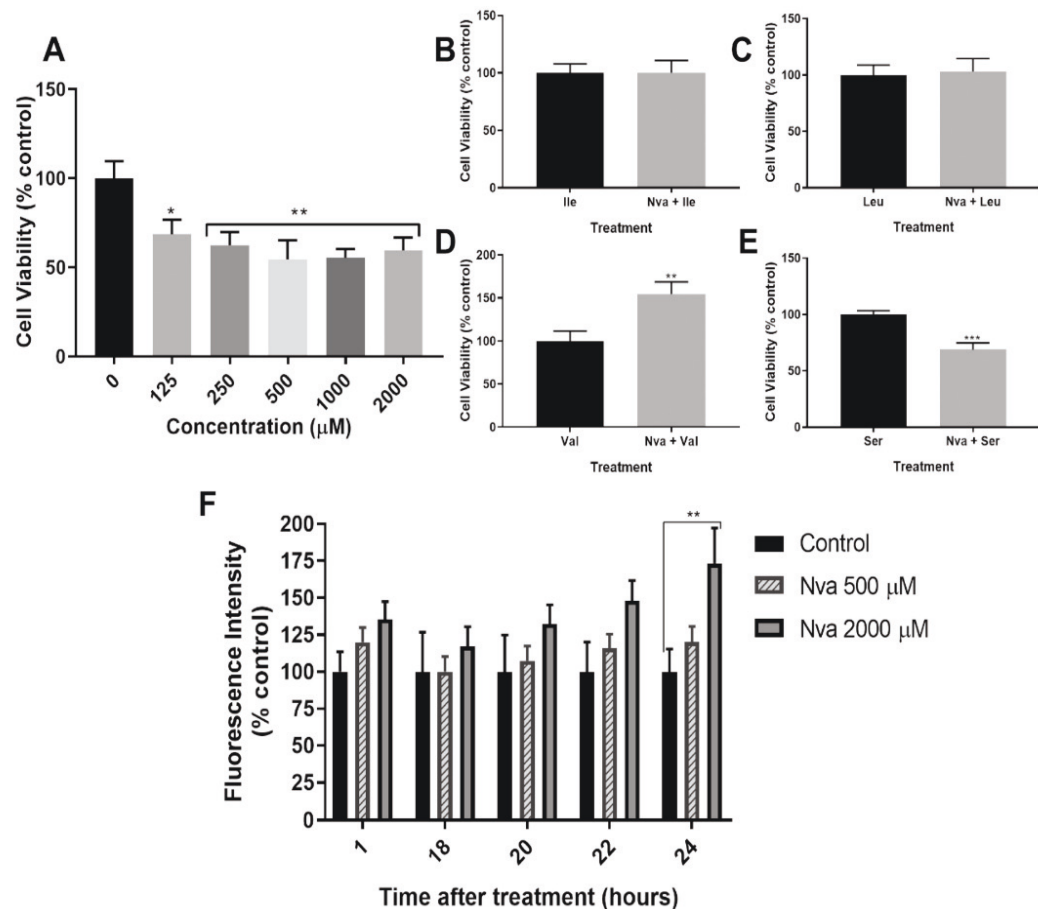
**Fig. 1.** Viability of SH-SH5Y neuroblastoma cells following 24 h l-norvaline treatment. Panel A shows viability at a range of concentrations in EMEM medium. Panels B- E show viability following 24 h treatment with 500 μM L-norvaline (Nva) in EMEM medium and supplemented with 1000 μM l-isoleucine (Ile) (B),l-leucine (Leu) (C) l-valine (Val) (D) and l-serine (Ser) as a negative control (E). Panel F shows viability as a measure of propidium iodide fluorescence intensity 1, 18, 20, 22 and 24 h after l-norvaline treatment. Normalised to nuclei counts and expressed as a percentage of control. $N = 3$. Error bars show SEM. $^{*}P < .05$, $^{**}P < .01$, $^{***}P < .001$.

## 3. Results

### 3.1. Exposure of SH-SY5Y cells to l-norvaline caused a time-dependent decrease in cell viability

Cell viability was assessed in SH-SY5Y cells over a range of l-norvaline concentrations using the Alamar Blue assay (Fig. 1A). Viability decreased to 68.5% at 125 μM l-norvaline ($P < .05$) and decreased further at 250 μM, 500 μM, 1000 μM and 2000 μM l-norvaline ($P < .01$).

### 3.2. The toxicity of l-norvaline was reduced in the presence of increased concentrations of structurally similar amino acids

To examine the protective effects of protein amino acid analogues, the Alamar Blue assay was performed in the presence of 500 μM l-norvaline and increased concentrations of the amino acids l-isoleucine, l-leucine, l-valine and l-serine relative to those present in the medium (EMEM) used in the previous viability experiment (Fig. 1A). l-serine was included as a structurally dissimilar protein amino acid. The basal concentrations of l-isoleucine, l-leucine, l-valine and l-serine in the DMEM medium were 800, 802, 400, and 0 μM respectively (Fig. 1A). The concentrations of each amino acid was increased to 1000 μM and cell viability determined in each case relative to identical medium

without l-norvaline (Fig. 1B-E). In contrast to the previous data (Fig. 1A), in the presence of increased concentrations of l-isoleucine and l-leucine there were no significant decline in viability in the l-norvaline treated cells relative to the control (Fig. 1B & 1C). Co-incubation with l-valine (Fig. 1D) significantly increased cell viability ($P < .01$) while co-incubation with l-serine (Fig. 1E) did not increase cell viability in l-norvaline treated cells ($P < .001$).

### 3.3. Time-course of l-norvaline-induced necrosis in live cells

In order to determine the time-course of l-norvaline induced toxicity we examined the uptake of PI by live cells treated with l-norvaline (500 and 2000 μM) over a 24 h period (Fig. 1F). PI uptake is indicative of irreversible cell membrane damage and necrotic cell death. At 2000 μM l-norvaline there was an increase in PI uptake differing significantly from the untreated cells after 24 h ($P < .01$). An increase in necrotic cell death relative to the control cells was not seen in cells treated with 500 μM l-norvaline.

### 3.4. Lysosome activity is unaffected by l-norvaline exposure

The number of lysosomal bodies in the cell was monitored over 24 h of exposure to l-norvaline using the dye LysoTracker Red DND-99 in EMEM. Fluorescence microscopy was used to visualise the lysosomes

**Fig. 2.** Lysotracker Red DND-99 (A) and Annexin V (B) fluorescent intensity of SH-SY5Y neuroblastoma cells measured every 6 h over a 24 h period of l-norvaline (Nva) treatment at 500 and 2000 μM. $N = 3$. Error bars show SEM. (For interpretation of the references to colour in this figure legend, the reader is referred to the web version of this article.)

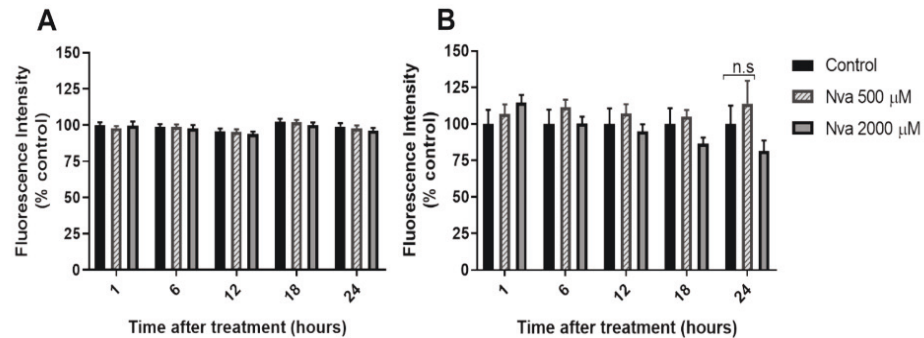and fluorescence intensity was then analysed using the software FIJI (Fig. 2A). L-norvaline treatment did not significantly affect lysosomal numbers, although a difference was observed in the positive control (data not shown).

### 3.5. L-norvaline exposure does not cause apoptotic cell death

The apoptotic activity of cells was monitored over 24 h of l-norvaline (2000 μM) treatment using Annexin V-FITC. Fluorescence microscopy and FIJI were used to visualise and analyse fluorescence (Fig. 2B). L-norvaline treatment did not induce apoptosis over the course of the treatment.

### 3.6. L-norvaline cytotoxicity is independent of glutamate and calcium

Cellular glutamate and calcium levels were measured following 24 h treatment with l-norvaline (2000 μM) using fluorometric assays (Fig. 3A & B). L-norvaline did not significantly affect glutamate concentration or calcium fluorescence.

### 3.7. L-norvaline induces morphological changes to mitochondria

Mitochondrial morphology following treatment with l-norvaline at 2000 μM was assessed using fluorescence microscopy (Fig. 4). Morphological changes pertaining to mitochondrial shape, size and connectivity were quantified using FIJI software and the macro Mito Morphology. Mitochondrial number was not significantly affected following l-norvaline treatment (Fig. 5A) however mitochondrial area significantly decreased ($P < .0001$) (Fig. 5B) while the mitochondrial elongation score significantly increased ($P < .0001$) (Fig. 5C) and mitochondrial interconnectivity significantly decreased ($P < .001$) (Fig. 5D).

### 3.8. Mitochondrial bioenergetics is affected by l-norvaline treatment in the presence of l-NAME

Mitochondrial bioenergetics was analysed by measuring OCR after 24 h of l-norvaline treatment at 500 and 2000 μM. Neither basal respiration (Fig. 6A), ATP production (Fig. 6B), maximal respiration (Fig. 6C) nor non-mitochondrial respiration (Fig. 6D) were significantly affected by the treatment. Upon the addition of 200 μM l-NAME, an NO inhibitor, significant changes were observed to all measurements at 2000 μM l-norvaline while non-mitochondrial respiration also significantly decreased at 500 μM l-norvaline (Fig. 6A–D). Basal and maximal OCR decreased by 20.7% and 26.1% respectively. ATP production decreased by 26.6% while non-mitochondrial respiration decreased by 29.9% at 500 μM and 25.5% at 2000 μM.

## 4. Discussion

L-norvaline is an NPAA synthesised by multiple strains of bacteria including *Bacillus subtilis* (*B. subtilis*) and *Serratia marcesens* (Nandi and Sen, 1953; Kisumi et al., 1976). In *B. subtilis* l-norvaline is a component of an antifungal peptide consisting of nine other amino acids (Nandi and Sen, 1953). Although the antifungal action of this peptide has been documented in several test organisms including the fungal plant pathogen *Fusarium* sp., no mechanisms for this activity have been proposed.

While investigating the fidelity of protein sythesis, the inhibition of bacterial growth was demonstrated in leucyl-tRNA synthetase (LeuRS) editing defective strains of *E.coli* at concentrations starting at 100 μM in the absence of competing amino acids and 300 μM when l-isoleucine, l-leucine and l-valine were added at threefold concentrations (Cvetesic et al., 2014). Another study also using *E. coli* with a LeuRS editing defect reported an l-norvaline IC50 of 4.2 mM (Karkhanis et al., 2007). Plant growth inhibition has been observed in the duckweed *Lemna*
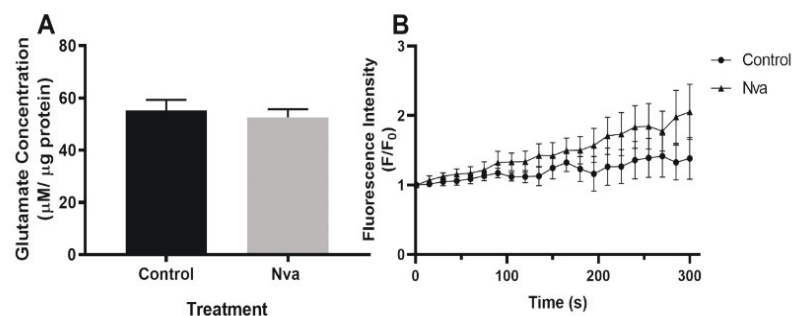


**Fig. 3.** Glutamate concentration (A) and intracellular calcium measured by Fluo-8/AM fluorescence intensity (B) of SH-SY5Y neuroblastoma cells following 24 h l-norvaline (Nva) treatment at 2000 μM. Fluorescence intensity (F) is shown relative to baseline ($F_0$). $N = 3$. Error bars show SEM.
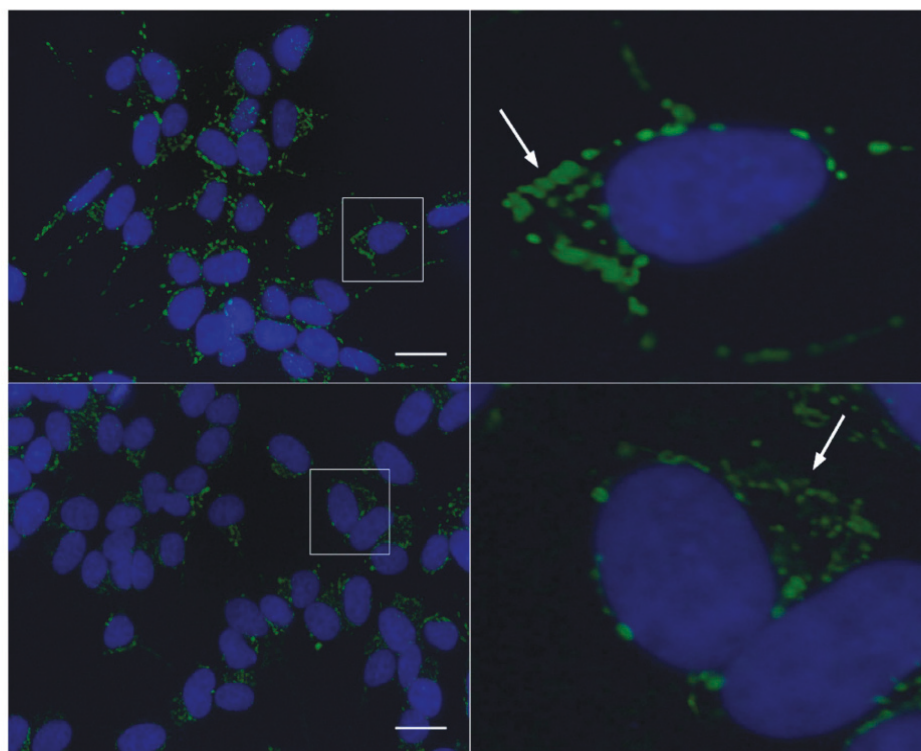
**Fig. 4.** Fluorescence microscopy (60 x magnification) of effects of l-norvaline on SH-SY5Y neuroblastoma cell mitochondria following 24 h treatment. Cells are stained with an anti-mitochondria antibody (green) and nucleic acid stain DAPI (blue). Control cells are shown in the top panel and cells in the bottom panel were treated with 2000 μM l-norvaline. Scale bar 10 μm. (For interpretation of the references to colour in this figure legend, the reader is referred to the web version of this article.)

*minor* at much lower concentrations ($LD_{50}$ between 25 and 30 μM) (Gulati et al., 1981). The consumption of l-norvaline by humans is fairly recent, and due to less stringent regulations on supplements compared to pharmaceuticals, few studies have investigated its toxicity in mammalian cells. This is especially pertinent since l-norvaline is now readily available for purchase and consumption and it is common to consume up to 400 mg per day.

Using the Alamar Blue assay we provided evidence that l-norvaline
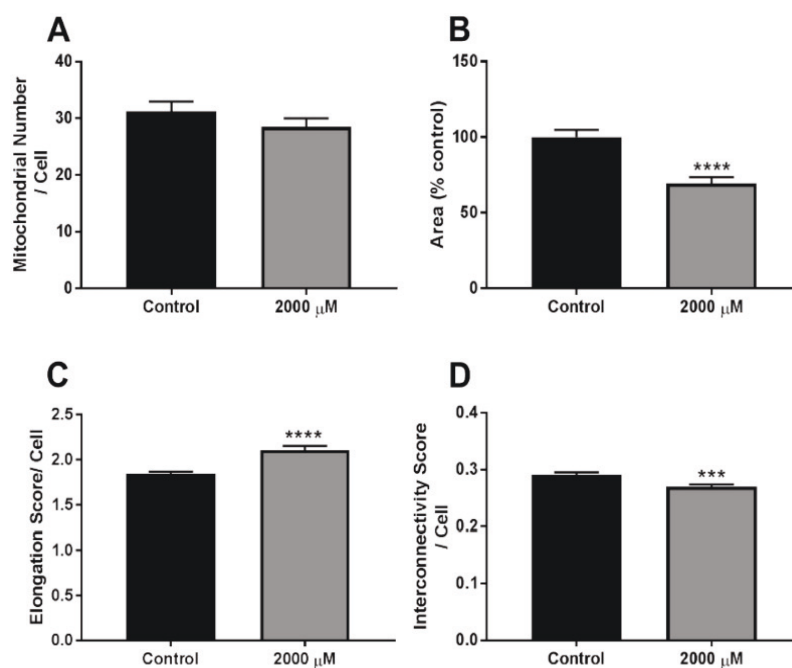


**Fig. 5.** Mitochondrial morphology in SH-SY5Y neuroblastoma cells following 24 h l-norvaline treatment. Panel A shows mitochondrial number, panel B shows mitochondrial area, panel C shows the mitochondrial elongation score and panel D shows the mitochondrial interconnectivity score. $N = 3$. Error bars show SEM. ***$P < .001$, ****$P < .0001$.
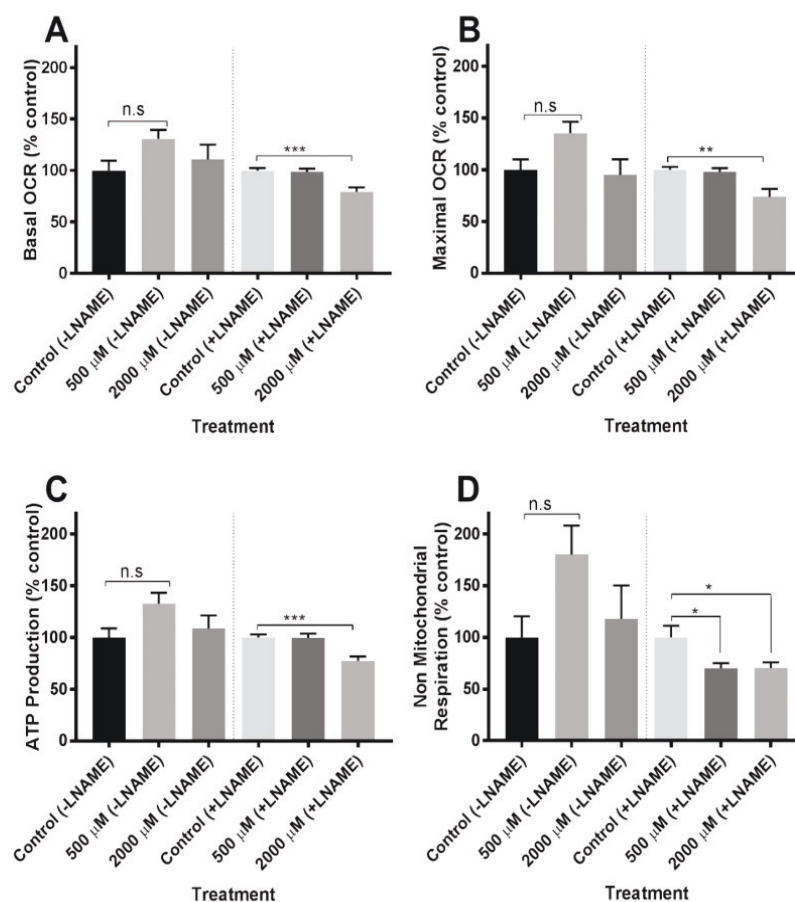
**Fig. 6.** Mitochondrial bioenergetics of SH-SY5Y neuroblastoma cells following l-norvaline treatment for 24 h in the absence and presence of the NO inhibitor l-NAME. Panel A shows basal respiration, panel B shows maximal respiration, as measured by oxygen consumption rate (OCR), panel C shows ATP production and panel D shows non-mitochondrial respiration. $N = 3$. Error bars show SEM. $^*P < .05$, $^{**}P < .01$, $^{***}P < .001$.

is toxic to mammalian cells at concentrations as low as 125 μM (Fig. 1A). In this assay, resazurin is reduced to resorufin, which is highly fluorescent and provides a sensitive measure of the reducing activity in living cells. Reducing activity is dependent on the activity of a wide range of cytosolic and mitochondrial enzymes, so the assay is a general indicator of cell health which can be related to toxicity, viability or proliferation (Rampersad, 2012). In the present studies resorufin fluorescence was normalised to protein concentration, thus the observed fluorescence was not related to proliferation. To determine if the significant decrease in reducing activity was accompanied by cell death we monitored necrosis over a 24 h period. By continuously monitoring cell membrane permeability we found that necrotic cell death was significantly increased after 24 h of l-norvaline exposure but this only occurred with 2000 μM l-norvaline (Fig. 1F). It should be noted that these changes were observed in cells that were cultured in the presence of the relatively high levels of protein amino acids commonly used in cell culture.

If l-norvaline was mistakenly used in cytosolic protein synthesis the presence of l-norvaline- containing proteins could potentially cause cytosolic protein misfolding and aggregation (Chan et al., 2012), triggering autophagic removal. However, after 24 h incubation with l-norvaline we observed no significant changes in lysosomal numbers (Fig. 2A). Interestingly, the autophagy inhibitor mTOR is activated by the BCAAs l-leucine and l-isoleucine (Perl, 2016; Laplante and Sabatini, 2009). It may be possible that l-norvaline is incorrectly binding to the activation site in place of the two BCAAs, resulting in the deleterious inhibition of autophagic removal. Similarly, when we monitored

apoptotic cell death we found no increase when cells were exposed to 2000 μM (Fig. 2B) which is consistent with l-norvaline having an antiapoptotic effect (Franek et al., 2002). It would appear that over this time-course the cell death observed is independent of autophagic and apoptotic cell death pathways.

By increasing the concentration of the three protein amino acids most closely related to l-norvaline in structure (l-isoleucine, l-leucine or l-valine) it was possible to fully protect against the toxic effects of l-norvaline (Fig. 1B–D). l-serine, an amino acid that has no structural similarity to l-norvaline, had no effect on viability while increasing the concentration of l-valine in the culture medium to 1000 μM (rather than 400 μM) resulted in an increased viability in the presence of l-norvaline. This may be due to l-valine's reported ability to increase dendritic cell function (Zhang et al., 2017). It is more likely that l-valine firstly inhibits l-norvaline's toxicity and then complements its arginase inhibitory effects (Carvajal and Cederbaum, 1986), resulting in a more pronounced increase in NO production than the other BCCAs since l-valine forms the most stable enzyme-inhibitor complex with arginase (Fujimoto et al., 1976). It has been previously reported by Gansauge et al. that increased NO bioavailability will increase cellular proliferation (Gansauge et al., 1997). However, as previously mentioned, in the present study resofurin fluorescence was normalised to protein content and therefore, we can only conclude that the combination of l-valine and l-norvaline provides protection from cytotoxicity while increasing the activity of enzymes involved in reducing resazurin.

We have not, however, identified if l-norvaline mimics any one specific branched chain amino acid (BCAA) and on the contrary, our

data suggests l-norvaline might compete with all structurally similar BCAAs since l-isoleucine, l-leucine and l-valine all provided some protection against l-norvaline cytotoxicity whereas the structurally unrelated amino acid l-serine did not (Fig. 1E). Another possibility is that the presence of these BCAAs inhibit l-norvaline's uptake into the cell by blocking system L transporters, the group responsible for transporting large, neutral amino acids such as BCAAs into the cell (Christensen, 1990). A decrease in uptake would be unlikely though given the very modest increase in the BCAA concentrations that produced the protective effects: for l-isoleucine and l-leucine the concentration was increased from 800 μM to 1000 μM and for l-valine 400 μM to 1000 μM. Competition during protein synthesis is another potential mechanism of protection. In fact, an *E.coli* based kinetic assay capable of identifying NPAAs that compromise the fidelity of protein synthesis has previously linked l-norvaline to l-leucine (Cvetesic et al., 2014). Cvetešić and colleagues found the protein elongation factor Tu binds l-norvaline to LeuRS with the same affinity as l-leucine in a step that may precede misincorporation (Cvetesic et al., 2013). A follow-up study identified l-norvaline as the prime physiological target of LeuRS proofreading (Cvetesic et al., 2014). L-norvaline is also a substrate for branched-chain aminotransferase (BCAT) which catalyses the conversion of BCAAs and α-ketoglutarate into branched chain-α- keto- acids and glutamate (Harper et al., 1984). Therefore we investigated whether the cytotoxic effects of l-norvaline were glutamate or Ca$^{2+}$- mediated and detected no significant changes to intracellular glutamate or Ca$^{2+}$ levels (Fig. 3A & B). L-norvaline has previously been found to incorporate into human recombinant hemoglobin expressed in *E. coli* in place of the BCAA l-leucine and the protection offered by BCAAs strongly suggests 'protein' amino acid mimicry as a mechanism of l-norvaline's cytotoxicity (Apostol et al., 1997). It is also worthwhile noting that the present studies are the first to investigate the BCAA mimicry of l-norvaline in a mammalian cell line.

Microscopy analysis of l-norvaline treated cells revealed marked morphological changes to mitochondria (Fig. 4) and detailed image analysis demonstrated a significant decrease in mitochondrial area and interconnectivity as well as increased elongation (Fig. 5). Lower interconnectivity scores are indicative of fragmentation and higher elongation scores indicate more abstract shapes (an elongation score of 1 would be a perfect circle) (Wiemerslage and Lee, 2016). Fragmentation contributes to mitochondrial dysfunction in diseases states such as Alzheimer's disease (AD) while elongation has been observed during cell cycle-mediated cell death in mouse neurons (Wang et al., 2014; DuBoff et al., 2012). Marked morphological changes such as these would be expected to result in mitochondrial dysfunction and a decrease in bioenergetics, however when we analysed mitochondrial respiration, non-mitochondrial respiration and ATP synthesis (Fig. 6) we found no significant changes suggesting the involvement of a secondary mechanism.

In mammalian cells l-norvaline stimulates NO production which triggers the generation of cGMP and indirectly fuels mitochondrial biogenesis, increasing respiration and ATP synthesis (Nisoli et al., 2004; Schwarz et al., 2004). To test if this secondary mechanism may have cancelled out the damaging effects of l-norvaline on mitochondrial function we repeated the analysis in the presence of the nitric oxide synthase inhibitor l-NAME. This allowed us to determine the effects of l-norvaline on mitochondrial bioenergetics independent of its action on the NO pathway. The observed decreases in basal and maximal respiration, ATP production and non-mitochondrial respiration in the presence of l-NAME are consistent with mitochondrial dysfunction and support the view that the NO pathway is compensating for this damage. This observation is particularly concerning given the association between mitochondrial dysfunction and many diseases, including neurodegeneration (Lin and Beal, 2006).

Metabolic dysfunction increases the risk of arginase overexpression and has been hypothesised to contribute to the development of Alzheimer's disease (AD) (Zhang et al., 2001; Sonntag et al., 2017).

Consequently, l-norvaline treatment has been studied in a mouse model of AD. A 6-week treatment of 40–50 mg/kg/day significantly improved memory deficits in 3xTransgenic mice and decreased protein aggregate formation in the cortex with no reported negative side effects (Polis et al., 2018). A 80 kg human would need to consume 3200–4000 mg/day, 10-fold higher than the current dosage, to achieve such effects and while the therapeutic potential of l-norvaline is promising, the results of the current study indicate that additional studies examining neurological function and aggregates in more detail may be warranted.

Despite presenting strong evidence of cytotoxicity and mitochondrial dysfunction, the exact mechanism whereby toxicity is elicited still is unclear, as is the primary cellular target of l-norvaline's toxic effects. Mitochondrial tRNAs consist of non-canonical cloverleaf structures and therefore mitochondrial proteins may be more susceptible to misincorporation than cytosolic proteins (Suzuki et al., 2011; Ye et al., 2015). Due to the structural differences between mitochondrial and cytosolic tRNAs, mitochondrial aminoacyl-tRNA synthetases (Mt aaRS) are often prone to incorrect aminoacylation. Consequently, mitochondrial proofreading and the discriminatory ability of Mt. aaRS are considered 'relaxed,' making them more susceptible to misincorporation (Ye et al., 2015). Given the absence of apoptotic and lysosomal changes, cell cycle arrest leading to necrotic cell death may also be a potential mechanism. This would result in positive toxicity results similar to those observed in the present study (Solhaug et al., 2012; Lee et al., 2007; Wang et al., 2016). We recommend future studies investigate the progression of the cell cycle following l-norvaline treatment and examine cells for nuclear or mitochondrial DNA damage that may initiate cell cycle arrest.

## 5. Conclusions

We have presented evidence of toxicity and mitochondrial dysfunction that question the safety of l-norvaline consumption and reaffirms the need to investigate the safety and efficacy of NPAAs that are analogues of protein amino acids. Furthermore, l-norvaline alone did not significantly alter ATP synthesis, contradicting its purported benefits and casting doubt on whether it should be consumed in the first place. This is especially relevant given that l-norvaline dietary supplementation has also been associated with reduced amino acid concentrations *in vivo* (Tews and Harper, 1986).

## References

Apostol, I., Levine, J., Lippincott, J., Leach, J., Hess, E., Glascock, C.B., Weickert, M.J., Blackmore, R., 1997. Incorporation of norvaline at leucine positions in recombinant human hemoglobin expressed in Escherichia coli. J. Biol. Chem. 272 (46), 28980–28988.

Bailey, R.L., Gahche, J.J., Lentino, C.V., Dwyer, J.T., Engel, J.S., Thomas, P.R., Betz, J.M., Sempos, C.T., Picciano, M.F., 2011. Dietary supplement use in the United States, 2003–2006. J. Nutr. 141 (2), 261–266.

Bell, E.A., 2003. Nonprotein amino acids of plants: significance in medicine, nutrition, and agriculture. J. Agric. Food Chem. 51 (10), 2854–2865.

Bertin, C., Weston, L.A., Huang, T., Jander, G., Owens, T., Meinwald, J., Schroeder, F.C., 2007. Grass roots chemistry: meta-Tyrosine, an herbicidal nonprotein amino acid. Proc. Natl. Acad. Sci. 104 (43), 16964–16,969.

Carvajal, N., Cederbaum, S.D., 1986. Kinetics of inhibition of rat liver and kidney arginases by proline and branched-chain amino acids. Biochim. Biophys. Acta Protein Struct. Mol. Enzymol. 870 (2), 181–184.

Chan, S.W., Dunlop, R.A., Rowe, A., Double, K.L., Rodgers, K.J., 2012. L-DOPA is incorporated into brain proteins of patients treated for Parkinson's disease, inducing toxicity in human neuroblastoma cells in vitro. Exp. Neurol. 238 (1), 29–37.

Christensen, H.N., 1990. Role of amino acid transport and countertransport in nutrition and metabolism. Physiol. Rev. 70 (1), 43–77.

Crick, F.H., Barnett, L., Brenner, S., Watts-Tobin, R.J., 1961. General nature of the genetic code for proteins. Nature 192 (4809), 1227–1232.

Cvetesic, N., Akmacic, I., Gruic-Sovulj, I., 2013. Lack of discrimination against non-proteinogenic amino acid norvaline by elongation factor Tu from. Croat. Chem. Acta 86 (1), 73–82.

Cvetesic, N., Palencia, A., Halasz, I., Cusack, S., Gruic-Sovulj, I., 2014. The physiological target for LeuRS translational quality control is norvaline. EMBO J. 33 (15), 1639–1653.

Cynober, L., 2013. Amino acid metabolism. In: Lane, W.J.L.D. (Ed.), Encyclopedia of

Biological Chemistry. Academic Press, Waltham, pp. 91–96.

Dagda, R.K., Cherra, S.J., 3rd, S.M. Kulich, Tandon, A., Park, D., Chu, C.T., 2009. Loss of PINK1 function promotes mitophagy through effects on oxidative stress and mitochondrial fission. J. Biol. Chem. 284 (20), 13843–13855.

De, A., Singh, M.F., Singh, V., Ram, V., Bisht, S., 2016. Treatment effect of l-Norvaline on the sexual performance of male rats with streptozotocin induced diabetes. Eur. J. Pharmacol. 771, 247–254.

DuBoff, B., Götz, J., Feany, Mel B., 2012. Tau promotes neurodegeneration via DRP1 mislocalization in vivo. Neuron 75 (4), 618–632.

El-Bassossy, H.M., El-Fawal, R., Fahmy, A., Watson, M.L., 2013. Arginase inhibition alleviates hypertension in the metabolic syndrome. Br. J. Pharmacol. 169 (3), 693–703.

Franek, F., Fismolova, I., Eckschlager, T., 2002. Antiapoptotic and proapoptotic action of various amino acids and analogs in starving MOLT-4 cells. Arch. Biochem. Biophys. 398 (1), 141–146.

Fujimoto, M., Kameji, T., Kanaya, A., Hagihira, H., 1976. Purification and properties of rat small intestinal arginase. J. Biochem. 79, 441–449.

Gansauge, S., Gansauge, F., Nussler, A.K., Rau, B., Poch, B., Schoenberg, M.H., Beger, H.G., 1997. Exogenous, but not endogenous, nitric oxide increases proliferation rates in senescent human fibroblasts. FEBS Lett. 410 (2), 160–164.

Gulati, D.K., Chambers, C.L., Rosenthal, G.A., Sabharwal, P.S., 1981. Comparative toxicity of some naturally occuring and synthetic non-protein amino acids. Environ. Exp. Bot. 21 (2), 225–230.

Hambræus, L., 2014. Protein and amino acids in human nutrition. In: Reference Module in Biomedical Sciences, (Elsevier).

Harper, A.E., Miller, R.H., Block, K.P., 1984. Branched-chain amino acid metabolism. Ann. Rev. Nutr. 4.

Häusler, R.E., Ludewig, F., Krueger, S., 2014. Amino acids – a life between metabolism and signalling. Plant Sci. 229, 225–237.

Hunter, A., Downs, C.E., 1945. The inhibition of arginase by amino acids. J. Biol. Chem. 157.

Karkhanis, V.A., Mascarenhas, A.P., Martinis, S.A., 2007. Amino acid toxicities of Escherichia coli that are prevented by leucyl-tRNA synthetase amino acid editing. J. Bacteriol. 189 (23), 8765–8768.

Kisumi, M., Sugiura, M., Kato, J., Chibata, I., 1976. L-Norvaline and L-homoisoleucine formation by Serratia marcescens. J. Biochem. 79 (5).

Laplante, M., Sabatini, D.M., 2009. mTOR signalling at a glance. J. Cell Sci. 122 (20), 3589.

Lee, S., Kim, S., Sun, X., Lee, J.H., Cho, H., 2007. Cell Cycle-Dependent Mitochondrial Biogenesis and Dynamics in Mammalian Cells. (0006-291× (Print)).

Lemon, P.W., 2000. Beyond the Zone: Protein Needs of Active Individuals. (0731–5724 (Print)).

Lin, M.T., Beal, M.F., 2006. Mitochondrial dysfunction and oxidative stress in neurodegenerative diseases. Nature 443 (7113), 787–795.

Ming, X.F., Barandier, C., Viswambharan, H., Kwak, B.R., Mach, F., Mazzolai, L., Hayoz, D., Ruffieux, J., Rusconi, S., Montani, J., Yang, Z., 2004. Thrombin stimulates human endothelial arginase enzymatic activity via RhoA/ROCK pathway: implications for atherosclerotic endothelial dysfunction. Circulation 110 (24).

Ming, X.F., J.M. Rajapakse Carvas, C.J. Jean, J. Ruffieux, Z. Yang, Inhibition of S6K1 accounts partially for the anti-inflammatory effects of the arginase inhibitor L-norvaline. 2009(1471–2261 (Electronic)).

Monte-Silva, K., Liebetanz, D., Grundey, J., Paulus, W., Nitsche, M.A., 2010. Dosage-Dependent Non-Linear Effect of L-Dopa on Human Motor Cortex Plasticity. (1469–7793 (Electronic)).

Nandi, P., Sen, G.P., 1953. An Antifungal Substance from a Strain of B. subtilis. Nature 172, 871.

Nisoli, E., Falcone, S., Tonello, C., Cozzi, V., Palomba, L., Fiorani, M., Pisconti, A., Brunelli, S., Cardile, A., Francolini, M., Cantoni, O., Carruba, M.O., Moncada, S., Clementi, E., 2004. Mitochondrial biogenesis by NO yields functionally active mitochondria in mammals. Proc. Natl. Acad. Sci. U. S. A. 101 (47), 16507.

Osowska, S., Moinard, C., Neveux, N., Loï, C., Cynober, L., 2004. Citrulline Increases Arginine Pools and Restores Nitrogen Balance After Massive Intestinal Resection. (0017–5749 (Print)).

Perl, A., 2016. Activation of mTOR (mechanistic target of rapamycin) in rheumatic diseases. Nat. Rev. Rheumatol. 12 (3), 169–182.

Polis, B., Srikanth, K.D., Elliott, E., Gil-Henn, H., Samson, A.O., 2018. L-norvaline reverses cognitive decline and synaptic loss in a murine model of Alzheimer's disease. Neurotherapeutics 15 (4), 1036–1054.

Rampersad, S.N., 2012. Multiple applications of Alamar Blue as an indicator of metabolic function and cellular health in cell viability bioassays. Sensors (Basel) 12 (9), 12347–12360.

Rodgers, K.J., Shiozawa, N., 2008. Misincorporation of amino acid analogues into proteins by biosynthesis. Int. J. Biochem. Cell Biol. 40 (8), 1452–1466.

Rosenthal, G.A., 2001. L-Canavanine: a higher plant insecticidal allelochemical. Amino Acids 21, 319–330.

Schindelin, J., Arganda-Carreras, I., Frise, E., Kaynig, V., Longair, M., Pietzsch, T., Preibisch, S., Rueden, C., Saalfeld, S., Schmid, B., Tinevez, J.Y., White, D.J., Hartenstein, V., Eliceiri, K., Tomancak, P., Cardona, A., 2012. Fiji: an open-source platform for biological-image analysis. Nat. Methods 9 (7), 676–682.

Schwarz, K.R., Pires, P.R., Mesquita, L.G., Chiaratti, M.R., Leal, C.L., 2004. Effect of nitric oxide on the cyclic guanosine monophosphate (cGMP) pathway during meiosis resumption in bovine oocytes. (1879–3231 (Electronic)).

Sharp, D.P.M., Pearson, D.R., 2010. Amino Acids supplements and recovery from high-intensity resistance training. J. Strength Cond. 24 (4).

Smith, P.K., Krohn, R.I., Hermanson, G.T., Mallia, A.K., Gartner, F.H., Provenzano, M.D., Fujimoto, E.K., Goeke, N.M., Olson, B.J., Klenk, D.C., 1985. Measurement of protein using bicinchoninic acid. Anal. Biochem. 150 (1), 76–85.

Sobolev, M.S., Faitelson, A.V., Gudyrev, O.S., Rajkumar, D.S.R., Dubrovin, G.M., Anikanov, A.V., Koklina, N.U., Chernomortseva, E.S., 2018. Study of endothelio- and osteoprotective effects of combination of rosuvastatin with L-norvaline in experiment. J. Osteoporos. 2018, 1585749.

Solhaug, A., Vines, L.L., Ivanova, L., Spilsberg, B., Holme, J.A., Pestka, J., Collins, A., Eriksen, G.S., 2012. Mechanisms involved in alternariol-induced cell cycle arrest. Mutat. Res./Fundam. Mol. Mech. Mutagen. 738 (739), 1–11.

Song, Y., Zhou, H., Vo, M.N., Shi, Y., Nawaz, M.H., Vargas-Rodriguez, O., Diedrich, J.K., Yates, J.R., Kishi, S., Musier-Forsyth, K., Schimmel, P., 2017. Double mimicry evades tRNA synthetase editing by toxic vegetable-sourced non-proteinogenic amino acid. Nat. Commun. 8 (1), 2281.

Sonntag, K.C., Ryu, W.I., Amirault, K.M., Healy, R.A., Siegel, A.J., McPhie, D.L., Forester, B., Cohen, B.M., 2017. Late-onset Alzheimer's disease is associated with inherent changes in bioenergetics profiles. Sci. Rep. 7 (1), 14038.

Suzuki, T., Nagao, A., Suzuki, T., 2011. Human mitochondrial tRNAs: biogenesis, function, structural aspects, and diseases. Annu. Rev. Genet. 45 (1), 299–329.

Tews, J.K., Harper, A.E., 1986. Tissue amino acids in rats fed norleucine, norvaline, homoarginine or other amino acid analogues. J. Nutr. 116 (8), 1464–1472.

Thompson, J.F., Morris, C.J., Smith, I.K., 1969. New naturally occurring amino acids. Annu. Rev. Biochem. 38 (1), 137–158.

Vickery, H.B., Schmidt, C.L.A., 1931. The history of the discovery of the amino acids. Chem. Rev. 9 (2), 169–318.

Wang, X., Wang, W., Li, L., Perry, G., Lee, H.-g., Zhu, X., 2014. Oxidative stress and mitochondrial dysfunction in Alzheimer's disease. Biochim. Biophys. Acta (BBA) – Mol. Basis Dis. 1842 (8), 1240–1247.

Wang, L., Zhang, X., Cui, G., Chan, J.Y.-W., Wang, L., Li, C., Shan, L., Xu, C., Zhang, Q., Wang, Y., Di, L., Lee, S.M.-Y., 2016. A novel agent exerts antitumor activity in breast cancer cells by targeting mitochondrial complex II. Oncotarget 7 (22), 32054–32,064.

Wiemerslage, L., Lee, D., 2016. Quantification of mitochondrial morphology in neurites of dopaminergic neurons using multiple parameters. J. Neurosci. Methods 262, 56–65.

Wu, G., 2009. Amino acids: metabolism, functions, and nutrition. Amino Acids 37 (1), 1–17.

Yamazaki, M., Chiba, K., 2006. Expression of Functional Nitric Oxide Synthase for Neuritogenesis in PC12h Cells. J. Health Sci. 52 (6).

Ye, Q., Wang, M., Fang, Z.P., Ruan, Z.R., Ji, Q.Q., Zhou, X.L., Wang, E.D., 2015. Degenerate connective polypeptide 1 (CP1) domain from human mitochondrial leucyl-tRNA synthetase. J. Biol. Chem. 290 (40), 24391–24402.

Zhang, C., Hein, T.W., Wang, W., Chang, C.I., Kuo, L., 2001. Constitutive expression of arginase in microvascular endothelial cells counteracts nitric oxide-mediated vasodilatory function 1. FASEB J. 15 (7), 1264–1266.

Zhang, S., Zeng, X., Ren, M., Mao, X., Qiao, S., 2017. Novel metabolic and physiological functions of branched chain amino acids: a review. J. Anim. Sci. Biotechnol. 8, 10.

58

# Chapter Four:

Investigation into L-azetidine-2-carboxylic

acid toxicity

# CHAPTER FOUR: INVESTIGATION INTO L-AZETIDINE-2-CARBOXYLIC ACID TOXICITY

**Compound Abstract**

The previous two chapters highlighted the need to investigate commonly consumed NPAAs for evidence of toxicity to human cells and mitochondrial dysfunction, identifying that the supplement L-norvaline was cytotoxic and induced mitochondrial morphological and bioenergetic changes. This chapter performs the same investigation on another frequently ingested NPAA, L-azetidine-2-carboxylic acid. This chapter was published in the journal *Amino Acids*.

**Certificate of Authorship and Originality**

This paper was published in *Amino Acids*. The following is a copy reprinted with permission from Springer-Verlag GmbH Austria, part of Springer Nature © 2019. I certify that the work present in chapter four of this thesis has not been previously submitted as part of the requirements for a degree. I also certify that I carried out all the experimental work, analysis and interpretation of the data presented in this paper.

The remaining author listed on this manuscript contributed in the following way:

- Kenneth Rodgers: Assisted in experimental design, manuscript direction and proofreading

Principal Supervisor                                   Student

Kenneth Rodgers                                        Kate Samardzic

Production Note:                                       Production Note:
Signature removed                                      Signature removed
prior to publication.                                  prior to publication.

Signature                                              Signature

11/12/2019                                             16/06/2020

Date                                                   Date

**ORIGINAL ARTICLE**

# Cell death and mitochondrial dysfunction induced by the dietary non-proteinogenic amino acid L-azetidine-2-carboxylic acid (Aze)

Kate Samardzic[1] · Kenneth J. Rodgers[1]

## Abstract

In addition to the 20 protein amino acids that are vital to human health, hundreds of naturally occurring amino acids, known as non-proteinogenic amino acids (NPAAs), exist and can enter the human food chain. Some NPAAs are toxic through their ability to mimic protein amino acids and this property is utilised by NPAA-containing plants to inhibit the growth of other plants or kill herbivores. The NPAA L-azetidine-2-carboxylic acid (Aze) enters the food chain through the use of sugar beet (*Beta vulgaris*) by-products as feed in the livestock industry and may also be found in sugar beet by-product fibre supplements. Aze mimics the protein amino acid L-proline and readily misincorporates into proteins. In light of this, we examined the toxicity of Aze to mammalian cells in vitro. We showed decreased viability in Aze-exposed cells with both apoptotic and necrotic cell death. This was accompanied by alterations in endosomal–lysosomal activity, changes to mitochondrial morphology and a significant decline in mitochondrial function. In summary, the results show that Aze exposure can lead to deleterious effects on human neuron-like cells and highlight the importance of monitoring human Aze consumption via the food chain.

**Keywords** Non-protein amino acid · Azetidine-2-carboxylic acid · Mitochondria · Multiple sclerosis

## Introduction

Hundreds of non-proteinogenic amino acids (NPAAs) exist in nature and fulfil diverse biological roles. Less common than their protein amino acid counterparts, yet more abundant, NPAAs have historically been overlooked in favour of research into the biological roles of the protein-encoded amino acids. As secondary metabolites in plants, NPAAs are not essential to normal growth, development or reproduction. In fact, in some cases, their role in plants is much more sinister and NPAAs are thought to have evolved to protect plants from the attacks of predators, pathogens, or

to adversely affect competing plants (Bertin et al. 2007; Rosenthal 2001). This phenomenon arises from the structural similarity of some NPAAs to protein amino acids, and as such, they are termed amino acid analogues (Thompson et al. 1969). NPAAs that are known to inhibit biological processes are close structural analogues of protein amino acids. This structural similarity to their respective corresponding protein amino acids has been attributed to their toxicity through a process dubbed protein 'misincorporation' or amino acid 'mimicry' (Song et al. 2017), where the NPAAs are mistakenly utilised in protein synthesis with the error resulting in potentially deleterious effects (Rodgers and Shiozawa 2008; Dunlop et al. 2011). Several other amino acid analogues have been shown to misincorporate in place of their parent amino acid (Rodgers and Shiozawa 2008) and among them is the NPAA L-azetidine-2-carboxylic acid (Aze) (Alescio 1973). Misincorporation is a random process in which the NPAA competes with a protein amino acid for charging to the transfer RNA (Rodgers 2014). The NPAA can then be inserted into any newly synthesised proteins encoded for that protein amino acid provided it can by-pass the proof-reading process (Song et al. 2017).

✉ Kenneth J. Rodgers
  kenneth.rodgers@uts.edu.au

1   Neurotoxin Research Group, School of Life Sciences
    (04.06.340), University of Technology, Harris Street,
    Sydney, NSW 2007, Australia

Aze is produced by sugar beets (*Beta vulgaris*) and lilies (*Convallaria majalis*) and is a structural analogue of the protein-encoded amino acid L-proline (Fig. 1) (Fowden 1956, 1972). While the Aze containing lily also contains acutely toxic cardiac glycosides and, therefore, eschews human consumption (Löffelhardt et al. 1979), sugar beets do provide an avenue for human exposure to Aze. Even though sugar beets themselves are rarely consumed in quantities that would warrant concern over Aze exposure, over 250 million tonnes of sugar beets are grown annually worldwide (FAO 2014). Such large quantities are demanded due to the role of sugar beets as the starting material for approximately 20% of the world's commercial sugar production (FAO 2014). Aze containing by-products of this process, known as sugar beet pulp or fibre, are used primarily as feed for livestock and as human dietary fibre supplements (Harland et al. 2009; Golini et al. 2017; Habeeb et al. 2017). In addition to concerns over direct human exposure, humans may be indirectly exposed to Aze through bioaccumulation in dairy and meat products (Rubenstein et al. 2009). Rubenstein et al. (2006) detected Aze in four varieties of garden beets at a ratio of 1–5% Aze to L-proline, which based on the current US National Nutrient Database findings would relate to 0.49–2.45 mg Aze per cup (246 g) of beets consumed (Rubenstein et al. 2006). Rubenstein et al. (2009) also quantified Aze concentration in sugar beet by-products, detecting up to 0.34 mg/100 mg.

Since Aze was first discovered in plants in the 1950s, there has been much speculation about its ability to mimic protein amino acids and thereby exert a toxic effect in humans. A known plant toxin, the ability of Aze to incorporate in place of L-proline has been shown in multiple plant models (Vaughan et al. 1974; Lee et al. 1996). In addition, Lee et al. (1996) found that 5 mM Aze treatment induced a heat shock-like response, which is often produced by cells in response to abnormal protein synthesis (Rodgers et al. 2009). Aze incorporates into the L-proline-rich myelin basic protein of *Escherichia coli* (*E. coli*) and is toxic to chick embryos due to incorrectly formed collagen, another L-proline-rich protein (Bessonov et al. 2010; Lane et al. 1970; Fraser and Deber 1985). These findings are particularly pertinent to humans, since the worldwide distribution of the neurodegenerative disorder multiple sclerosis (MS) correlates with regions of high sugar beet production (Poskanzer et al. 1980;

Karni et al. 2003; Sarasoja et al. 2004; Beck et al. 2005; Rubenstein 2008). MS is a demyelinating condition and the loss of myelin basic protein function is known to trigger this process. Given that Aze is capable of misincorporating into myelin basic protein and the potential for both direct and indirect human consumption, the present study aims to examine the effect of Aze on the viability and function of human neuroblastoma cells.

## Materials and methods

### Reagents

Dulbecco's Modified Eagle's Medium (DMEM), Eagle's Minimal Essential Medium (EMEM, deficient in L-proline), and L-azetidine-2-carboxylic acid were from Sigma Chemical Co., St Louis, MO. All aqueous solutions and buffers were prepared using 18 mU water. All the other chemicals and solvents were of cell-culture grade.

### Cell culture

SH-SY5Y human neuroblastoma cells (American Tissue Culture Collection, catalogue number CRL-2266) were cultured as follows; DMEM was supplemented with 10% heat-inactivated Foetal Bovine Serum (FBS) (US origin, Gibco Carlsbad, CA, USA), and 100 X GlutaMAX (Thermo Fisher Scientific, Waltham, MA, USA). Cells were maintained at 37 °C with 5% $CO_2$ in 175 $cm^2$ flasks until they were plated for specific experiments. During treatment, DMEM culture medium was substituted with L-proline deficient EMEM. Experiments were performed between passages 17 and 26.

### Cell viability

Cells were plated in 96 well plates at 30,000 cells/well, allowed to adhere overnight and then treated in triplicate with the following concentrations of Aze: 125 μM, 250 μM, 500 μM, 1000 μM, and 2000 μM. Cells were treated for 24 h and then incubated with 10% Alamar Blue cell viability reagent (Thermo Fisher) for 2 h. Fluorescence was read at ex 570/em 585. Protein concentration was determined with the bicinchoninic acid (BCA) assay (Smith et al. 1985) and fluorescence was normalised to protein concentration.

### Live cell imaging cell viability time course

Cells were plated into 24 well plates at 60,000 cells/well, allowed to adhere overnight, then stained with Hoechst 33258 nuclei stain for 15 min and treated in duplicate with Aze at 500 μM and 2000 μM in EMEM containing propidium iodide (PI) and placed in a microscope-heated chamber
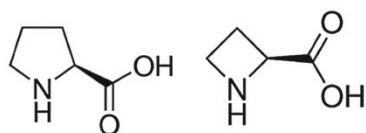


**Fig. 1** Structural representations of the protein amino acid L-proline and the non-proteinogenic amino acid (NPAA) L-azetidine-2-carboxylic acid (Aze)

62

warmed to 37 °C with 5% $CO_2$. Images were captured with a high-speed charge-coupled device (CCD) camera using the NIS-Elements acquisition software mounted on a Nikon Ti inverted fluorescence microscope equipped with 20X objective lens (Plan Apo NA 1.4 aperture) and the Perfect Focus System™ for continuous maintenance of focus. Hoechst was monitored with a bandpass 470 emission filter and PI was monitored at emission 636. Time-lapse images were collected every 30 min over a 24 h period with two fields of view from each well imaged. Exposure time and brightness/contrast setting were kept constant for each using the NIS-Elements acquisition software. Images were analysed in FIJI (Schindelin et al. 2012) following background subtraction with a rolling ball radius. PI staining was measured using the mean grey value and fluorescence was normalised to the number of Hoechst positive nuclei.

### Acidic vesicle activity

Cells were plated into 24 well plates at 60,000 cells/well, allowed to adhere overnight, and then stained with Hoechst 33258 nuclei stain as above. The acidotropic dye LysoTracker Red DND-99 was then diluted in EMEM containing Aze at 2000 µM and added to wells in triplicate. The plate was then placed in a microscope-heated chamber warmed to 37 °C with 5% $CO_2$ and images were then captured using the Nikon Ti and NIS-Elements at emission 470 for Hoechst 33258 and emission 636 for LysoTracker Red DND-99. Time-lapse images were collected every 30 min over a 24 h period with 2 fields of view from each well imaged. Exposure time and brightness/contrast setting were kept constant for each using the NIS-Elements acquisition software. Images were analysed in FIJI following background subtraction with a rolling ball radius. Acid vesicle intensity was measured using the mean grey value of LysoTracker uptake and fluorescence was normalised to the number of Hoechst positive nuclei.

### Cathepsin B activity

The activity of the lysosomal cysteine protease cathepsin B (CatB) was measured by the linear increase in fluorescence following the cleavage of 7-amino-4-methylcoumarin (AMC) from the peptide substrate Z-Arg-Arg-AMC (where z is benzyloxycarbonyl) [as described in Dunlop Rachael et al. (2008)]. Briefly, cells were subcultured onto 6 well plates at 400,000 cells/well and treated in triplicate with 2000 µM Aze in EMEM for 24 h. Cultures were washed three times in phosphate-buffered saline (PBS) and harvested by scraping into 200 µL of cathepsin assay buffer [0.1 M phosphate buffer (pH 6) containing 5 mM EDTA, 0.005% Brij 30, 1 µM pepstatin A and 5 mM benzamidine]. Cells underwent three freeze/thaw cycles and then lysates

were centrifuged at $10,000 \times g$ for 10 min to remove particulates. A 20 µL aliquot of the supernatant was activated with dithiothreitol (DTT) (final concentration 2.5 mM) and assay buffer wad added, in triplicate, to a 96 well plate. Following addition of 50 µM substrate, changes in fluorescence (ex 360/em 460) were measured every 1 min for 29 min. Results were normalised to protein concentration using a BCA assay and activity was expressed as the change in fluorescence over time ($\Delta F/t$).

### Apoptotic activity

The apoptotic activity of cells was determined using the Annexin V-fluorescein isothiocyanate (FITC) Apoptosis Detection Kit (Abcam, Cambridge, UK) as recommended by the manufacturer. Cells were plated into 24 well plates at 60,000 cells/well, allowed to adhere overnight, and then stained with Hoechst 33258 nuclei stain as above. The Annexin V-FITC was then diluted in EMEM containing Aze at 2000 µM and added to wells in duplicate. The plate was then placed in a microscope-heated chamber warmed to 37 °C with 5% $CO_2$ and images were then captured as above.

### Mitochondrial morphology

To examine mitochondrial morphology, cells were seeded on sterile glass coverslips that were placed in 12 well plates. The next day, the cells were treated with 2000 µM Aze. At 24 h post-treatment, the cells were fixed with 2% paraformaldehyde for 20 min, quenched in 100 mM glycine for 5 min, blocked in 2% bovine serum albumin (BSA) in PBS for 1 h, permeabilised in 0.5% Triton X-100 for 5 min, and incubated with mitochondrial mouse monoclonal antibody MTC02 (Abcam) overnight at 4 °C. Next, the cells were incubated with a mouse secondary antibody conjugated to CF488A for 1 h at RT in the dark, followed by 4',6-diamidino-2-phenylindole (DAPI) nucleic acid stain (Thermo Fisher) for 5 min. Slides were then prepared with one drop of Dako and sealed using nail varnish. Images were obtained at 60× using a DeltaVision Elite microscope and the DAPI and FITC channels. Images were analysed in FIJI using the macro Mito Morphology (Dagda et al. 2009). Briefly, the green channel of cells stained with the anti-mitochondria antibody was extracted to greyscale, inverted to show mitochondria-specific fluorescence as black pixels, and thresholded to optimally resolve all individual mitochondria per cell. The macro-traced mitochondrial outlines using "analyse particles." The area measurement refers to the average area of all mitochondria analysed per cell and the mean area/perimeter ratio was employed as an index of mitochondrial interconnectivity. Mitochondrial elongation was measured as inverse circularity. For each condition, a total of 81 cells

were measured from three independent experiments (27 each).

## Mitochondrial bioenergetics

A mitochondrial bioenergetics analysis was performed by measuring the oxygen consumption rate (OCR) of cultured cells using the Seahorse XFe24 Extracellular Flux analyser (Agilent, Santa Clara, CA, USA). Cells were plated at 30,000 cells/well and left overnight to adhere. Cells were then treated with Aze at 2000 μM for 24 h. The Mito Stress Test (Agilent) was then performed according to manufacturer's instructions. Cells were then washed in Seahorse assay media and prepared using the manufacturer's protocol and kit reagents [oligomycin (1 μM), FCCP (1 μM) and antimycin A/rotenone (0.5 μM)]. OCR values were normalised to protein concentration using the BCA assay. Basal respiration, maximal respiration, ATP production, and non-mitochondrial respiration were then calculated using the Seahorse XF Cell Mito Stress Test Report Generator. Calculations are as follows: non-mitochondrial respiration equates to the minimum rate measurement after antimycin A/rotenone injection, basal respiration equates to last rate measurement before oligomycin injection subtracted from non-mitochondrial respiration, maximal respiration equates to maximum rate measurement after FCCP injection subtracted from non-mitochondrial respiration, and ATP production equates to last rate measurement before oligomycin injection subtracted from the minimum rate after oligomycin injection.

## Statistical analysis

Statistical analyses were evaluated using GraphPad software (CA, USA) Prism 7 version 7.03 using either one- or two-way ANOVA with Dunnett's multiple comparison post-tests to compare replicate means between different treatments across the samples or Welch's $t$ test. Differences were considered significant at $P < 0.05$.

## Results

### Exposure of SH-SY5Y cells to Aze caused a decrease in cell viability

Cell viability was assessed in SH-SY5Y cells over a range of Aze concentrations for 24 h using the Alamar Blue assay (Fig. 2a). Cell viability was unchanged at concentrations up to 1000 μM Aze, but decreased to 65% at 2000 μM Aze ($P < 0.0001$).

## Time course of Aze-induced necrosis in live cells

To determine the time course of Aze-induced toxicity, we examined the uptake of PI on live cells treated with Aze (500 and 2000 μM) over a 24 h period (Fig. 2b). PI uptake is indicative of irreversible cell membrane damage and necrotic cell death. At 2000 μM Aze, there were significant increases in PI uptake relative to untreated cells after 12 h, 18 h ($P < 0.05$), and 24 h ($P < 0.01$). An increase in necrotic cell death relative to the control cells was not seen in cells treated with 500 μM Aze. The full-time course and representative images are included within the Electronic Supplementary Material (Supplementary Figures 1 and 2)

## Lysotracker intensity is increased by Aze exposure, while lysosomal protease CatB activity decreased

The fluorescence intensity of acidic bodies in the cell was monitored over 24 h of exposure to 2000 μM Aze using the dye LysoTracker Red DND-99. Fluorescence microscopy was used to visualise the acidic vesicles (Supplementary Figure 3) and fluorescence intensity of the images was then analysed using the software FIJI (Fig. 2c). Aze treatment significantly increased Lysotracker intensity compared to the untreated cells after 18 h ($P < 0.01$) and 24 h ($P < 0.0001$). CatB activity was measured directly through the cleavage of a fluorescent substrate peptide (Fig. 2e) and small, but significant decrease in activity was observed in cells treated with 2000 μM Aze for 24 h ($P < 0.0001$).

### Aze exposure leads to apoptotic cell death

The apoptotic activity of cells was monitored over 24 h of Aze (2000 μM) treatment using Annexin V-FITC. Fluorescence microscopy and FIJI software were used to visualise and analyse fluorescence (Fig. 2d). The fluorescence intensity of Annexin V-FITC was significantly increased 18 and 24 h after Aze treatment ($P < 0.0001$), indicating an increase in apoptotic cell death. Representative images are included in the Electronic Supplementary Material (Supplementary Figure 4).

### Aze induces morphological changes to mitochondria

Mitochondrial morphology following treatment with Aze at 2000 μM was assessed using fluorescence microscopy (Fig. 3a–d). Morphological changes pertaining to mitochondrial shape, size, and connectivity were quantified using FIJI software and the macro Mito Morphology. Following Aze treatment, the number of mitochondria per cell significantly decreased by 13.1% ($P < 0.05$) (Fig. 4a) and mitochondrial area
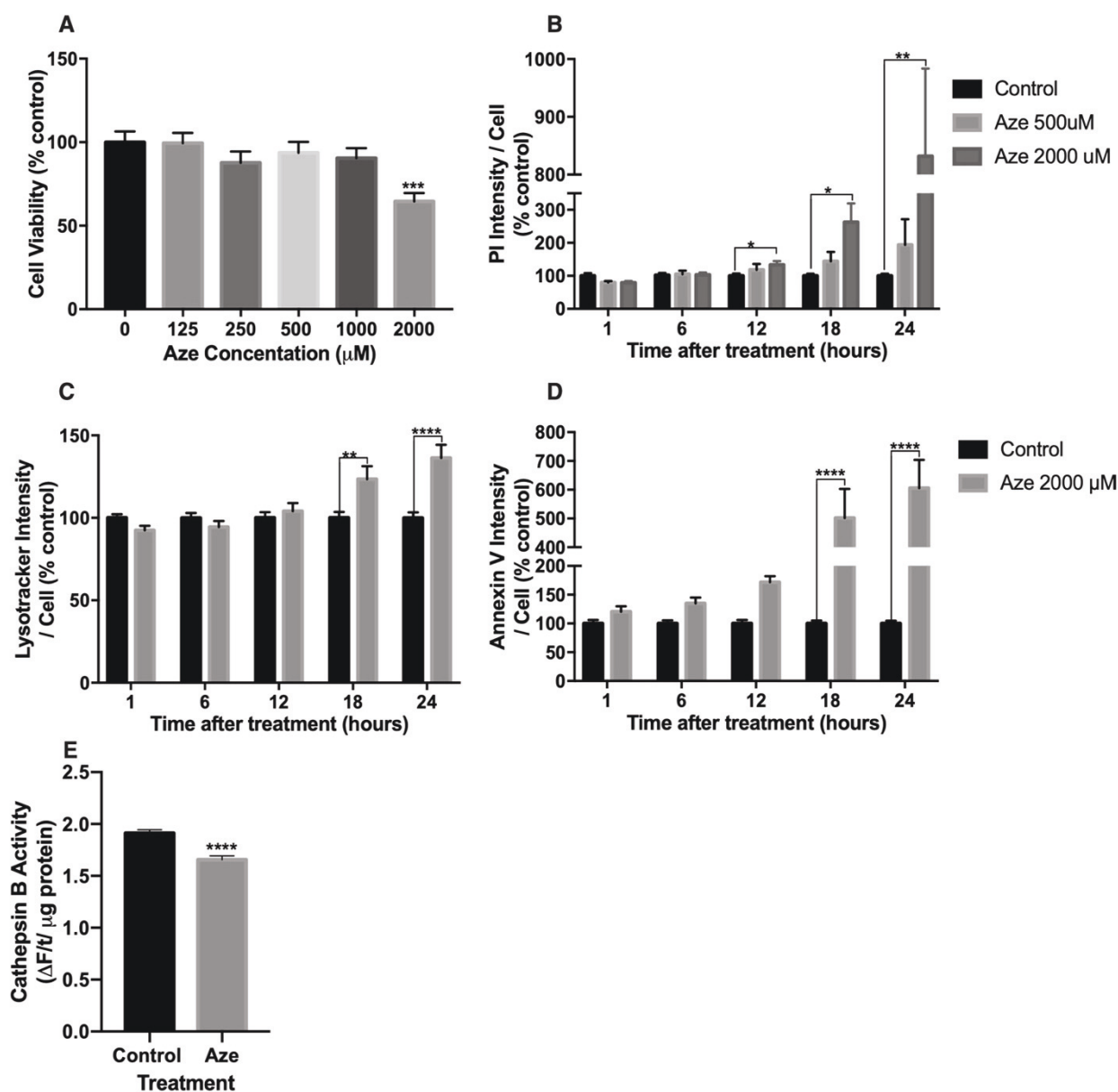
**Fig. 2** Effects of Aze treatment on SH-SY5Y neuroblastoma cells: **a** cells were exposed to a range of Aze concentrations and viability after 24 h was measured using the Alamar Blue assay; **b** cell viability as a measure of propidium iodide fluorescence intensity measured over 24 h of Aze treatment using live cell imaging; **c** Lysotracker Red DND-9 staining measured over 24 h of Aze treatment using live cell imaging; **d** Annexin V fluorescent intensity measured over 24 h of Aze treatment using live cell imaging; **e** cathepsin B activity following 24 h treatment with 2000 μM Aze, expressed as a change in fluorescence over time per μg cell protein ($\Delta F/t$). $N = 3$. Error bars show SEM with significance relative to control represented by *$P < 0.05$, **$P < 0.01$, ***$P < 0.001$, ****$P < 0.0001$

decreased by 17.7% ($P < 0.001$) (Fig. 4b). The mitochondrial elongation score was not affected (Fig. 4c) and mitochondrial interconnectivity significantly decreased by 6.6% ($P < 0.001$) (Fig. 4d).

## Mitochondrial bioenergetics are affected by Aze treatment

Mitochondrial bioenergetics were analysed by measuring OCR after 24 h of Aze treatment at 2000 μM (Fig. 5a).

**Fig. 3** Fluorescence microscopy images (×60 magnification) of the effects of 2000 μM Aze on SH-SY5Y cell mitochondria following 24 h treatment. Cells were stained with an anti-mitochondria antibody (green) and nuclei visualised using DAPI (blue). **a** Control; **b** magnified image of white box in **a**; **c** Aze treated cells; **d** magnified image of white box in **c**. Scale bar 10 μm for **a** and **c**
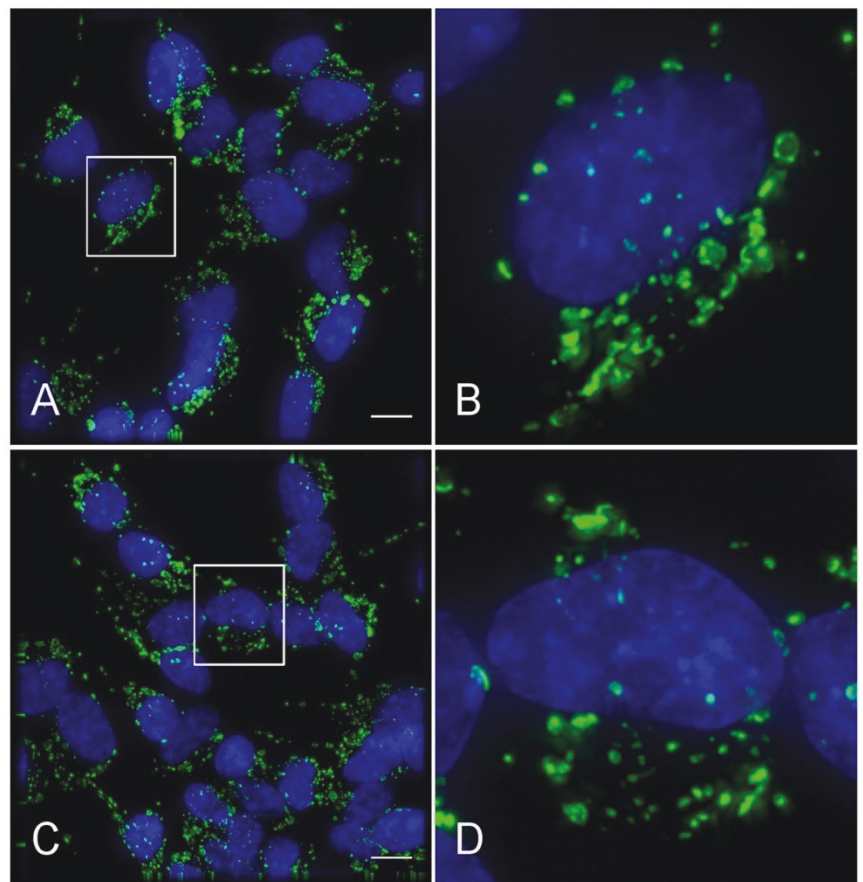


**Fig. 4** Comparison of mitochondrial morphology in Aze 2000 μM treated SH-SY5Y neuroblastoma cells and control cells after 24 h. **a** Mitochondrial number; **b** mitochondrial area; **c** mitochondrial elongation score; **d** mitochondrial interconnectivity score. $N=3$. Error bars show SEM with significance relative to control represented by $*P < 0.05$, $**P < 0.01$, $***P < 0.001$
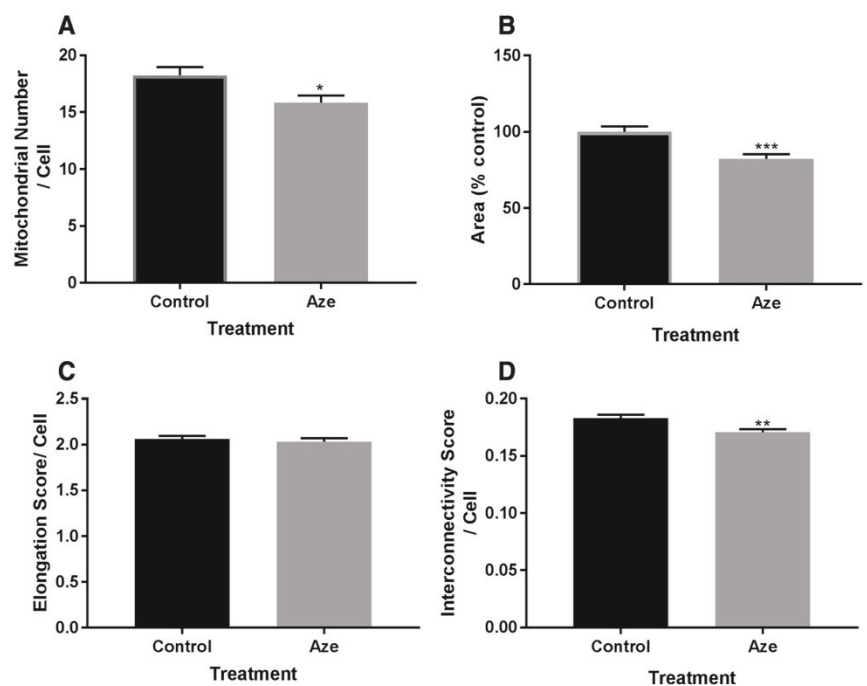
Fig. 5 Mitochondrial bioenergetics of SH-SY5Y neuroblastoma cells following 2000 μM Aze treatment for 24 h. **a** Oxygen consumption rate (OCR) measured using the Seahorse XFe24 analyser with oligomycin, FFCP and antimycin A/rotenone injections; **b** basal respiration; **c** maximal respiration; **d** ATP production; **e** non-mitochondrial respiration. $N = 3$. Error bars show SEM with significance relative to control represented by $*P < 0.05$, $***P < 0.001$



## Discussion
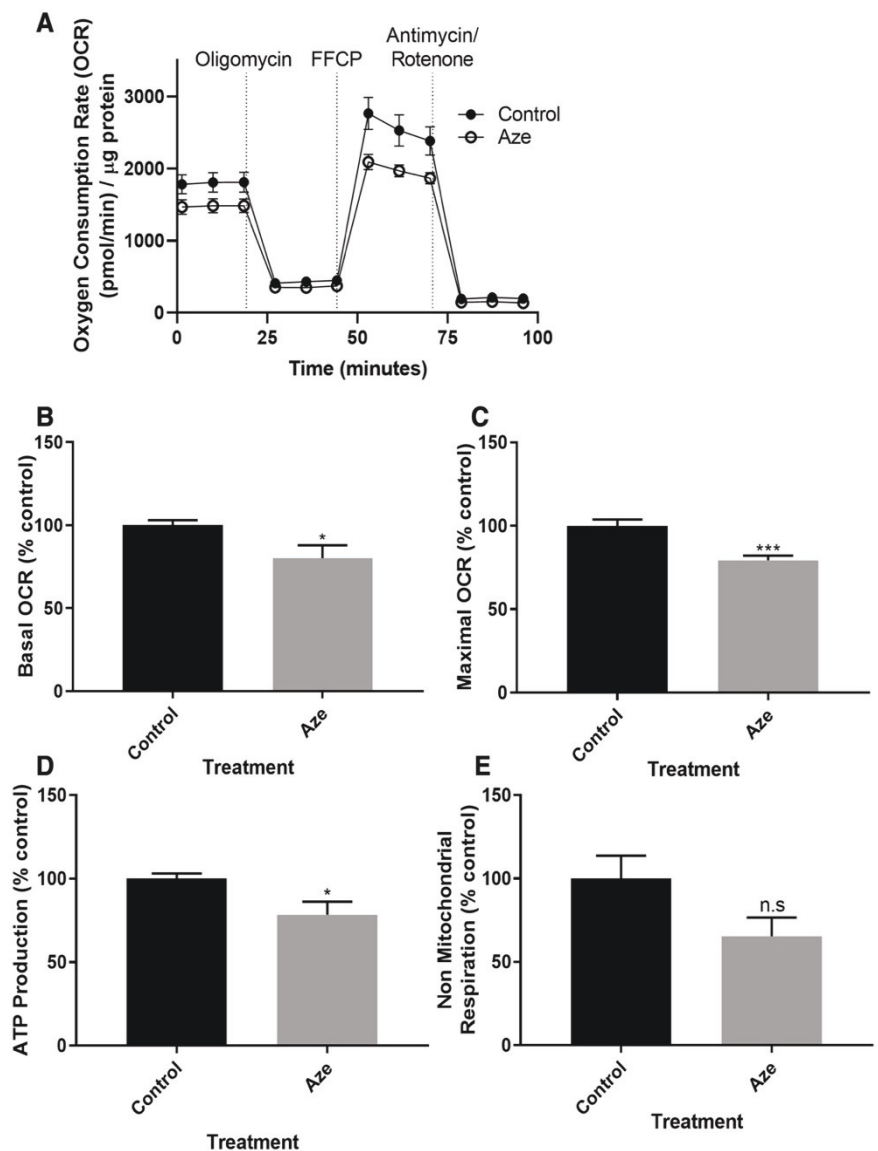
Basal respiration (Fig. 5b), which is the oxygen consumption used to meet cellular adenosine triphosphate (ATP) demand under baseline conditions, was significantly decreased by 19.8% ($P < 0.05$). Maximal respiration (Fig. 5c), which is the maximal oxygen consumption rate attained following addition of the uncoupler FCCP, decreased by 20.7% ($P < 0.001$). ATP production is derived from the decrease in oxygen consumption following oligomycin injection and shows the portion of basal respiration used to drive mitochondrial ATP production. This was also significantly affected with a decrease of 21.5% ($P < 0.05$) (Fig. 5d). The oxygen consumption that persists following antimycin A/rotenone injection, termed non-mitochondrial respiration, was unaffected (Fig. 5e).

In the present studies, we observed significant decreases in SH-SY5Y cell viability after exposure to 2000 μM Aze for 24 h (Fig. 2a). The toxicity was similar to that previously reported in HeLa cells (Song et al. 2017) and it is worthwhile noting that in the study by Song et al., the toxicity induced by 5000 μM Aze was rescued using the structural analogue L-proline at 1000 μM, but protein amino acids with no structural similarity to L-proline did not provide any protection (Song et al. 2017). A cell viability time course, employing continuous live cell imaging, demonstrated Aze toxicity in mammalian cells as early as 12 h of Aze treatment (Fig. 2b). In a similar study by Roest et al., much higher

concentrations (10–25 mM) of Aze were required to induce cell death in HeLa cells at similar timepoints (Roest et al. 2018). The previously reported length of time required for Aze incorporation in *E. coli* was 3 h (Grant et al. 1975). Mammalian cell studies using the NPAA beta-methylamino-L-alanine (BMAA) reported an exponential increase in protein bound $^3$H BMAA within 9 and 16 h treatment periods and this was accompanied by apoptotic but not necrotic cell death (Main et al. 2018; Dunlop et al. 2013).

Our data are consistent with a delayed cytotoxic response due to the synthesis and accumulation of non-native proteins. Aze is a weak competitor for prolyl aminoacyl-tRNA synthetase and can become randomly incorporated into newly synthesised proteins (Rodgers and Shiozawa 2008). The consequences of this could be loss of protein function or alteration in protein structure. In some cases, misfolded proteins are rapidly degraded, but they can also resist degradation and form aggregates, possibly through the interaction of exposed hydrophobic regions (Dunlop Rachael et al. 2008). Protein aggregates are known to be cytotoxic (Bucciantini et al. 2002). Significant conformational changes to protein structure are caused by Aze insertion, and these are discussed in detail elsewhere (Zagari et al. 1990, 1994; Rubenstein 2008). Interestingly, Aze-containing peptides may be oxygenated by prolyl hydroxylases resulting in potential damage of the protein by a reverse aldol of the hydroxyazetidine (Liu et al. 2015), contributing further to the deleterious effects of Aze. Despite the low rate of Aze for L-proline substitution, adverse effects of Aze have been reported in plants (Fowden 1963; Verbruggen et al. 1992; Lee et al. 2016a), algae (Kim et al. 2006) and in vivo models (Lane et al. 1970; Rojkind 1973; Joneja 1981) and occur even in the presence of normal L-proline production (Fichman et al. 2015).

Since Aze can be incorporated into certain proteins in place of L-proline, we then examined the cells to determine if they were responding to an increased load of non-native proteins. Consistent with this, the fluorescence intensity of acidic vesicles detected by the Lysotracker dye significantly increased following 18 h of Aze treatment when compared to control cells (Fig. 2c). A further increase was observed after 24 h exposure. The accumulation of the Lysotracker dye represents expansion of acidified compartments such as late endosomal or lysosomal organelles (Huotari and Helenius 2011). As one of the major systems for the degradation of misfolded proteins, protein aggregates, or damaged organelles (Ciechanover and Kwon 2015), an increase in the activity of the endosomal–lysosomal system may be in response to proteins containing misincorporated Aze. The activity of the lysosomal protease CatB, however, showed a small but significant decrease following Aze treatment (Fig. 2e). It has previously been reported that the activity of the lysosomal proteinases can be adversely affected by

the rapid delivery of damaged or aggregated proteins to the endosomal–lysosomal system (Rodgers et al. 2004). Cells can then respond by an increase in cathepsin delivery to lysosomes resulting in a rapid increase in lysosomal protease activity (Rodgers et al. 2004). Inhibition of cathepsins has previously been shown to increase Lysotracker staining due to the accumulation of immature cathepsins, reducing the degradative ability of lysosomes and resulting in apoptosis (Jung et al. 2015). Jung et al. reported an increase in the levels of the autophagy marker lipidated microtubule-associated protein light-chain 3 (LC3-II), independent of cathepsin activation, which is consistent with the previous findings that Aze treatment elevates LC-II (Roest et al. 2018). We hypothesise that the accumulation of misfolded Aze-containing proteins impairs lysosomal function and this can also contribute to cell death.

To examine if programmed cell death played a role in the decline in viability we observed, cells were stained with the apoptosis marker Annexin V. On treatment with Aze the intensity of Annexin V staining gradually increased, and was significantly elevated after 18 h (Fig. 2d). Annexin V positive cells were previously observed following 12 h treatment with 2500 μM Aze in primary fibroblasts (Gu et al. 2004). Cross-talk between the endosomal–lysosomal system and apoptotic pathway often occurs following endoplasmic reticulum (ER) stress and ER stress can induce both autophagy and apoptosis (Nikoletopoulou et al. 2013; Ding et al. 2007). Although the present study did not investigate ER stress, Gu et al. (2004) used Aze to induce ER stress, and in addition, Roest et al. recently found that Aze activates both the protein kinase RNA-like ER kinase (PERK) and activating transcription factor 6 (ATF6) arms of the unfolded protein response (Roest et al. 2018). Other NPAAs are also known to induce ER stress (Okle et al. 2013; Jin et al. 2010; Main et al. 2016). Furthermore, ER stress occurs in response to the formation of misfolded proteins and is a common feature of neurodegenerative disorders (Hoozemans and Scheper 2012).

Mitochondria play a key role in the regulation of apoptosis, and dysfunctional mitochondria have been linked to a number of disease pathologies, including neurodegenerative disease (Witte et al. 2014; Su et al. 2010; Wang et al. 2014). In the present studies, we detected changes to mitochondrial numbers, area, and interconnectivity. The observed decreases in size and interconnectivity are consistent with the formation of mitochondrial fragments during apoptosis, a process facilitated by the mitochondrial fission machinery (Youle and Karbowski 2005; Parone and Martinou 2006). While mitochondrial fragmentation occurs in many forms of apoptosis, damage to mitochondrial proteins may also contribute to the induction of apoptosis. Lee et al. reported that cells depleted of the fusion protein mitofusin 1 were more susceptible to fragmentation and apoptosis upon

toxin exposure (Lee et al. 2016b). Furthermore, inhibition of the antiapoptotic mitochondrial protein Bcl-2 is known to induce apoptosis (Mallick et al. 2016). Mitochondria are comprised of around 1000 proteins that, with the exception of 13, are nuclear encoded, translated in the cytosol and the precursor proteins imported into the mitochondria (Backes and Herrmann 2017). The imported proteins generally require proteolytic processing and chaperone assisted folding before they can assume their native conformation (Backes and Herrmann 2017). Even intermittent protein misfolding as could occur due to Aze incorporation could cause proteotoxic stress in the mitochondria and cause morphological changes as observed in the present studies. Proteins synthesised in the mitochondria may also be more susceptible to NPAA incorporation due to inherent differences in their proof-reading machinery, aminoacyl-tRNA synthetases, and NPAA-induced mitochondrial protein instability has previously been demonstrated by Konovalova et al. using L-canavanine, an NPAA present in jack beans and wild potato (Suzuki et al. 2011; Konovalova et al. 2015). In addition to fragmentation, the number of mitochondria per cell also decreased. Reductions in mitochondrial numbers have also been observed in cultured mouse neurons expressing a frontotemporal dementia-related tau mutation, suggesting that decreased mitochondrial numbers may be associated with early stage development of the disease (Rodríguez-Martín et al. 2016).

Basal and maximal respirations were significantly decreased following Aze treatment, as was ATP production (Fig. 5). Protein dysfunction in the respiratory chain could contribute to this decrease, and of the 13 proteins encoded by mitochondria, the L-proline-rich ATP synthase protein 8 (Complex V subunit) might be particularly susceptible to misincorporation with 16.2% L-proline content (The UniProt 2018). Mitochondrial bioenergetic collapse is also a well characterised marker of apoptotic and necrotic cell death (Skulachev 2006; Izyumov et al. 2004). While it is clear Aze exposure induces apoptosis, the exact cellular events that precede this downstream response remain unknown. While ER stress has previously been mentioned, as one potential apoptosis evoking event, DNA damage, oxidative stress, and damage to mitochondrial proteins are also events that warrant investigation in the future (Roos and Kaina 2006; Chandra et al. 2000). This is the first study to show that Aze causes mitochondrial dysfunction and is especially important given the link between mitochondrial dysfunction, apoptosis, and neurodegenerative disease, in particular MS (Dutta et al. 2006; Mahad et al. 2008, 2009).

The results of the present study are particularly pertinent, given that the production of Aze containing sugar beets has been historically linked to the development of MS and it has been hypothesised that Aze misincorporation may trigger the onset of MS in genetically predisposed individuals (Rubenstein 2008). MS is an autoimmune demyelinating disease of the central nervous system and came to prominence in the middle nineteenth century, some 50 years after the popularisation of sugar beet production (Loma and Heyman 2011; Rubenstein 2008; Murray 2009). In the same way that a neurodegenerative disorder known as amyotrophic lateral sclerosis–Parkinson's dementia complex has been linked to exposure to the cyanotoxic NPAA BMAA on Guam and has been proposed to have contributed to clusters of amyotrophic lateral sclerosis in New Hampshire (Caller et al. 2012), cases of MS are increased in areas that produce sugar beets. In Canada, the region at the centre of the Canadian sugar beet industry coincides with the highest incidence of MS in the country (Beck et al. 2005). Similarly, the Japanese region of Tokachi has the highest MS prevalence in Asia (Houzen et al. 2008). Tokachi also produces 45% of Japan's sugar beets (Rubenstein 2008). This pattern of high MS incidence in synchrony with sugar beet producing regions has also been observed in Sardinia, Scotland's Orkney Islands, the Middle East and Finland (Pugliatti et al. 2001; Poskanzer et al. 1980; Karni et al. 2003; Sarasoja et al. 2004). Although the present studies do not provide direct evidence of a link between Aze exposure and MS, the spectrum of in vitro toxicity identified suggests that it has the potential to damage the human nervous system. Further studies investigating levels of human exposure to Aze and its in vivo effects would be justified.

## Conclusions

Aze is toxic to human neuron-like cells and induced mitochondrial damage that is accompanied by an increase in apoptotic. The toxicity observed in this study is important, because Aze-containing sugar beets are grown in over 40 countries for the production of sugar (Geng and Yang 2015), and this is set to increase as sugar beets become a source of biofuels such as ethanol (Haankuku et al. 2015). Furthermore, there is significant potential for Aze to enter the human food chain and elicit harmful effects.

## Compliance with ethical standards

**Conflict of interest** The authors declare that they have no conflict of interest.

**Research involving human participants and/or animals** This article does not contain any studies with human participants or animals performed by any of the authors.

**Informed consent** This article does not contain individual participants requiring informed consent.

# References

Alescio T (1973) Effect of a proline analogue, azetidine-2-carboxylic acid, on the morphogenesis in vitro of mouse embryonic lung. J Embryol Exp Morphol 29:439–451

Backes S, Herrmann JM (2017) Protein translocation into the intermembrane space and matrix of mitochondria: mechanisms and driving forces. Front Mol Biosci 4:83. https://doi.org/10.3389/fmolb.2017.00083

Beck CA, Metz LM, Svenson LW, Patten SB (2005) Regional variation of multiple sclerosis prevalence in Canada. Mult Scler J 11(5):516–519

Bertin C, Weston LA, Huang T, Jander G, Owens T, Meinwald J, Schroeder FC (2007) Grass roots chemistry: meta-tyrosine, an herbicidal nonprotein amino acid. Proc Natl Acad Sci USA 104(43):16964–16969. https://doi.org/10.1073/pnas.0707198104

Bessonov K, Bamm VV, Harauz G (2010) Misincorporation of the proline homologue Aze (azetidine-2-carboxylic acid) into recombinant myelin basic protein. Phytochemistry 71(5–6):502–507. https://doi.org/10.1016/j.phytochem.2009.12.010

Bucciantini M, Giannoni E, Chiti F, Baroni F, Formigli L, Zurdo J, Taddei N, Ramponi G, Dobson CM, Stefani M (2002) Inherent toxicity of aggregates implies a common mechanism for protein misfolding diseases. Nature 416(6880):507–511. https://doi.org/10.1038/416507a

Caller TA, Field NC, Chipman JW, Shi X, Harris BT, Stommel EW (2012) Spatial clustering of amyotrophic lateral sclerosis and the potential role of BMAA. Amyotroph Lateral Sci 13(1):25–32

Chandra J, Samali A, Orrenius S (2000) Triggering and modulation of apoptosis by oxidative stress. Free Radic Biol Med 29(3):323–333. https://doi.org/10.1016/S0891-5849(00)00302-6

Ciechanover A, Kwon YT (2015) Degradation of misfolded proteins in neurodegenerative diseases: therapeutic targets and strategies. Exp Mol Med 47:e147. https://doi.org/10.1038/emm.2014.117

Dagda RK, Cherra SJ 3rd, Kulich SM, Tandon A, Park D, Chu CT (2009) Loss of PINK1 function promotes mitophagy through effects on oxidative stress and mitochondrial fission. J Biol Chem 284(20):13843–13855. https://doi.org/10.1074/jbc.M808515200

Ding WX, Ni HM, Gao W, Hou YF, Melan MA, Chen X, Stolz DB, Shao ZM, Yin XM (2007) Differential effects of endoplasmic reticulum stress-induced autophagy on cell survival. J Biol Chem 282(7):4702–4710. https://doi.org/10.1074/jbc.M609267200

Dunlop Rachael A, Dean Roger T, Rodgers Kenneth J (2008) The impact of specific oxidized amino acids on protein turnover in J774 cells. Biochem J 410(1):131

Dunlop RA, Brunk UT, Rodgers KJ (2011) Proteins containing oxidized amino acids induce apoptosis in human monocytes. Biochem J 435(1):207–216. https://doi.org/10.1042/BJ20100682

Dunlop RA, Cox PA, Banack SA, Rodgers KJ (2013) The non-protein amino acid BMAA is misincorporated into human proteins in place of L-serine causing protein misfolding and aggregation. PLoS One 8(9):1–6. https://doi.org/10.1371/journal.pone.0075376

Dutta R, McDonough J, Yin X, Peterson J, Chang A, Torres T, Gudz T, Macklin WB, Lewis DA, Fox RJ, Rudick R, Mirnics K, Trapp BD (2006) Mitochondrial dysfunction as a cause of axonal degeneration in multiple sclerosis patients. Ann Neurol 59(3):478–489. https://doi.org/10.1002/ana.20736

FAO (2014) FAO statistical yearbook. In: FAOSTAT (ed)

Fichman Y, Gerdes SY, Kovács H, Szabados L, Zilberstein A, Csonka LN (2015) Evolution of proline biosynthesis: enzymology, bioinformatics, genetics, and transcriptional regulation. Biol Rev 90(4):1065–1099. https://doi.org/10.1111/brv.12146

Fowden L (1956) Azetidine-2-carboxylic acid: a new cyclic imino acid occurring in plants. Biochem J 64(2):323–332

Fowden L (1963) Amino-acid analogues and the growth of seedlings. J Exp Bot 14(3):387–398. https://doi.org/10.1093/jxb/14.3.387

Fowden L (1972) Amino acid complement of plants. Phytochemistry 11(7):2271–2276. https://doi.org/10.1016/S0031-9422(00)88389-2

Fraser PE, Deber CM (1985) Structure and function of the proline-rich region of myelin basic protein. Biochemistry 24(17):4593–4598. https://doi.org/10.1021/bi00338a017

Geng G, Yang J (2015) Sugar beet production and industry in China. Sugar Technol 17(1):13–21. https://doi.org/10.1007/s12355-014-0353-y

Golini J, Jones WL, Clift IC (2017) The effect of increased fiber ingestion on lipid levels and body mass: a 4-week trial. J Food Sci Nut 3(1):1–3

Grant MM, Brown AS, Corwin LM, Troxler RF, Franzblau C (1975) Effect of L-azetidine 2-carboxylic acid on growth and proline metabolism in Escherichia coli. Biochim Biophys Acta 404(2):180–187

Gu F, Nguyen DT, Stuible M, Dube N, Tremblay M, Chevet E (2004) Protein tyrosine phosphatase 1B potentiates IRE1 signaling during endoplasmic reticulum stress. J Biol Chem 279(48):49689–49693

Haankuku C, Epplin FM, Kakani VG (2015) Industrial sugar beets to biofuel: field to fuel production system and cost estimates. Biomass Bioenergy 80:267–277. https://doi.org/10.1016/j.biombioe.2015.05.027

Habeeb AAM, Gad AE, EL-Tarabany A, Mustafa MM, Atta A (2017) Using of sugar beet pulp by-product in farm animals feeding. IJSRST 3(3)

Harland JI, Jones CK, Hufford C (2009) Co-products. In: Draycott AP (ed) Sugar beet. Blackwell Publishing, Oxford, UK, pp 443–463

Hoozemans JJM, Scheper W (2012) Endoplasmic reticulum: the unfolded protein response is tangled in neurodegeneration. Int J Biochem Cell Biol 44(8):1295–1298. https://doi.org/10.1016/j.biocel.2012.04.023

Houzen H, Niino M, Hata D, Nakano F, Kikuchi S, Fukazawa T, Sasaki H (2008) Increasing prevalence and incidence of multiple sclerosis in northern Japan. Mult Scler J 14(7):887–892. https://doi.org/10.1177/1352458508090226

Huotari J, Helenius A (2011) Endosome maturation. EMBO J 30(17):3481–3500. https://doi.org/10.1038/emboj.2011.286

Izyumov DS, Avetisyan AV, Pletjushkina OY, Sakharov DV, Wirtz KW, Chernyak BV, Skulachev VP (2004) "Wages of Fear": transient threefold decrease in intracellular ATP level imposes apoptosis. Biochim Biophys Acta Bioenerg 1658(1):141–147. https://doi.org/10.1016/j.bbabio.2004.05.007

Jin CM, Yang YJ, Huang HS, Kai M, Lee MK (2010) Mechanisms of L-DOPA-induced cytotoxicity in rat adrenal pheochromocytoma cells: implication of oxidative stress-related kinases and cyclic AMP. Neuroscience 170(2):390–398. https://doi.org/10.1016/j.neuroscience.2010.07.039

Joneja MG (1981) Teratogenic effects of proline analogue L-azetidine-2-carboxylic acid in hamster fetuses. Teratology 23(3):365–372. https://doi.org/10.1002/tera.1420230311

Jung M, Lee J, Seo H-Y, Lim JS, Kim E-K (2015) Cathepsin inhibition-induced lysosomal dysfunction enhances pancreatic beta-cell apoptosis in high glucose. PLoS One 10(1):e0116972. https://doi.org/10.1371/journal.pone.0116972

Karni A, Kahana E, Zilber N, Abramsky O, Alter M, Karussis D (2003) The frequency of multiple sclerosis in Jewish and Arab populations in greater Jerusalem. Neuroepidemiology 22(1):82–86

Kim J-S, Kim J-C, Lee S, Lee B-H, Cho KY (2006) Biological activity of L-2-azetidinecarboxylic acid, isolated from *Polygonatum odoratum* var. *pluriflorum*, against several algae. Aquat Bot 85(1):1–6. https://doi.org/10.1016/j.aquabot.2006.01.003

Konovalova S, Hilander T, Loayza-Puch F, Rooijers K, Agami R, Tyynismaa H (2015) Exposure to arginine analog canavanine induces aberrant mitochondrial translation products, mitoribosome stalling, and instability of the mitochondrial proteome. Int J Biochem Cell Biol 65:268–274. https://doi.org/10.1016/j.biocel.2015.06.018

Lane JM, Dehm P, Prockop DJ (1970) Effect of the proline analogue azetidine-2-carboxylic acid on collagen synthesis in vivo. Biochim Biophys Acta 236:517–527

Lee YRJ, Nagao RT, Lin CY, Key JL (1996) Induction and regulation of heat-shock gene expression by an amino acid analog in soybean seedlings. Plant Physiol 110(1):241–248

Lee J, Joshi N, Pasini R, Dobson RC, Allison J, Leustek T (2016a) Inhibition of Arabidopsis growth by the allelopathic compound azetidine-2-carboxylate is due to the low amino acid specificity of cytosolic prolyl-tRNA synthetase. Plant J 88(2):236–246. https://doi.org/10.1111/tpj.13246

Lee W-C, Chiu C-H, Chen J-B, Chen C-H, Chang H-W (2016b) Mitochondrial fission increases apoptosis and decreases autophagy in renal proximal tubular epithelial cells treated with high glucose. DNA Cell Biol 35(11):657–665. https://doi.org/10.1089/dna.2016.3261

Liu Z, Jenkinson SF, Vermaas T, Adachi I, Wormald MR, Hata Y, Kurashima Y, Kaji A, Yu CY, Kato A, Fleet GW (2015) 3-Fluoro-azetidine carboxylic acids and *trans,trans*-3,4-difluoroproline as peptide scaffolds: inhibition of pancreatic cancer cell growth by a fluoroazetidine iminosugar. J Org Chem. https://doi.org/10.1021/acs.joc.5b00463

Löffelhardt W, Kopp B, Kubelka W (1979) Intracellular distribution of cardiac glycosides in leaves of *Convallaria majalis*. Phytochemistry 18(8):1289–1291. https://doi.org/10.1016/0031-9422(79)83009-5

Loma I, Heyman R (2011) Multiple sclerosis: pathogenesis and treatment. Curr Neuropharmacol 9(3):409–416. https://doi.org/10.2174/157015911796557911

Mahad DJ, Ziabreva I, Lassmann H, Turnbull D (2008) Mitochondrial defects in acute multiple sclerosis lesions. Brain 131(7):1722–1735. https://doi.org/10.1093/brain/awn105

Mahad DJ, Ziabreva I, Campbell G, Lax N, White K, Hanson PS, Lassmann H, Turnbull DM (2009) Mitochondrial changes within axons in multiple sclerosis. Brain 132(5):1161–1174. https://doi.org/10.1093/brain/awp046

Main BJ, Dunlop RA, Rodgers KJ (2016) The use of L-serine to prevent β-methylamino-L-alanine (BMAA)-induced proteotoxic stress in vitro. Toxicon 109:7–12. https://doi.org/10.1016/j.toxicon.2015.11.003

Main BJ, Italiano CJ, Rodgers KJ (2018) Investigation of the interaction of β-methylamino-L-alanine with eukaryotic and prokaryotic proteins. Amino Acids 50(3):397–407. https://doi.org/10.1007/s00726-017-2525-z

Mallick A, More P, Syed MM, Basu S (2016) Nanoparticle-mediated mitochondrial damage induces apoptosis in cancer. ACS Appl Mater Interfaces 8(21):13218–13231. https://doi.org/10.1021/acsami.6b00263

Murray TJ (2009) The history of multiple sclerosis: the changing frame of the disease over the centuries. J Neurol Sci 277:S3–S8. https://doi.org/10.1016/S0022-510X(09)70003-6

Nikoletopoulou V, Markaki M, Palikaras K, Tavernarakis N (2013) Crosstalk between apoptosis, necrosis and autophagy. Biochim Biophys Acta Mol Cell Res 1833(12):3448–3459. https://doi.org/10.1016/j.bbamcr.2013.06.001

Okle O, Stemmer K, Deschl U, Dietrich DR (2013) L-BMAA induced ER stress and enhanced caspase 12 cleavage in human neuroblastoma SH-SY5Y cells at low nonexcitotoxic concentrations. Toxicol Sci 131(1):217–224. https://doi.org/10.1093/toxsci/kfs291

Parone PA, Martinou J-C (2006) Mitochondrial fission and apoptosis: an ongoing trial. Biochim Biophys Acta Mol Cell Res 1763(5):522–530. https://doi.org/10.1016/j.bbamcr.2006.04.005

Poskanzer DC, Prenney LB, Sheridan JL, Kondy JY (1980) Multiple sclerosis in the Orkney and Shetland Islands. I: epidemiology, clinical factors, and methodology. J Epidemiol Community Health 34(4):229–239. https://doi.org/10.1136/jech.34.4.229

Pugliatti M, Sotgiu S, Solinas G, Castiglia P, Rosati G (2001) Multiple sclerosis prevalence among Sardinians: further evidence against the latitude gradient theory. Neurol Sci 22(2):163–165. https://doi.org/10.1007/s100720170017

Rodgers KJ (2014) Non-protein amino acids and neurodegeneration: the enemy within. Exp Neurol 253:192–196. https://doi.org/10.1016/j.expneurol.2013.12.010

Rodgers KJ, Shiozawa N (2008) Misincorporation of amino acid analogues into proteins by biosynthesis. Int J Biochem Cell Biol 40(8):1452–1466. https://doi.org/10.1016/j.biocel.2008.01.009

Rodgers KJ, Hume PM, Dunlop RA, Dean RT (2004) Biosynthesis and turnover of DOPA-containing proteins by human cells. Free Radic Biol Med 1(37):1756–1764

Rodgers KJ, Ford JL, Brunk UT (2009) Heat shock proteins: keys to healthy ageing? Redox Rep 14(4):147–153. https://doi.org/10.1179/135100009X392593

Rodríguez-Martín T, Pooler AM, Lau DHW, Mórotz GM, De Vos KJ, Gilley J, Coleman MP, Hanger DP (2016) Reduced number of axonal mitochondria and tau hypophosphorylation in mouse P301L tau knockin neurons. Neurobiol Dis 85:1–10. https://doi.org/10.1016/j.nbd.2015.10.007

Roest G, Hesemans E, Welkenhuyzen K, Luyten T, Engedal N, Bultynck G, Parys JB (2018) The ER stress inducer L-azetidine-2-carboxylic acid elevates the levels of phospho-eIF2α and of LC3-II in a Ca(2+)-dependent manner. Cells 7(12):239. https://doi.org/10.3390/cells7120239

Rojkind M (1973) Inhibition of liver fibrosis by L-Azetidine-2-carboxylic acid in rats treated with carbon tetrachloride. J Clin Investig 52:2451–2456

Roos WP, Kaina B (2006) DNA damage-induced cell death by apoptosis. Trends Mol Med 12(9):440–450. https://doi.org/10.1016/j.molmed.2006.07.007

Rosenthal GA (2001) L-Canavanine: a higher plant insecticidal allelochemical. Amino Acids 21:319–330

Rubenstein E (2008) Misincorporation of the proline analog azetidine-2-carboxylic acid in the pathogenesis of multiple sclerosis: a hypothesis. J Neuropathol Exp Neurol 67(11):1035–1040. https://doi.org/10.1097/NEN.0b013e31818add4a

Rubenstein E, Zhou H, Krasinska KM, Chien A, Becker CH (2006) Azetidine-2-carboxylic acid in garden beets (*Beta vulgaris*). Phytochemistry 67(9):898–903. https://doi.org/10.1016/j.phytochem.2006.01.028

Rubenstein E, McLaughlin T, Winant RC, Sanchez A, Eckart M, Krasinska KM, Chien A (2009) Azetidine-2-carboxylic acid in the food chain. Phytochemistry 70(1):100–104. https://doi.org/10.1016/j.phytochem.2008.11.007

Sarasoja T, Wikström J, Paltamaa J, Hakama M, Sumelahti ML (2004) Occurrence of multiple sclerosis in central Finland: a regional and temporal comparison during 30 years. Acta Neurol Scand 110(5):331–336

Schindelin J, Arganda-Carreras I, Frise E, Kaynig V, Longair M, Pietzsch T, Preibisch S, Rueden C, Saalfeld S, Schmid B, Tinevez JY, White DJ, Hartenstein V, Eliceiri K, Tomancak P, Cardona A (2012) Fiji: an open-source platform for biological-image analysis. Nat Methods 9(7):676–682. https://doi.org/10.1038/nmeth.2019

Skulachev VP (2006) Bioenergetic aspects of apoptosis, necrosis and mitoptosis. Apoptosis 11(4):473–485. https://doi.org/10.1007/s10495-006-5881-9

Smith PK, Krohn RI, Hermanson GT, Mallia AK, Gartner FH, Provenzano MD, Fujimoto EK, Goeke NM, Olson BJ, Klenk DC (1985) Measurement of protein using bicinchoninic acid. Anal Biochem 150(1):76–85. https://doi.org/10.1016/0003-2697(85)90442-7

Song Y, Zhou H, Vo MN, Shi Y, Nawaz MH, Vargas-Rodriguez O, Diedrich JK, Yates JR, Kishi S, Musier-Forsyth K, Schimmel P (2017) Double mimicry evades tRNA synthetase editing by toxic vegetable-sourced non-proteinogenic amino acid. Nat Commun 8(1):2281. https://doi.org/10.1038/s41467-017-02201-z

Su B, Wang X, Zheng L, Perry G, Smith MA, Zhu X (2010) Abnormal mitochondrial dynamics and neurodegenerative diseases. Biochim Biophys Acta Mol Basis Dis 1802(1):135–142. https://doi.org/10.1016/j.bbadis.2009.09.013

Suzuki T, Nagao A, Suzuki T (2011) Human mitochondrial tRNAs: biogenesis, function, structural aspects, and diseases. Annu Rev Genet 45(1):299–329. https://doi.org/10.1146/annurev-genet-110410-132531

The UniProt C (2018) UniProt: a worldwide hub of protein knowledge. Nucleic Acids Res 47(D1):D506–D515. https://doi.org/10.1093/nar/gky1049

Thompson JF, Morris CJ, Smith IK (1969) New naturally occurring amino acids. Annu Rev Biochem 38(1):137–158. https://doi.org/10.1146/annurev.bi.38.070169.001033

Vaughan D, Dekock PC, Cusens E (1974) Effects of hydroxyproline and other amino acid analogues on the growth of pea root segments. Physiol Plant 30(3):255–259. https://doi.org/10.1111/j.1399-3054.1974.tb03652.x

Verbruggen N, van Montagu M, Messens E (1992) Synthesis of the proline analogue [2,3-3H]azetidine-2-carboxylic acid. Uptake and incorporation in Arabidopsis thaliana and Escherichia coli. FEBS Lett 308(3):261–263

Wang X, Wang W, Li L, Perry G, Lee H-G, Zhu X (2014) Oxidative stress and mitochondrial dysfunction in Alzheimer's disease. Biochim Biophys Acta Mol Basis Dis 1842(8):1240–1247. https://doi.org/10.1016/j.bbadis.2013.10.015

Witte ME, Mahad DJ, Lassmann H, van Horssen J (2014) Mitochondrial dysfunction contributes to neurodegeneration in multiple sclerosis. Trends Mol Med 20(3):179–187. https://doi.org/10.1016/j.molmed.2013.11.007

Youle RJ, Karbowski M (2005) Mitochondrial fission in apoptosis. Nat Rev Mol Cell Biol 6(8):657–663

Zagari A, Nemethy G, Scheraga HA (1990) The effect of L-azetidine-2-carboxylic acid residue on protein conformation. 1. Conformations of the residue and of dipeptides. Biopolymers 30:951–959

Zagari A, Palmer KA, Gibson KD, Nemethy G, Scheraga HA (1994) The effect of the L-azetidine-2-carboxylic acid residue on protein conformation. IV. Local substitutions in the collagen triple helix. Biopolymers 34(1):51–60. https://doi.org/10.1002/bip.360340107

Author Names: Kate Samardzic and Kenneth J. Rodgers
Affilidation and Email Address of Corresponding Author: University of Technology Sydney, kenneth.rodgers@uts.edu.au
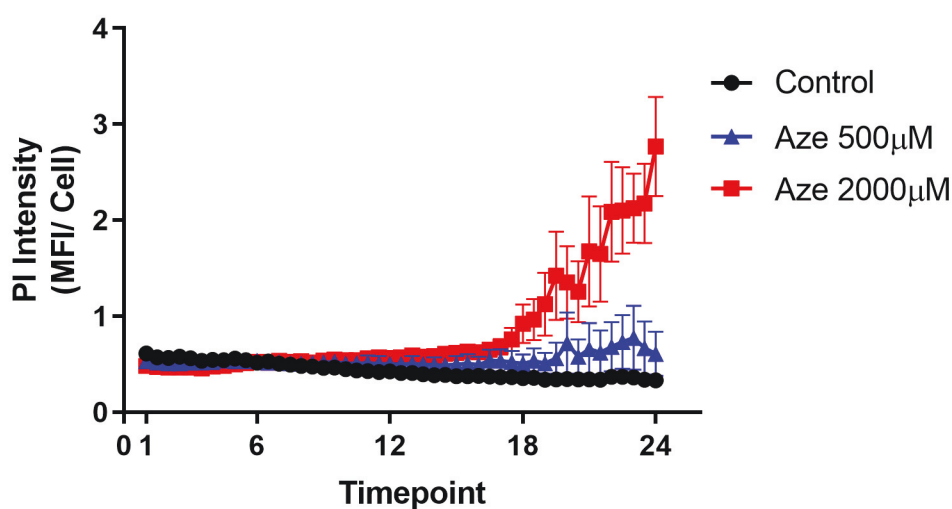
**Supplementary Fig 1. Time course of Propidium Iodide (PI) staining following Aze treatment in SH-SY5Y cells.** PI staining is shown as mean fluorescence intensity (MFI) and normalised to nuclei number. Measurements were taken every 30 min for 24 h following treatment with Aze 500 µM (blue) and 2000 µM (red) and untreated control (black).
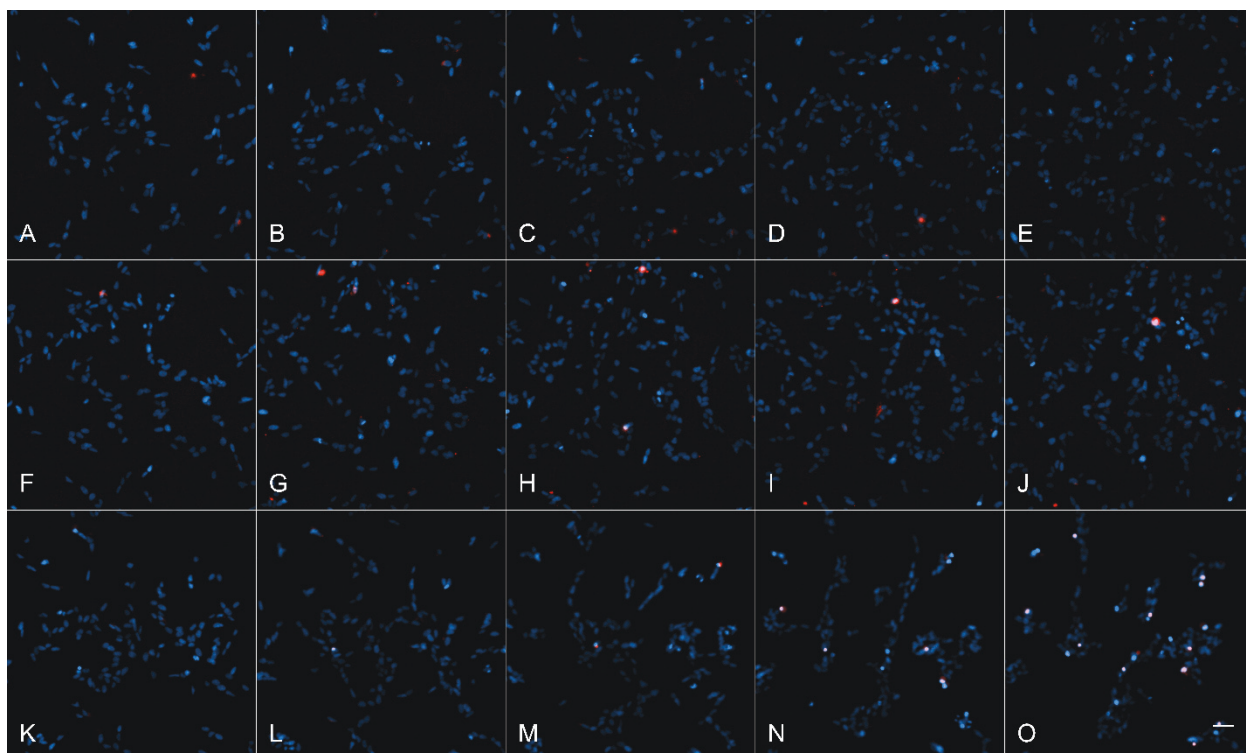
**Supplementary Fig 2. Representative images of Propidium Iodide (PI) and Hoeschst 33258 staining on SH-SY5Y cells following Aze treatment.** PI (red) and Hoeschst 33258 (blue) stained nuclei are overlayed in each image. Panels A-E show untreated cells at 1, 6, 12, 18 and 24 hours. Panels F-J show cells treated with 500 µM Aze 1, 6, 12, 18 and 24 hours following treatment while panels K-O show cells treated with 2000 µM Aze 1, 6, 12, 18 and 24 hours following treatment. Scale bar shows 50 µm. All images were captured on a Nikon Ti inverted fluorescence microscope with a 20X objective.
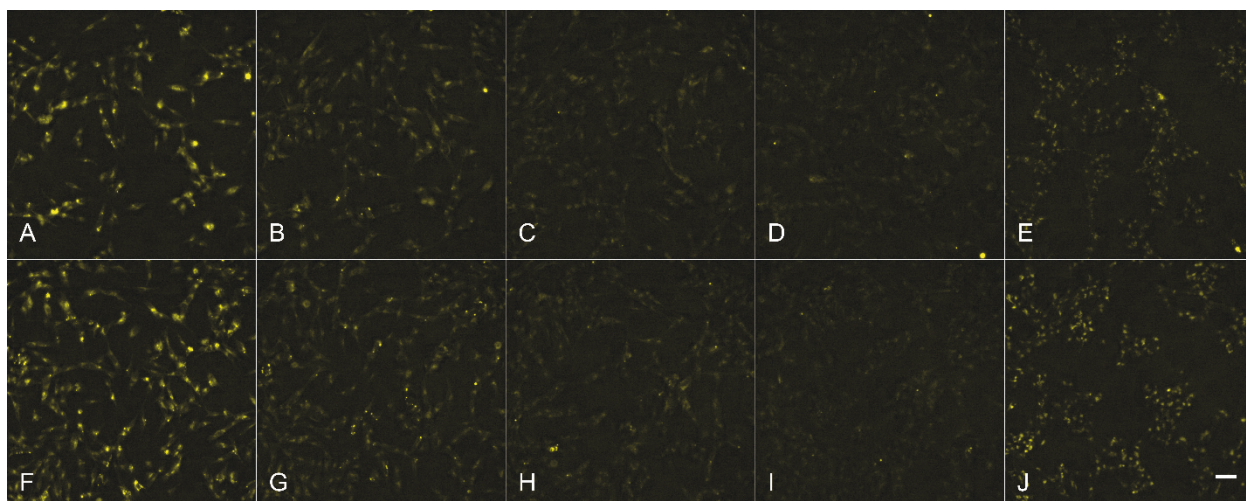
**Supplementary Fig 3. Representative images of Lysotracker Red DND-99 staining (yellow) on SH-SY5Y cells following Aze treatment**. Panels A-E show untreated cells at 1, 6, 12, 18 and 24 hrs. Panels F-J show cells treated with 2000 µM Aze following 1, 6, 12, 18 and 24 hours. For clarity, the images are presented in yellow. For further analysis Lysotracker fluorescence was normalised to nuclei number using Hoeschst 33258 staining (not shown). Scale bar shows 50 µm. All images were captured on a Nikon Ti inverted fluorescence microscope with a 20X objective.
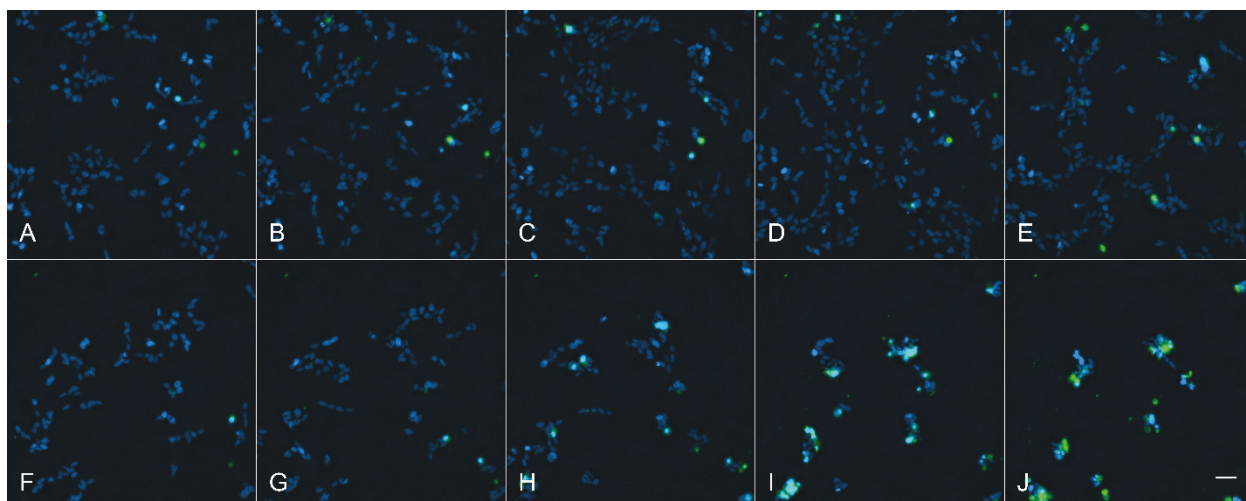
**Supplementary Fig 4. Representative images of Annexin V and Hoeschst 33258 staining on SH-SY5Y cells following Aze treatment.** Annexin V (green) and Hoeschst 33258 (blue) are overlayed in each image. Panels a-e show untreated cells at 1, 6, 12, 18 and 24 hrs. Panels f-j show cells 1, 6, 12, 18 and 24 hrs following treatment with 2000 µM. Scale bar shows 50 µm. All images were captured on a Nikon Ti inverted fluorescence microscope with a 20X objective.

# Chapter Five:

Proteomic characterisation of SH-SY5Y neuroblastoma cells following NPAA exposure

# CHAPTER FIVE: PROTEOMIC CHARACTERISATION OF SH-SY5Y NEUROBLASTOMA CELLS FOLLOWING NPAA EXPOSURE

## 5.1 Introduction

Proteomics, a combination of the terms "protein" and "genomics", is defined as: "the use of quantitative protein-level measures of gene expression to characterise biological processes (e.g., disease processes and drug effects) and decipher the mechanism of gene expression control" [213]. Early proteomic studies uncovered strong functional relationships between drug treatments, protein expression and physiological effects, and since then the study of proteomics has been applied in research studying toxins, termed 'toxicoproteomics' [213,214]. Thus, proteomics has the potential to prove useful when investigating the mechanisms behind NPAAs' toxic effects as observed in the previous chapters.

The field of quantitative proteomics is bolstered by the use of mass spectrometry, a technique which relies upon the production, separation and measurement of fragmented gas-phase ions of a given molecule according to their mass-to-charge (m/z) ratios. These ions are detected in proportion to their relative abundance, and together, this data produces a mass spectrum [215]. Though mass spectrometry techniques have been utilised in the field of physics dating back to the early 20th century, it wasn't until the 1990s, when mass spectrometry was coupled with liquid chromatography and soft ionisation techniques, that these techniques were applied to the field of proteomics [216].

Though there are various methods of proteome analysis, the methods described in this chapter utilise "bottom-up" or "shotgun" proteomics, which is the characterisation of a mixture of proteins using peptide fragments released through proteolysis. The mass spectra derived from the peptide fragments are then compared to a database of protein sequences for identification, following which the identified proteins can be investigated for abundance changes using peptide abundance and bioinformatics. The converse method, "top-down" proteomics, analyses intact proteins and can lead to difficulties with protein fractionation, ionisation and fragmentation at the gas stage. While

fragmentation difficulties can be overcome when top-down strategies such as electron capture dissociation or electron transfer dissociation are used, the other difficulties are also overcome when a bottom-up approach is used [217-219]. Additionally, the analysis of smaller molecules leads to increased sensitivity [219].

Proteomic studies that measure protein abundance changes in neurodegenerative disease have become increasingly common as a means to further understand the mechanisms behind disease progression. The ability to quickly and reproducibly quantify and identify large numbers of proteins in the diseased brain and then compare them to control brains has provided an excellent tool in the investigation of neurodegenerative diseases. A number of protein expression alterations have been identified in various disease pathologies using human and animal models including AD [220-222], PD [223,224] and MS [225,226]. These tools are especially useful when investigating expression changes following exposure to toxins with unclear mechanisms as they may identify the molecular pathways involved in toxicity and can also be utilised in *in vitro* models of toxicity.

As mentioned in section 2.3, many toxicological studies into NPAAs occurred prior to the advent of proteomics and as such, relatively few NPAAs have had their effects investigated in this manner. Fewer still have been scrutinised via bottom-up proteomics and this is largely because mass spectrometry has mainly been solicited to detect NPAAs, namely BMAA, in complex mixtures from environmental and patient samples. These analytical chemistry methods are targeted and differ from untargeted bottom-up proteomics in both instrumentation and data analysis. Sacks et al. used liquid chromatography-mass spectrometry (LC-MS) to detect protein-associated BMAA in brain samples from Guamanian ALS-PDC patients, a study which has provided the foundation for much of the research into NPAAs and their link to neurodegenerative disease [109]. In addition, Murch et al. used a triple quadrupole mass spectrometer in an *in vitro* cell free protein expression system to detect incorporated BMAA [227]. While both the aforementioned studies used methods that involve the hydrolysis of proteins to their constituent amino acids, resulting in increased sensitivity for NPAA, LC-MS based

bottom-up proteomics has also recently been utilised to show Nva misincorporates into *E.coli* proteins [228,229].

Research investigating expression changes following BMAA exposure in rats has observed decreases in the abundance of histone H2B and myelin basic proteins, which could relate to changes in chromatin regulation, myelination and cytoskeletal function [230]. Meanwhile, a study using a zebrafish model detected changes in the abundance of proteins linked to protein homeostasis such as translation initiation factors (increased) and ribosomal protein subunit 21 (decreased), reactive oxygen species and neuronal cell death [231]. Though BMAA has been the subject of a limited number of studies into protein abundance changes, there is currently no data investigating the NPAAs Nva and Aze in this manner.

Following the generation of large proteomic datasets, raw data must undergo bioinformatic processing for functional analysis. Functional analysis, as part of an integrated proteomics workflow, utilises various software packages and can identify relevant pathways and interactions [232]. In this chapter, this is performed by connecting each identified protein with its associated Gene Ontology (GO) term. This process uses an enrichment algorithm to associate proteins to hierarchically clustered terms that relate to their molecular function, biological process or cellular local [233]. Limitations of this process are the incomplete nature of the term list and its shifting nature as new discoveries are made [234]. Furthermore, the majority of functional annotations are based on computational, rather than manual, analysis of experimental results [234]. Despite these drawbacks, functional analysis using GO terms is a valuable tool to filter, characterise and interpret large proteomic datasets.

Of the numerous software packages available to perform GO analysis, the open-sourced packages Biological Networks Gene Ontology tool (BiNGO) and ClueGO integrates Gene Ontology (ClueGO) were selected due to their compatibility with the freely available data visualisation program Cytoscape. BiNGO identifies enriched terms  using a hypergeometric test and determines the probability that "*x* or more genes belong to a

functional category *C* shared by *n* of the *N* genes in the reference set [235]." Similarly, ClueGO performs an enrichment test for terms based the hypergeometric distribution [236]. The output of both packages is a p-value, however, following a validation study that compared BiNGO output to clustered DNA microarray data, excessive dependence on an exact p-value during data interpretation was warned against due to the potential for incomplete annotation data to bias results [237]. The allowance for statistical improvements such as a false discovery rate and p-value adjustments partly mitigates this issue and the overall conclusion was one of reliability. These techniques may be used to complement existing findings, as they were used in this chapter, or to generate hypotheses that can then be validated by additional experimentation. Hence, the overarching aim of the studies presented in this chapter was to analyse the protein abundance changes and pathways enriched in SH-SY5Y neuroblastoma cells following exposure to Nva and Aze, in order to further understand the mechanisms at the heart of their toxicity.

## 5.2 Methods

### 5.2.1 Reagents

Dulbecco's Modified Eagle's Medium (DMEM), Nva, Aze, ammonium bicarbonate, urea, bovine serum albumin, tris(2-carboxyethyl)phosphine (TCEP), dithiothreitol (DTT), formic acid and acrylamide monomers were purchased from Sigma Chemical Co. (MO, USA). Sequence grade trypsin was from Promega (Wi, USA). Acetonitrile was high-performance liquid chromatography grade and purchased from Sigma Chemical Co.  All aqueous solutions and buffers were prepared using 18 mU water.

### 5.2.2 Cell Culture

SH-SY5Y human neuroblastoma cells (American Tissue Culture Collection, catalogue number CRL-2266) were cultured as follows; DMEM was supplemented with 10% heat-inactivated Foetal Bovine Serum (FBS) (US origin, Gibco, CA, USA), and 2 mM GlutaMAX (Thermo Fisher Scientific, MA, USA). Cells were maintained at 37 °C with 5% $CO_2$ in 175 cm2 flasks until they were plated for experiments. During treatment, DMEM culture

medium was substituted with L-isoleucine, L-leucine, L-valine and L-proline deficient Eagle's Minimum Essential Medium (EMEM). Experiments were performed at passage 15.

### 5.2.3 Treatment

Cells were plated in 6-well plates at 400,000 cells/well, allowed to adhere overnight and were then treated in triplicate with 2000 µM of Nva or Aze. Following 24 h treatment, cells were detached using TrypLE and washed 3 times in phosphate buffered saline (PBS) prior to being snap frozen in $LN_2$.

### 5.2.4 Protein Precipitation and Mass Spectrometry

The cell pellet was solubilised in 8 M urea and 100 mM ammonium bicarbonate. Disulphide bonds were then reduced in 5 mM TCEP and alkylated with 20 mM acrylamide monomers at room temperature for 90 min. Excess alkylating agents were then quenched in 20 mM DTT prior to sonication at 80% power on ice (3 x 30 sec) to shear DNA. The cells were then centrifuged and a 5 µL sample of the supernatant was diluted in ammonium bicarbonate prior to quantification with a BCA assay [238]. A 50 µg sample was then diluted using ammonium bicarbonate and trypsin (1:50 trypsin: protein ratio) and digested overnight at 37°C. Solid phase extraction was then performed using the method described by Rappsilber, Mann and Ishihama [239] using Styrene Divinylbenzene-Reversed Phase Sulfonate media.

Using an Acquity M-class nanoLC system (Waters, MA, USA), 5 µL of the sample (1 µg) was loaded at 15 µL/min for 3 minutes onto a nanoEase Symmetry C18 trapping column (180 µm x 20mm) before being washed onto a PicoFrit column (75 µmID x 250 mm; New Objective, MA, USA) packed with Magic C18AQ resin (3 micron; Michrom Bioresources, CA, USA). Peptides were eluted from the column and into the ESI source of a Q Exactive Plus mass spectrometer (Thermo Fisher) using the following program: 5-30% MS buffer B (98% Acetonitrile + 0.2% Formic Acid) over 90 minutes, 30-80% MS buffer B over 3 minutes, 80% MS buffer B for 2 minutes, 80-5% for 3 min. The eluting peptides were ionised at 2000V. A Data Dependent MS/MS (dd-MS$^2$) experiment was performed, with

a survey scan of 350-1500 Da performed at 70,000 resolution for peptides of charge state 2+ or higher with an AGC target of 3e6 and maximum injection time of 50 ms. The top 12 peptides were selected fragmented in the higher-energy collisional dissociation cell using an isolation window of 1.4 m/z, an AGC target of 1e5 and maximum injection time of 100 ms. Fragments were scanned in the Orbitrap analyser (Thermo Fisher) at 17,500 resolution and the product ion fragment masses measured over a mass range of 120-2000 Da. The mass of the precursor peptide was then excluded for 30 seconds.

### 5.2.5 Generation of Protein Quantification Data

Proteins were identified with the Andromeda search engine integrated into MaxQuant version 1.6.1 [240]. Protein sequences were downloaded from the human UniProt proteome database (accessed February 5th 2018) and supplemented with frequently observed contaminants. Trypsin specificity was set to allow for up to 4 miscleaved sites, deamidation (of L-arginine), oxidation (of L-methionine), N-terminal acetylation and propionamide (on L-cysteine) were set as variable modifications. Peptides and proteins were accepted with a false discovery rate (FDR) of less than 1%. The decoy mode was set to the default mode, 'revert'. In this mode a reverse database of the original search database, consisting of all protein sequences read from the end to the beginning, was used in the target-decoy database strategy to control for false discoveries.

Proteins were quantified in MaxQuant using maximum (pairwise) peptide ratio information from peptide ion intensities, normalised using MaxLFQ and computed as label free quantification (LFQ) values [241]. Further analysis was performed in Perseus version 1.6.1.3 [242]. Data was loaded in Perseus and log2 transformed. Scatter plots with Pearson correlation coefficients between LFQ intensities from biological replicates in the experimental groups were generated, as was a numeric Venn diagram. Missing LFQ data were then imputed with intensities with an imputation width of 0.3 and a shift of 0.8. Proteins with significantly changed abundance were analysed with a two-tailed t-test, where p-values were corrected for multiple testing by a permutation-based FDR with a threshold of 0.05. A fold change cut off was determined by s0 and set to 2 for Nva and 0.1 for Aze and fold changes are expressed as 'Student's T-test Difference,' which

corresponds to a log2(fold change). The fold change cut off was lowered (s0=0.1) for the Aze dataset due to the relatively low number of unique proteins detected.

The datasets of unique proteins were then uploaded into the software platform Cytoscape [243] and the apps ClueGO [236], ClusterONE [244] and BiNGO [235] were used to study GO annotations. A functional analysis was performed in ClueGO using a Fisher Exact enrichment test, showing only showing only pathways with a p-value < 0.05 and corrected with the Bonferroni step-down method. Protein-protein interaction network clustering was analysed with ClusterONE. Significant clusters contained proteins that had edge weights, determined using nodes imported from STRING version 10.5 [245], satisfying p < 0.05 in a one-sided Mann-Whitney U test. The clusters were then enriched for GO terms in BiNGO using a Fisher Exact test with a Benjamini-Hochberg FDR of 0.05.

## 5.3 Results

### 5.3.1 L-Norvaline

#### *5.3.1.1 Proteomic Findings*

Samples collected from the control and Nva experimental groups were digested and analysed by LC-MS/MS without any fractionation. The reproducibility of the biological replicates was assessed by scatter plotting and the Pearson correlation coefficient was determined using LFQ intensities (Figure 5A). The Pearson correlations calculated for the experimental groups were deemed acceptable, ranging from 0.973- 0.986. A total of 2590 proteins were identified in averaged samples of the control group and 3137 proteins in pooled samples of the Nva treatment group respectively (Figure 5B). Of these, 2463 were common to both control and treatment groups. However, 127 proteins were unique to the control group and 238 (≥ 2 peptides) were unique to the Nva treatment. A scatter plot was used to study expression changes in the co-expressed proteins and excluded the unique proteins of either group (Figure 5C). From this plot, only one of the co-expressed proteins significantly changed in abundance, histone H2A type-2A.

**Figure 5. Proteomic characterization of Nva treated cells.**

Panel A shows scatter plot with Pearson correlation coefficients between LFQ intensities from biological replicates in the experimental groups, panel B shows Venn diagram of proteins identified. Panel C shows scatter plot of LFQ intensity ratios. One protein that significantly changed in abundance (black) was identified by mass spectrometry with permutation-based false discovery rate–corrected, two-tailed t test (threshold, FDR-adjusted p-value < 0.05; s0 = 2; n = 3). x axis, log2-transformed ratio of proteins in the control over Nva treatment; y axis, –log10-transformed p-values.


*5.3.1.2 Functional Annotations of Uniquely Expressed Proteins*

The unique proteins identified in the control and Nva treated groups were analysed in Cytoscape using ClueGo for enriched GO functional annotations. GO Cellular Compartment (CC) (Figure 6) analysis of proteins unique to the control revealed the pre-ribosome as the predominant cell localisation of proteins unique to the control group (50%), followed by microtubule end (25%) (p <0.01), kinesin complex (12.5%) and the nuclear inner membrane (12.5%) (p <0.05). Proteins classified as organellar small

ribosomal subunit made up 57.14% of proteins unique to the Nva treatment, followed by cell cortex part (21.43%), extrinsic component of the plasma membrane (7.14%), microtubule bundle (7.14%), and Wiskott–Aldrich syndrome protein and SCAR homolog (WASH) complex (7.14%) ($p < 0.01$). A full list of GO terms, p-values and protein identifications for each condition can be found in Supplementary Tables 1 and 2 of the Appendix.

GO Biological Process (BP) terms associated with proteins unique to each treatment were also analysed using ClueGO (Figure 7) and in the control group, negative regulation of supramolecular fiber (29.03%) and cleavage involved in rRNA processing (25.81%) were among the most significantly enriched terms ($p < 0.01$). In the Nva treated group microtubule polymerisation (40.74%), mitochondrial gene expression (33.33%), positive regulation of gliogenesis (11.11%), respiratory chain complex III assembly (7.41%), response to nitric oxide (3.7%) and chromatin remodelling (3.7%) were all significantly enriched terms ($p < 0.01$). A full list of GO terms, p-values and protein identifications for each cluster can be found in Supplementary Tables 3 and 4 of the Appendix.

Further GO BP analysis was performed using the using the apps ClusterONE and BiNGO (Figures 8 & 9). ClusterONE detects overlapping proteins in protein-protein interaction networks and the GO BP terms of proteins interacting within significant clusters ($p < 0.05$) are shown for each condition. The colour gradient of the cluster distribution network shows the p-value of each cluster associated with the GO term, with the darker colour (orange) indicating a lower p-value as a means to visualise GO terms that are significantly over-represented. The size of each node is proportional to the number of proteins in the unique protein dataset for each treatment. A full list of GO terms, p-values and protein identifications for each cluster can be found in Supplementary Tables 5 and 6 of the Appendix.
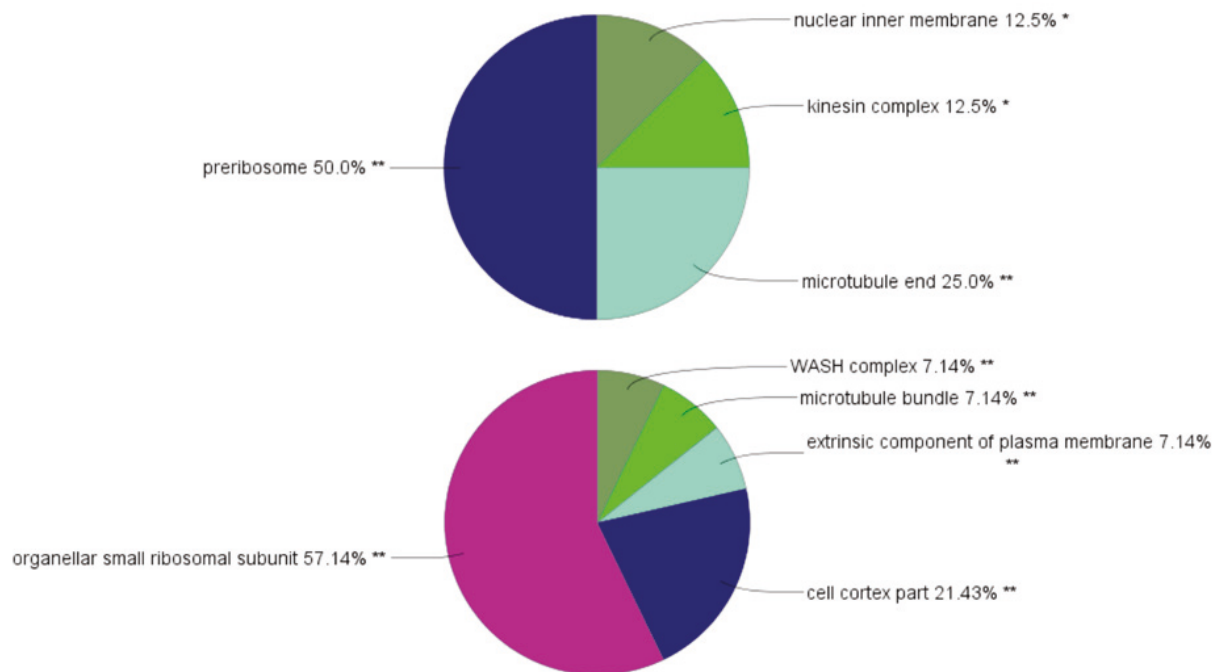
**Figure 6. Enriched ClueGO Gene Ontology (GO) Cellular Compartment (CC) terms**. GO CC terms for the unique proteins in the untreated (top) and Nva treated (bottom) groups. Percentage shows % of total enriched proteins in each group. * p < 0.05, ** p < 0.01.
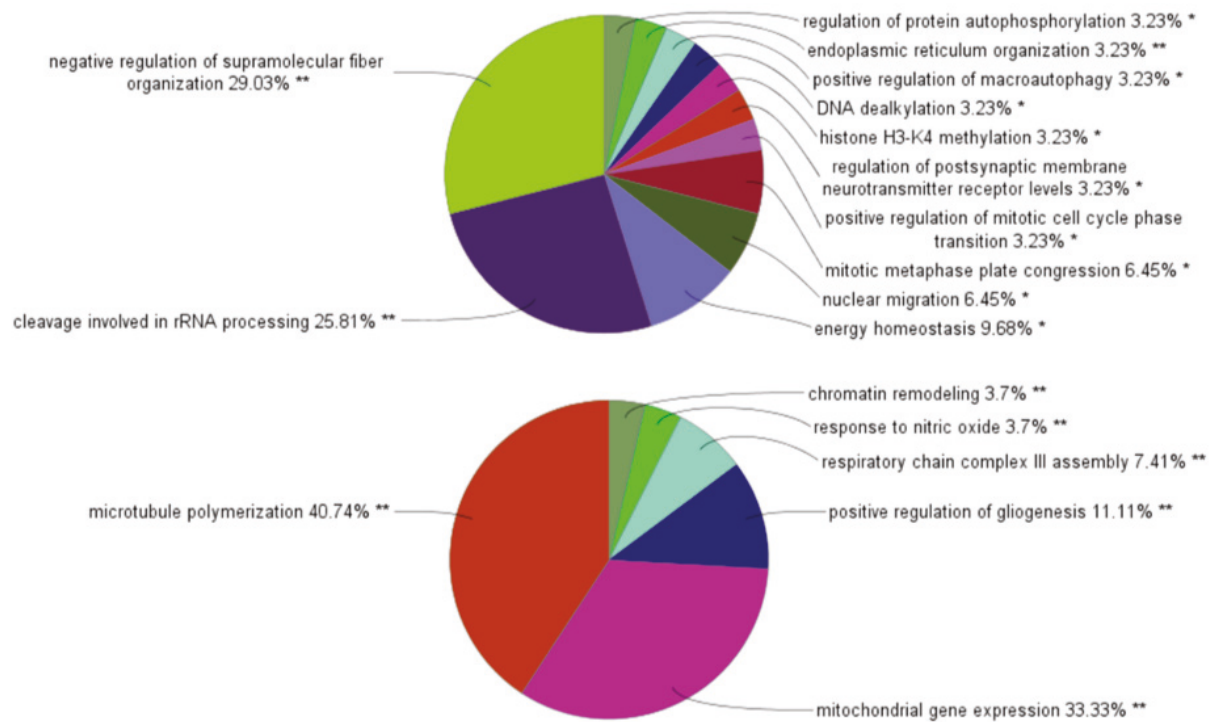
**Figure 7. Enriched ClueGO Gene Ontology (GO) Biological Process (BP) terms.**

GO BP terms for the unique proteins in the untreated (top) and Nva treated (bottom) groups. Percentage shows % of total enriched proteins in each group. * $p < 0.05$, ** $p < 0.01$.
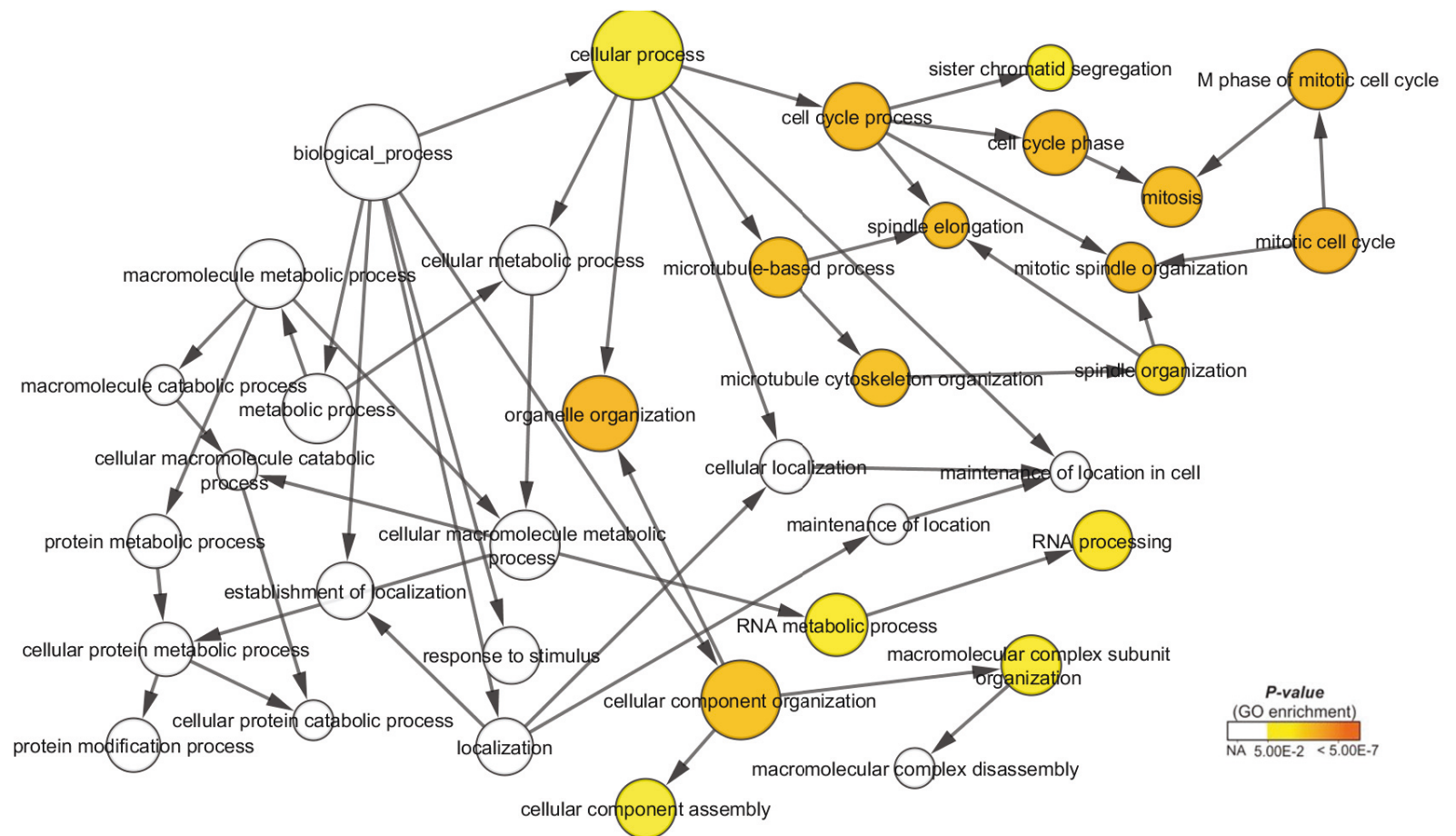
**Figure 8. GO BP terms associated with proteins interacting within ClusterONE significant clusters for the unique proteins in the untreated group.** The colour gradient of the cluster distribution network shows the p-value of each cluster associated with the term, while the darker orange indicates a lower p-value. The size of each node is proportional to the number of proteins in the set. See Supplementary Table 5 for complete GO terms, p-values and protein identification.

**Figure 9. GO BP terms associated with proteins interacting within ClusterONE significant clusters for the unique proteins in the Nva treated group.** The colour gradient of the cluster distribution network shows the p-value of each cluster associated with the term, while the darker orange indicates a lower p-value. The size of each node is proportional to the number of proteins in the set. See Supplementary Table 6 for complete GO terms, p-values and protein identification.

5.3.2 L-Azetidine-2-carboxylic acid

*5.3.2.1 Proteomic Findings*

Samples collected from the control and Aze experimental groups were digested and analysed by LC-MS/MS without any fractionation. The reproducibility of the biological replicates was assessed by scatter plotting and the Pearson correlation coefficient was determined using LFQ intensities (Figure 10A). The Pearson correlations calculated for the experimental groups were deemed acceptable, ranging from 0.938- 0.986. A total of 2627 proteins were identified in pooled samples of the control group and 2479 proteins in pooled samples of the Aze treatment group respectively (Figure 10B). Of these, 2420 were common to both control and treatment groups (Figure 11). 207 proteins were unique to the control group and 59 were unique to the Aze treatment. 55 proteins ($\geq 2$ peptides) in the pool of common proteins that either significantly increased or decreased in abundance were identified (Figure 11) and are described in Table 7.

GO BP analysis was performed on significantly differentially abundant proteins using the using the app BiNGO in Cytoscape (Figures 12 & 13). A full list of GO terms, p-values and protein identifications for each cluster can be found in Supplementary Tables 7 and 8 of the Appendix.
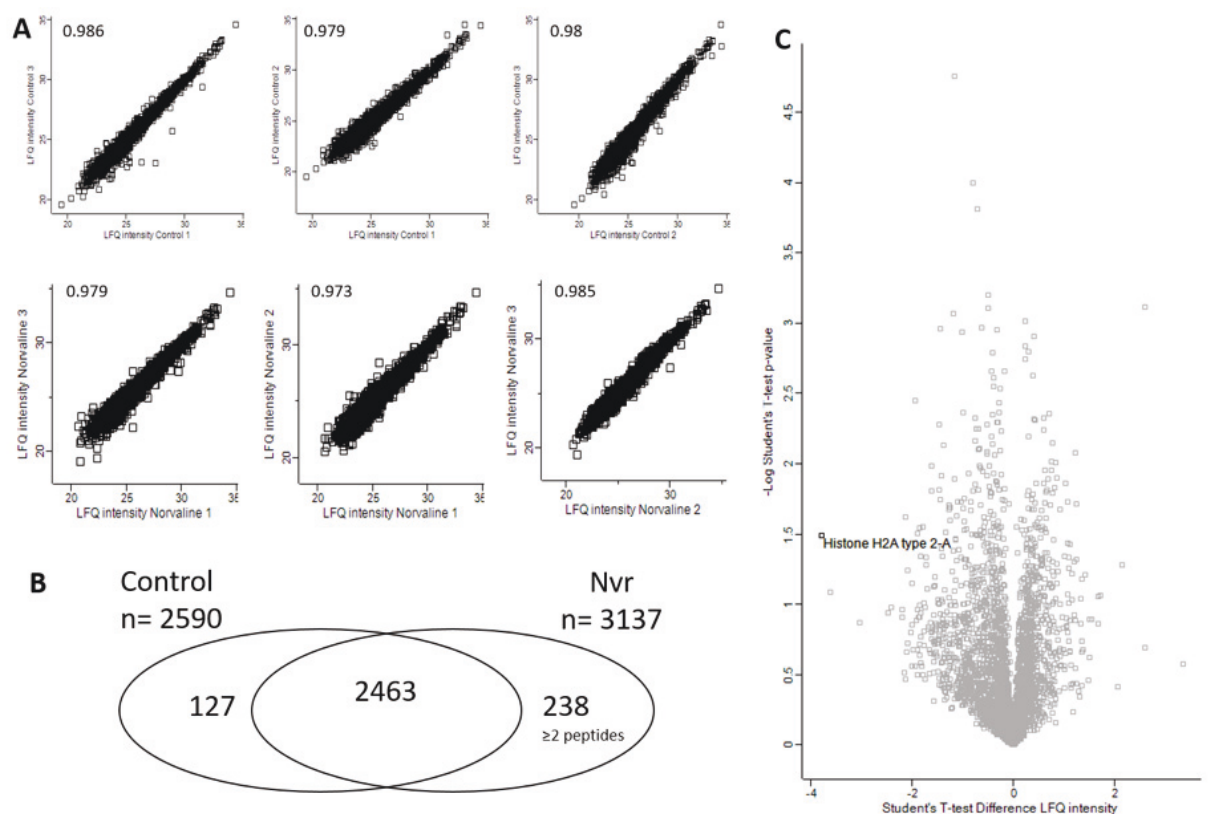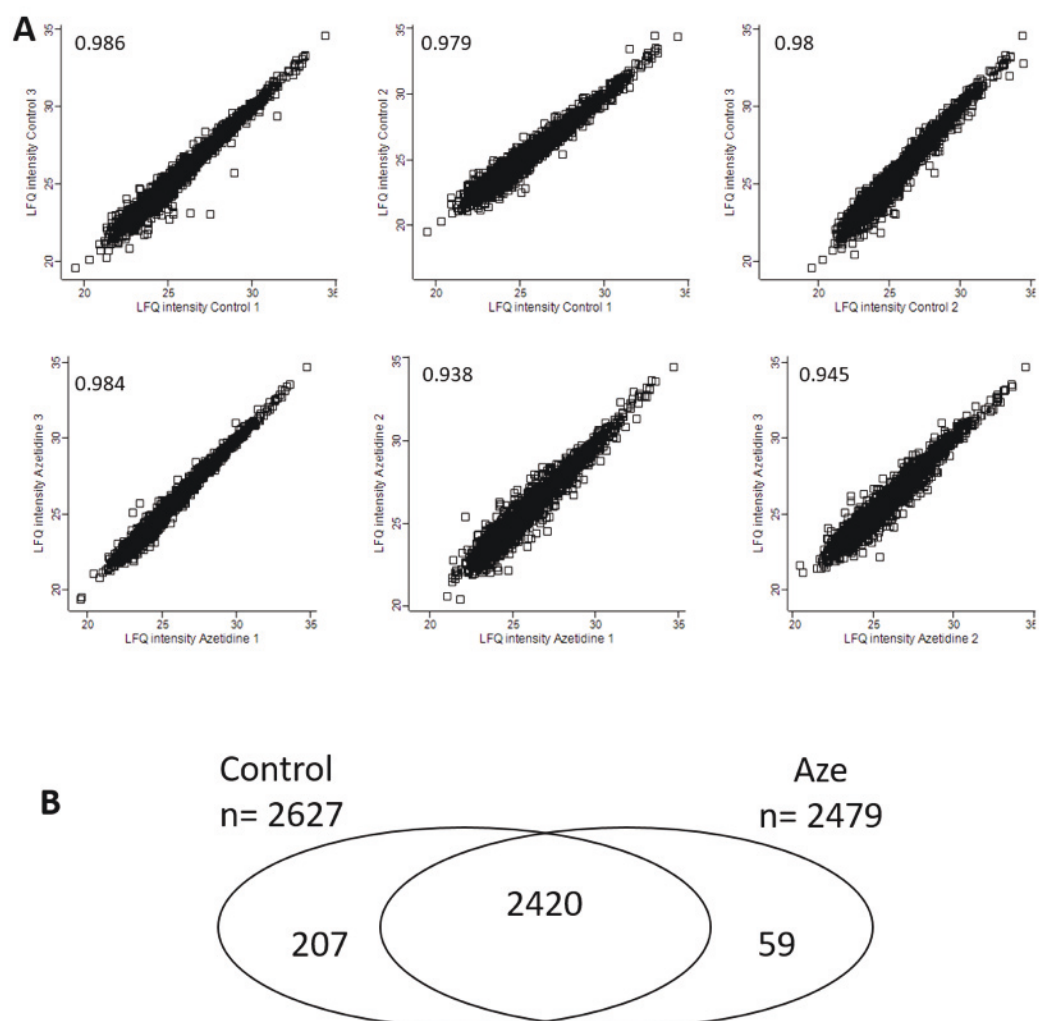
**Figure 10. Proteomic characterization of Aze treated cells.**

Panel A shows scatter plots with Pearson correlation coefficients between LFQ intensities from biological replicates in the experimental groups, panel B shows Venn diagram of proteins identified.
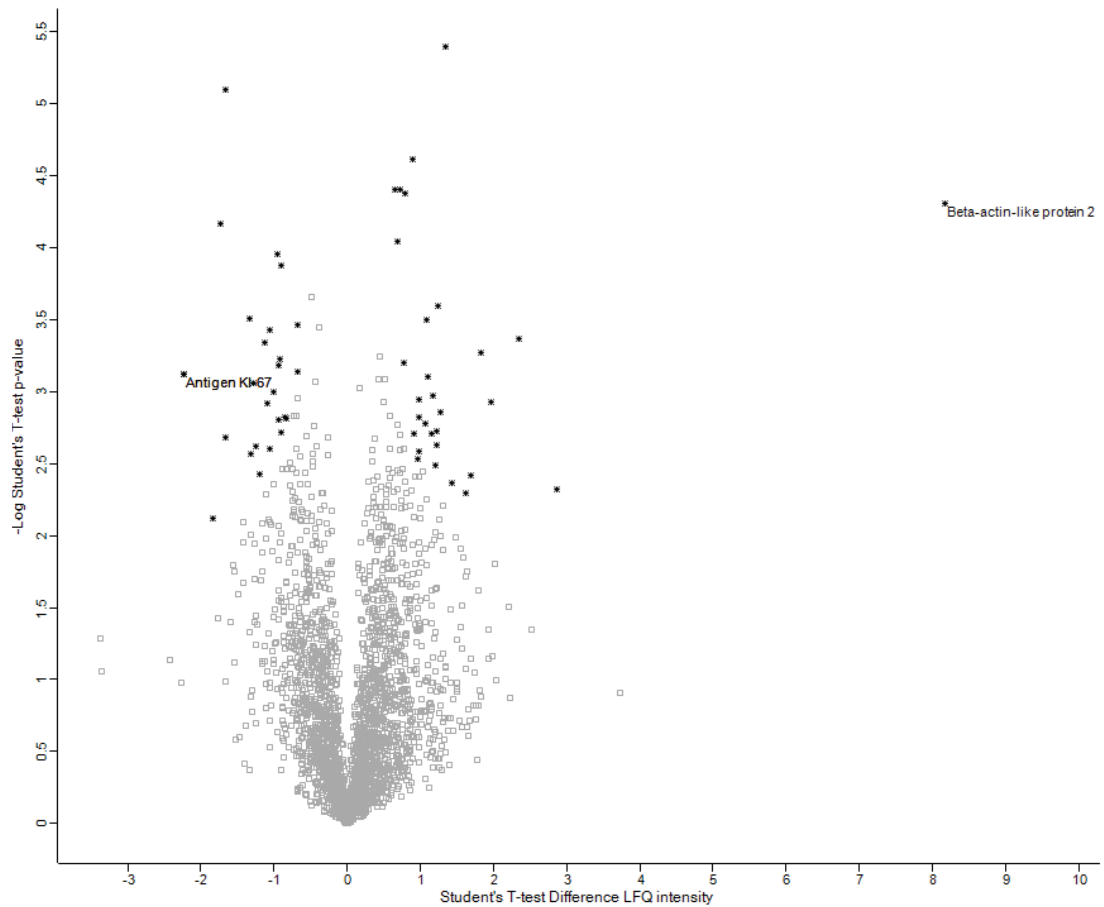
**Figure 11. Scatter plot of LFQ intensity ratios following Aze treatment**.

55 proteins that significantly changed in abundance (black) were identified by mass spectrometry with permutation-based false discovery rate–corrected, two-tailed t test (threshold, FDR-adjusted p-value < 0.05; s0 = 0.1; n = 3). x axis, log2-transformed ratio of proteins in the control over Aze treatment; y axis, –log10-transformed p-values.

**Table 7. SH-SY5Y neuroblastoma cell proteins with significantly (p< 0.05) differentially expressed abundance following 24 h treatment with Aze.** The fold change cut off was lowered (s0=0.1) due to the relatively low number of unique proteins in each condition.

| Protein ID | Protein Name | Student's T-test Difference (Log2(Fold Change)) |
|---|---|---|
| P46013 | Antigen KI-67 | -2.23851 |
| P16401 | Histone H1.5 | -1.83337 |
| Q99453 | Paired mesoderm homeobox protein 2B | -1.7255 |
| P16402 | Histone H1.3;Histone H1.4 | -1.66246 |
| P35251 | Replication factor C subunit 1 | -1.65702 |
| Q14966 | Zinc finger protein 638 | -1.32758 |
| G3XAG1 | Zinc finger protein 512 | -1.32335 |
| Q9P0M6 | Core histone macro-H2A.2;Histone H2A | -1.27865 |
| Q8NC51 | Plasminogen activator inhibitor 1 RNA-binding protein | -1.24885 |
| P35637 | RNA-binding protein FUS | -1.20004 |
| Q86V81 | THO complex subunit 4 | -1.11805 |
| Q96AG4 | Leucine-rich repeat-containing protein 59 | -1.09757 |
| Q9P0L0 | Vesicle-associated membrane protein-associated protein A | -1.0599 |
| O14813 | Paired mesoderm homeobox protein 2A | -1.0484 |
| P27816 | Microtubule-associated protein;Microtubule-associated protein 4 | -0.999165 |
| Q08380 | Galectin-3-binding protein | -0.957201 |
| P26358 | DNA (cytosine-5)-methyltransferase 1 | -0.943516 |
| Q8WTT2 | Nucleolar complex protein 3 homolog | -0.928965 |
| P42166 | Lamina-associated polypeptide 2, isoform alpha;Thymopentin;Thymopoietin | -0.914497 |
| Q9NWH9 | SAFB-like transcription modulator | -0.903877 |
| Q5SSJ5 | Heterochromatin protein 1-binding protein 3 | -0.896633 |
| O95239 | Chromosome-associated kinesin KIF4A | -0.854056 |
| O15294 | UDP-N-acetylglucosamine--peptide N-acetylglucosaminyltransferase 110 kDa subunit | -0.831539 |
| Q8N1G4 | Leucine-rich repeat-containing protein 47 | -0.680112 |
| P42765 | 3-ketoacyl-CoA thiolase, mitochondrial | -0.669971 |
| Q14974 | Importin subunit beta-1 | 0.655556 |
| O00303 | Eukaryotic translation initiation factor 3 subunit F | 0.694747 |
| O75306 | NADH dehydrogenase [ubiquinone] iron-sulfur protein 2, mitochondrial | 0.73226 |
| P26641 | Elongation factor 1-gamma | 0.779774 |
| Q00610 | Clathrin heavy chain;Clathrin heavy chain 1 | 0.787474 |
| Q5H909 | Melanoma-associated antigen D2 | 0.903817 |
| Q8NI27 | THO complex subunit 2 | 0.916466 |

| | | |
|---|---|---|
| O00410 | Importin-5 | 0.962305 |
| P08758 | Annexin;Annexin A5 | 0.97887 |
| Q96QK1 | Vacuolar protein sorting-associated protein 35 | 0.986816 |
| Q9Y295 | Developmentally-regulated GTP-binding protein 1 | 0.99206 |
| O43592 | Exportin-T | 1.06496 |
| Q9UIA9 | Exportin-7 | 1.09344 |
| Q92621 | Nuclear pore complex protein Nup205 | 1.09879 |
| J3QSV6 | Ribosomal L1 domain-containing protein 1 | 1.15489 |
| Q9Y2A7 | Nck-associated protein 1 | 1.17921 |
| Q00325 | Phosphate carrier protein, mitochondrial | 1.20822 |
| Q9BZE4 | Nucleolar GTP-binding protein 1 | 1.21908 |
| Q63HM9 | PI-PLC X domain-containing protein 3 | 1.22163 |
| O95373 | Importin-7 | 1.23524 |
| D6RAC5 | Single-stranded DNA-binding protein 2;Single-stranded DNA-binding protein 3;Single-stranded DNA-binding protein 4 | 1.27205 |
| P0DMV9 | Heat shock 70 kDa protein 1A;Heat shock 70 kDa protein 1B | 1.3422 |
| O14980 | Exportin-1 | 1.43816 |
| Q6PL18 | ATPase family AAA domain-containing protein 2 | 1.61961 |
| P48729 | Casein kinase I isoform alpha;Casein kinase I isoform alpha-like | 1.6946 |
| P41236 | Protein phosphatase inhibitor 2;Protein phosphatase inhibitor 2-like protein 3 | 1.82563 |
| LRWD1 | Leucine-rich repeat and WD repeat-containing protein 1 | 1.96518 |
| Q5SNT2 | Transmembrane protein 201 | 2.35003 |
| E9PF06 | 39S ribosomal protein L3, mitochondrial | 2.87131 |
| Q562R1 | Beta-actin-like protein 2 | 8.17366 |
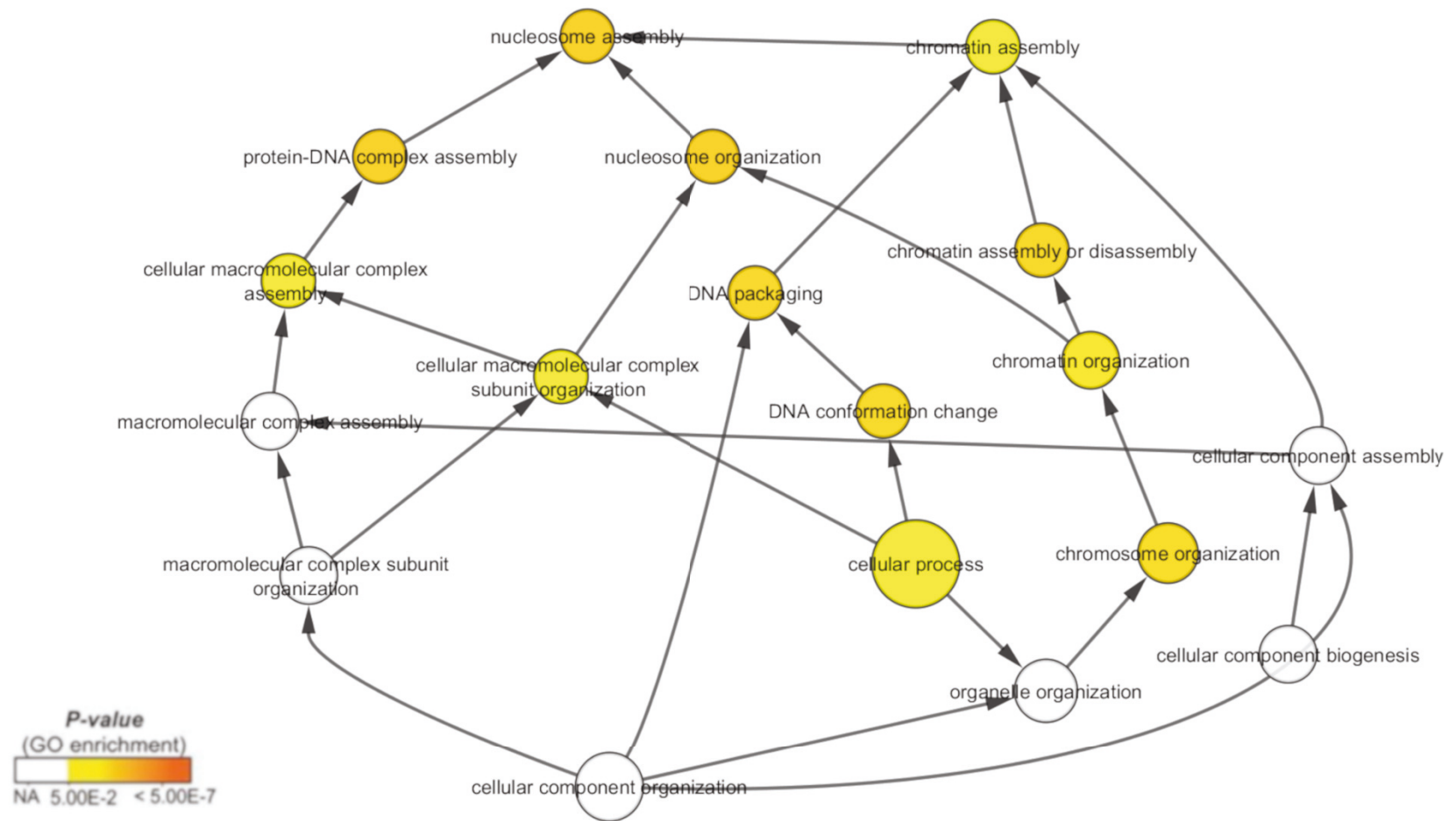
**Figure 12. GO BP terms associated with proteins downregulated following Aze treatment.** The colour gradient of the cluster distribution network shows the p-value of each cluster associated with the term, while the darker orange indicates a lower p-value. The size of each node is proportional to the number of proteins in the set. See Supplementary Table 7 for complete GO terms, p-values and protein identification.
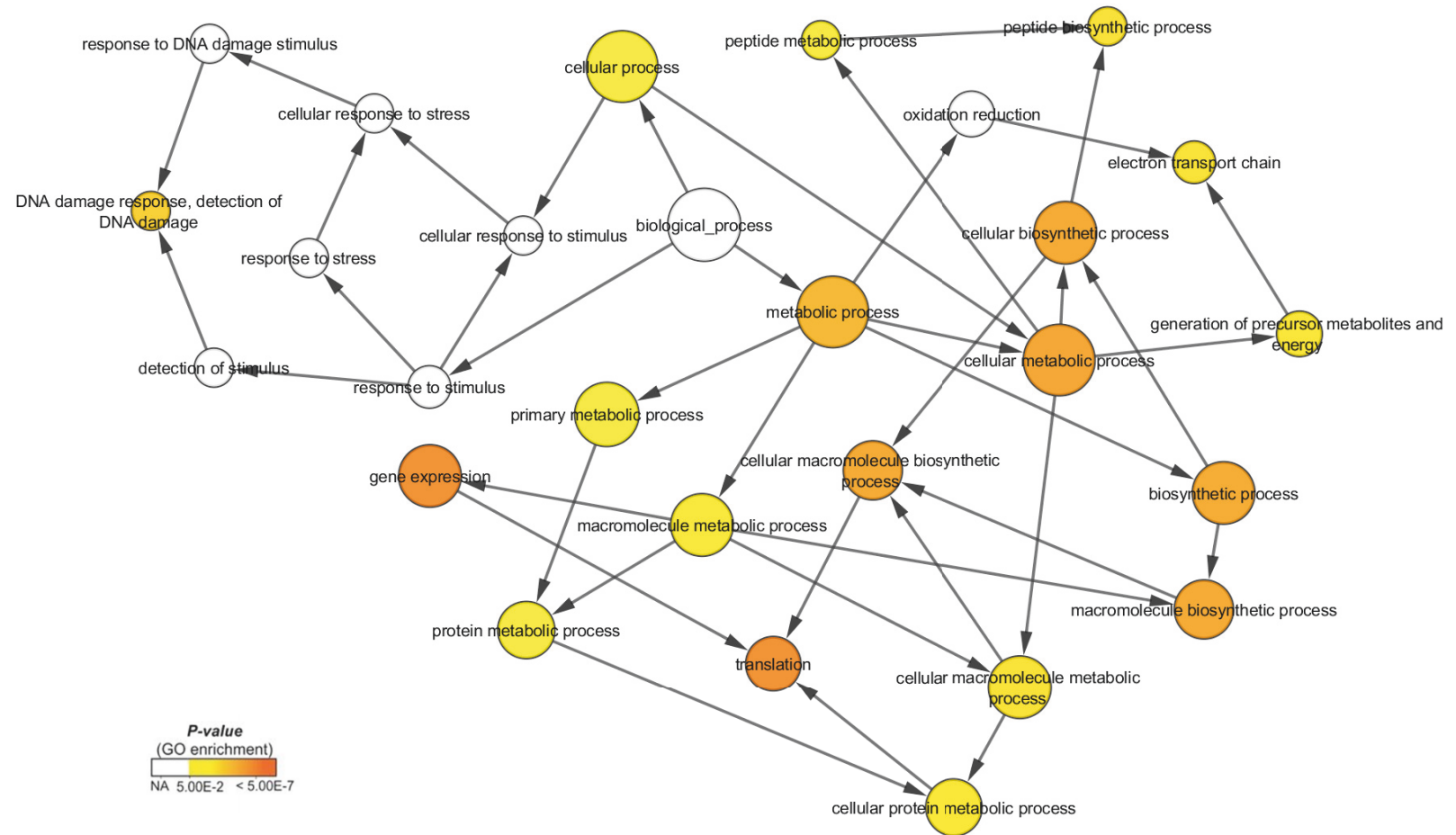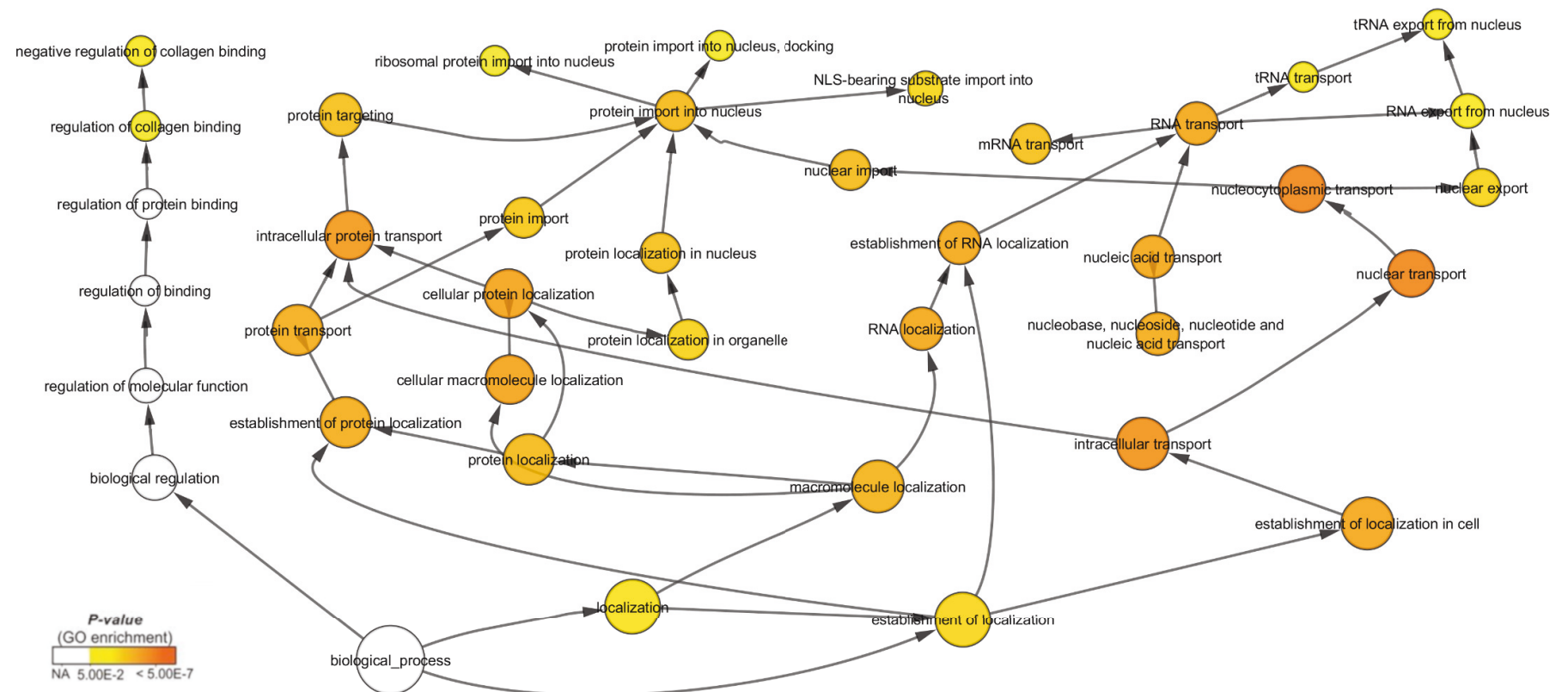
**Figure 13. GO BP terms associated with proteins upregulated following Aze treatment.** The colour gradient of the cluster distribution network shows the p-value of each cluster associated with the term, while the darker orange indicates a lower p-value. The size of each node is proportional to the number of proteins in the set. See Supplementary Table 8 for complete GO terms, p-values and protein identification

## 5.4 Discussion

5.4.1 L-Norvaline

This chapter aimed to perform a holistic proteomic investigation of cells exposed to Nva and Aze in order to further elucidate their mechanisms, and this section focuses on the changes to the proteome observed following Nva treatment. It is shown here that despite sharing 2463 proteins (Figure 5B), only one protein, histone H2A type-2A, was significantly reduced in abundance (Figure 5C). Histone proteins are at the core of nuclear chromatin, which in turn is responsible for the packaging of genetic material during gene expression [246,247]. Although little is known regarding histone H2A type-2A specifically, decreased histone expression in histone H2A variants type-1 and type-K has previously been observed following DNA damage [246] and such disruptions to the histone-DNA equilibrium can lead to errors in transcription and block cell cycle progression [248,249].

An analysis of the unique proteins using GO CC terms (Figure 6) identified the pre-ribosome as the predominant cellular location of proteins present in the control but below the limit of detection in the Nva treatment (henceforth referred to as 'absent'), with many overlapping with the second most common BP term, cleavage involved in ribosomal RNA processing (Figure 7). The absence of these proteins following Nva treatment suggests altered ribosome biogenesis. The absence of RRP1 and RRP9 homologs corresponds to the reduced processing and transport of pre-ribosomal RNA [250,251]. UTP18 and UTP20, components of the 90S small subunit pre-ribosome, are also absent after Nva treatment [252]. Furthermore, the absences of ribosome biogenesis protein BMS1 homolog and NOP14 are associated with decreased 40S ribosomal subunit assembly. The 40S ribosomal subunit is essential to the formation of the pre-initiation complex and is involved in the recognition of the mRNA start codon, which initiates protein translation [253].

Further analysis of the significant clusters and their functions within the control group implicated them in two distinct processes, spliceosomal mRNA processing and the

mitotic cell cycle (Figure 8). The cell cycle is essential to the replication of DNA and generation of daughter cells. Meanwhile, the spliceosome is a molecular machine integral to the processing of nascent precursor messenger RNA (pre-mRNA) to form the mature messenger RNA (mRNA) required for the correct translation of proteins. The ATP-dependent steps of pre-mRNA splicing require the DExD/H box family of proteins to unwind nucleic acids before splicing [254] and interestingly, the ATP binding RNA helicase DHX38 involved in this step of pre-mRNA splicing and proofreading is absent in the Nva treated group. In addition, the nuclei encoded mitochondrial RNA splicing machinery protein DEAH box protein 57 is also unique to the control. The splicing stabilising protein HuB and RNA splicing cofactor SON are upregulated in the Nva treated cells, suggesting inefficient or unstable spliceosome formation [255]. In keeping with the changes observed to histone H2A, SON is also involved in DNA replication and repair [256,257]. These changes suggest that Nva exposure disturbs cellular RNA processing and the molecular machinery that precedes protein translation.

Furthermore, the splicing factor hnRNP C, which is involved in internal ribosome entry site (IRES)-dependent translation during the G2/M phase of the cell cycle, is increased in abundance in the Nva treatment in what may be a compensatory response in the event of missing splicing machinery [258]. Splicing defects have been identified as one of two mechanisms responsible for mutations in the MAPT gene that encodes tau, a microtubule-associated protein that is associated with several neurological disorders characterised by dementia including AD, Pick's disease, and frontotemporal dementia and Parkinsonism linked to Chromosome 17 [259,260]

In addition to disruptions to IRES-dependant translation during G2/M phase of the cell cycle, further evidence of disruption to the cell cycle is presented by the absence of the cell division progression proteins sororin and CDK4 following Nva treatment. Sororin is required for the stable binding of sister chromatids during S and G2 phase and is very sensitive to defects in splicing machinery [261,262]. Additionally, its downregulation is known to suppress cancer cell growth [263]. CDK4 is important for G1 phase progression

and inhibitors of this protein kinase induce cyclic adenosine monophosphate G1 phase arrest [264].

Several enriched terms in the unique to control group were related and contained proteins involved in similar cellular processes. A quarter of enriched proteins were microtubule end constituents and the term negative regulation of supramolecular fiber was the most enriched BP term, also referring to microtubules. Furthermore, within the ClusterONE significant cluster, the term mitotic spindle organisation was highly enriched. The proteins in the first two groups, including CAMSAP2, CLASP1, KIF2C and HDAC6, relate to microtubule organisation and stabilisation during mitosis [265-268]. The third group contains proteins that are also essential to cytokinesis such as the regulator protein PRC1, which crosslinks microtubules during spindle formation [269], and KIF23, a component of the central spindle complex [270]. Together the decreased abundance of these proteins following Nva treatment further suggests disruption to the cell cycle and downregulation or inactivation of these proteins has previously been linked to disordered chromatid separation, G1 arrest and decreased proliferation [271-273].

In addition to changes in the abundance of cytoplasmic ribosomal proteins, Nva treatment also induced changes in abundance to mitochondrial ribosomal proteins indicated by the enriched BP term 'mitochondrial gene expression' (Figure 7). Although cell lysates were not fractionated and instead, whole cell lysates were analysed by LC-MS/MS, GO CC analysis identified 'organellar small ribosomal subunit' as the term with the most constituent proteins (Figure 6). These proteins were exclusively mitochondrial. Nuclear gene expression produces small and large mitochondrial ribosomal subunits, 28S and 39S respectively, that make up the 55S mitoribosome and synthesise the 13 essential proteins of oxidative phosphorylation (OXPHOS) complexes [274]. A total of 10 mitoribosome proteins, representing 13% of the 78 available, were unique to the Nva treatment and related to both the small and large ribosomal subunits [275,276]. The presence of mitochondrial transcription factor B2 (TFB2M), one of the basic components of mitochondrial transcription initiation machinery, and the marked absence of transcription termination factors suggests that, converse to cytoplasmic protein

translation, the synthesis of the 13 OXPHOS complexes in mitochondria continues following Nva treatment [277,278]. This is supported by the detection of UQCC1 and UQCC2, proteins related to the positive regulation of mitochondrial translation that function as assembly factors in the production of respiratory complex III, another enriched BP term ('respiratory complex III assembly') [279]. It is hypothesised that Nva's previously described action as an arginase inhibitor may be responsible, and in addition, a BP enrichment for the term 'response to nitric oxide' was detected.

Other mitochondrial proteins detected via proteomics were the mitochondrial apoptosis-related proteins BAX and endonuclease G, contradicting previous studies where apoptosis was not detected following Nva exposure [280-282]. However, as reported by Suzuki et al., apoptotic cells may not always externalise phosphatidyl-serine, which was how apoptosis was measured previously [282,283]. Mitochondrial fission has been previously observed after Nva treatment and, along with apoptosis, is associated with neurodegeneration [282,284]. Given the historical association between NPAAs and neurodegenerative disease, it is worth noting that several proteins and proteins encoded by genes linked with AD and HD were uniquely identified within the Nva treatment. These include mitochondrial proteins BAX [281], COX7A2L [285], NDUFB3 [286], CYC1 [287], NDUFV3 [288] and COX7A2 [289] and the intracellular proteins LRP1 [290], MAPK3 [285] and GNAQ [291].

The heat shock family of proteins are often expressed in response to cellular stress and the heat shock chaperone protein HSPA8 was unique to the Nva treated cells. HSPA8 plays an important role safeguarding proteostasis in human cells and assists in the proper folding of newly translated and misfolded proteins [292]. The microtubule-constituent beta-tubulin proteins TUBB3 and TUBB4A were also uniquely identified to the Nva treatment and work with chaperones to prevent aberrant protein aggregation in the cytoskeleton in response to ageing and neurodegenerative disease [293]. In contrast to the decreased abundance of cell division related microtubule proteins following Nva treatment, the term 'microtubule polymerization' was the most enriched BP term for the Nva treated cells. While initially this may seem contradictory, polymerization

fundamentally enables cytoskeletal reorganisation and these Nva induced changes may be an early response to microtubule instability [294]. Microtubules have a wide range of functions in neurons and microtubule instability, including the previously mentioned microtubule-associated protein tau, can result in neurological disorders [295].

The data in this section shows that despite only identifying one protein that significantly changed in abundance, the large number of proteins unique to each condition indicate that the proteome of cells exposed to 2000 µM Nva is subject to change following 24 h treatment. The decrease in histone H2A type-2A is suggestive of DNA damage and the absence of proteins involved in ribosome biogenesis proteins and the mitotic cell cycle are indicative of Nva interference with cell cycle progression. Surprisingly, the changes observed to mitochondrial proteins are related to the positive regulation of mitochondrial translation, and, as supported by the enriched term 'response to nitric oxide', are likely by-products of Nva's action as an arginase inhibitor. However, several other proteins detected following Nva treatment have been previously associated with cellular stress and neurodegenerative disease, and it is therefore important for future research to investigate Nva's effect on the proteome independent of its action on arginase. This could be performed using an NO synthase inhibitor, similar to experiments performed in Chapter three.

### 5.4.2 L-Azetidine-2-carboxylic acid

From a total pool of 2420 common proteins, 55 proteins that were differentially expressed were identified (Table 7). There were 30 proteins that significantly increased in abundance and 25 proteins that significantly decreased in abundance following Aze treatment. The most up and downregulated proteins were beta-actin-like protein 2 (ACTLB2) and antigen KI-67 (MKI67) respectively. ACTLB2 is a constituent of the beta-actin isoform of actin and is located in the cytoskeleton. Beta-actin plays an essential role in chromatin remodeling and its upregulation may be in response to abnormal chromatin structure, which would have deleterious effects on gene expression and cell division [296,297]. MKI67 is a nuclear proliferation marker protein and is required to maintain mitotic chromosomes [298]. Its downregulation would result in chromosome

collapse in the cytoplasm following nuclear envelope disassembly and inadequate chromosome segregation during cell division, prolonging mitosis [298]. The changes to both these proteins suggest Aze adversely affects cellular proliferation by interfering with the cell cycle.

The largest subunit of the DNA replication factor C (RFC) family is the fifth most downregulated protein, and while the RFC family is also involved in DNA repair, the downregulated subunit 1 is mainly involved in DNA replication. This is due to its direct interaction with proliferating cell nuclear antigen, which is then loaded onto DNA for subsequent replication by polymerase delta [299]. RFC subunit 1 expression has been associated with increased cell survival following DNA damage and its reduced abundance could be indicative of decreased cellular DNA replication and damage responses [300,301]. Zinc finger (ZnF) proteins 638 and 512 are the sixth and seventh proteins most reduced in abundance. Though ZnF proteins are a biologically abundant and diverse family of proteins, both ZnF 638 and 512 are DNA-binding transcription factors, and while their exact functions are poorly understood, these transcription factors may be downregulated due to insufficient DNA replication upstream [302-304]

This is supported by the downregulation of histones H1.5, H1.3, H2A and chromosome-associated kinesin KIF4A. Histones assist with chromatin formation following DNA replication during the S phase of the cell cycle and, as mentioned previously, their downregulation is associated with DNA damage [246,305]. Decreased histone expression at the G1 checkpoint has been observed following DNA damage induced G1 arrest [306]. Furthermore, a component of the heterochromatin form of chromatin, heterochromatin protein 1-binding protein 3, that maintains chromatin integrity and regulates cell cycle progression is also downregulated following Aze treatment [307]. These proteins fall under the GO BP enriched terms 'protein-DNA complex assembly' and 'nucleosome assembly' (Figure 12).

Interestingly, the most enriched GO BP term amongst the upregulated proteins is 'nucleocytoplasmic transport' (Figure 13). This term refers to the exchange of matter

between the nucleus and cytoplasm, and in the present study consists of several import (importins) and export (exportins) proteins (karyopherins) [308]. These proteins make up a system that facilitates the transport of histones, DNA and RNA polymerase and transcription factors to and from the nucleus [308,309]. An increase in the proteins responsible for the import of histones during the first step of chromatin assembly may be a compensatory response to insufficient protein-DNA complex formation. This is further supported by the upregulation of the nuclear pore complex protein Nup205, which helps maintain the channel by which these proteins are transported through the nuclear envelope, and the leucine-rich repeat and WD repeat-containing protein (LRWD1) [310]. LRWD1 binds to histones and is required for DNA replication initiation at the G1/S checkpoint [311].

The expression of several proteins related to mRNA processing is also significantly affected following Aze treatment. Plasminogen activator inhibitor 1 RNA-binding protein (PAI-RBP1) and FUS are both downregulated RNA-binding proteins, and while FUS binds to pre-mRNA and regulates splicing, PAI-RBP1 is thought to play a role in maintaining the stability of spliced mRNA [312,313]. The splicing of pre-mRNA is coupled with mRNA export and this process is also affected, as indicated by the reduced abundance of the mRNA export factor THO complex subunit 4 (THOC4) and increased abundance of THO complex subunit 2 (THOC2) [314]. These two THOC proteins make up the THO nuclear export complex, which is involved in synapse development and neuron survival in *Caenorhabditis elegans*, and the observed changes are indicative of altered THO complex assembly and may also be linked to decreased mRNA export following insufficient splicing [315].

Several of the upregulated proteins have been associated with neurodegenerative disease in the literature. Significant increases in ACTLB2 and transmembrane protein 201 have been identified disease states such as AD, HD and MS, while heat shock 70 kDa protein 1A is upregulated in the substantia nigra of PD patients [316,317].

Finally, a link to some of the seminal work into Aze toxicity was uncovered when the GO BP term 'negative regulation of collagen binding' was significantly enriched. As mentioned in Chapter two, Aze is incorporated into collagen, a L-proline rich protein, and the upregulation of this term, which contains nucleolar GTP-binding protein 1, may be linked to this process [164]. This is supported by previous research which has found Aze is an inhibitor of collagen synthesis in human fibrosarcoma cells, even at concentrations (250 and 500 µM) that do not induce cell death [318]. While the analysis methods used in the present experiment are insufficient to identify peptides containing incorporated Aze, a method to detect protein modifications resulting from mistranslation is currently being developed in the Rodgers lab in order to identify proteins and peptide sites susceptible to NPAA misincorporation.

The data in this section shows marked changes to chromatin formation and chromosome stability following treatment with 2000 µM Aze for 24 h. These are accompanied by changes to proteins such as DNA replication factor C subunit 1 and ZnF proteins which together suggest abnormal DNA replication and subsequent transcription. Proteins that regulate mRNA processing are also significantly affected following Aze treatment and may be linked to deficits in the mRNA splicing machinery. Like with Nva, several proteins that have been associated with neurodegenerative disease are significantly upregulated following Aze treatment, highlighting the importance of further investigations into the neurotoxic potential of both NPAAs.

## 5.5 Conclusions

This chapter utilised shotgun proteomics to characterise the proteome of cells exposed to Nva or Aze. Taken together, this data improves upon the current knowledge of the cellular mechanisms involved in Nva and Aze-mediated toxicity. Across both NPAAs, histone downregulation was observed, suggestive of altered chromatin formation and abnormal cell cycle progression, which may be mediated by damage to DNA. There is also evidence of alterations to RNA processing and mRNA splicing machinery, which precede protein translation. Finally, a number of the alterations observed following

NPAA exposure were in proteins positively linked to neurodegenerative disease. This data offers new insights into the mechanisms of Nva or Aze toxicity and highlights future areas for investigation in order to more fully understand how these NPAAs induce cytotoxicity, and their potential to cause neurodegeneration.

# Chapter Six:

Concluding remarks and future directions

# CHAPTER SIX: CONCLUDING REMARKS AND FUTURE DIRECTIONS

Amino acids are considered one of the chemical foundations for all life, as the variability among their unique R side chains enables proteins to be synthesised with an enormous diversity of functions from just 20 protein amino acids. This same variability allows for the existence of a large pool of NPAAs, and the formation of amino acid analogues within the wider pool of amino acids. Amino acid analogues have long been identified as inhibitors of biological processes. From the first plant toxicity studies in the 1960s, with bacterial studies closely following in the same decade, NPAA research has continued to grow over the ensuing six decades. The toxicity and mechanisms of some, such as L-canavanine, have been studied in mammals for almost this entire period and are consequently well characterised. However, the emergence of the neurotoxin BMAA reshaped the landscape of NPAA research and the link to neurodegenerative disease posed by the development of ALS-PDC in Guam provided the impetus for an era of renewed interest in NPAA toxicity.

Prior to the commencement of the present research, Nva and Aze were identified as analogous NPAAs with significant potential for human exposure and thus, this project aimed to investigate the toxicity and mechanisms of the two NPAAs. As a consequence, this project has provided the first in-depth toxicological studies of Nva and Aze in a human cell line. This overarching aim was addressed using four sub-aims. The first three were to determine whether either NPAA induced cell death, mitochondrial dysfunction, and which cell death pathways were activated; the results of which are presented in Chapters three and four. Prior to the studies presented in these chapters, evidence supporting the i*n vitro* toxicity of Nva and Aze in humans was significantly lacking. Though both NPAAs induced cytotoxicity, the cellular death pathways activated were different. Necrotic cell death was observed for both Nva and Aze while apoptosis only occurred following Aze treatment. As stated in Chapter three, this difference can be attributed to Nva's secondary mechanism as an arginase inhibitor and resulting antiapoptotic activity. Few studies since Fowden's seminal antimetabolite research in

1967 [38] have studied more than one NPAA concurrently and studying Nva and Aze alongside each other in the present research allowed for the distinction of molecular events that may be occurring as a consequence of misincorporation from those that are occurring independent of misincorporation or due to the activity of the molecule itself, such as Nva's action as an arginase inhibitor, which is supported by both the literature and the data in Chapters three and five. This was further exemplified whilst conducting studies into mitochondrial function. The studies presented in this thesis are the first to identify that treatment with Nva and Aze leads to mitochondrial dysfunction, thus joining the ranks of the few NPAAs implicated in mitochondrial dysfunction, namely L-canavanine and the recently reported L-DOPA [121,204], and presents an interesting area for future NPAA research. It should be noted though that Nva-induced bioenergetic dysfunction was masked by the molecule's additional mechanism and highlights the importance of carefully considering alternative mechanisms when designing experiments to study the effects of NPAA misincorporation.

Finally, the present thesis aimed to perform a holistic proteomic investigation of cells exposed to both NPAAs and, for the first time, a proteomic and pathway analysis of human cells exposed to Nva and Aze is presented in Chapter five. It was hypothesised that protein quality control pathways related to protein misfolding and aggregation such as the ubiquitin proteasomal system and autophagic degradation would be upregulated [319], however, most surprisingly, the alterations in protein abundance observed related to processes that precede protein translation. The finding that exposure to Nva and Aze causes disruptions to the processing of DNA and RNA during cell cycle progression represent the first reported effects of these NPAAs upstream of protein synthesis. However, it must be noted that the results of the current proteomic investigation require further validation and, in future, experiments assessing DNA damage through methods such as quantitative polymerase chain reaction or agarose gel electrophoresis would be beneficial [320].  Changes to the mRNA splicing machinery, such as those observed in Chapter five, are associated with cell cycle defects and aberrant splicing has been detected in tissues from patients with AD, HD and ALS [321,322]. Moving forward, further analysis of the transcriptome using RNA-sequencing would expand on our

current understanding of how these processes are affected following NPAA exposure [323].

The observed cytotoxicity and alterations to the proteome, whilst contributing to our knowledge of Nva and Aze toxicity, do little to confirm incorporation occurred under the present conditions. Thus, future research employing radiolabeled Nva and Aze, as utilised by Main et al. for BMAA [65], would identify whether the observed effects transpired concurrent to or independent of misincorporation. In addition, methods that confirm NPAA activation of aaRS such as an ATP/PPi exchange assay, which estimates the level of substrate activation, and analytical methods that detect incorporation such as the Mass Spectrometry Reporter for Exact Amino acid Decoding (MS-READ) approach could be utilised [324,325]. Furthermore, the proteomic investigation was carried out using whole cell lysates, rather than their fractionated subcellular components. Paulo et al. found that subcellular fractionation resulted in greater proteome coverage than whole cell lysate analysis, and future studies would benefit from utilising this technique to study the proteome of NPAA treated cells in greater detail [326]. All experiments presented in this thesis were conducted using an established secondary cell line and the use of the SH-SY5Y cell line in place of primary neuronal cells poses a limitation on the present studies. Although they have a neuroblast-like morphology when undifferentiated, this cell line does not express mature neuronal markers [327]. Since it is not known whether neurodegeneration targets immature or mature neurons [91], future studies would benefit from the use of differentiated cells. When differentiated, SH-SY5Y cells are morphologically similar to primary neurons with long dendritic processes and increased expression of neuron-specific markers [327]. Alternatively, since NPAAs have been linked to neuron disorders, the present research could be improved upon with the use of primary human neurons. This is because primary cultures are not derived from tumours and are therefore more likely to exhibit the properties of neuronal cells *in vivo* [327].

Another limitation is posed by the concentrations used. The majority of experiments were performed at 2000 μM, and this was chosen based on *in vitro* data available for

other NPAAs, such as BMAA, and following an initial viability assay at a range of concentrations as there is no data on the biologically relevant concentration for either NPAA presently available. While the human dosage for Nva in supplements can be calculated, it is difficult to calculate the dosage for Aze since it is usually consumed in the form of a supplement containing raw sugar beet by-products that have not been analysed to determine the concentration of Aze present. Future studies would benefit from the determination of biologically relevant concentrations that could then be used in subsequent research into the toxicity of these NPAAs. Such concentrations could be determined using urinary amino acid profiles or quantified from blood plasma or serum, the latter of which was used when Cox et al. studied vervets [169].

Overall, the present research was conducted to investigate the toxicity and mechanisms of Nva and Aze within the wider context of their potential to cause neurodegenerative disease. Though not conclusive, the toxicity and toxic phenotype observed provide convincing evidence that prolonged exposure to these NPAAs may contribute to the development of disease. As such, care must be taken to limit human exposure to these NPAAs whilst further research continues to characterise their neurotoxic potential.

# APPENDIX

**Supplementary Table 1. GO CC Enrichment of Proteins Unique to Control.**

| GO-ID | Description | Term p-value | Associated Proteins Found |
|-------|-------------|--------------|---------------------------|
| GO:0005637 | nuclear inner membrane | 1.02E-02 | [LBR, TMEM201, TMPO] |
| GO:0005871 | kinesin complex | 7.28E-03 | [KIF13B, KIF23, KIF2C] |
| GO:0005881 | cytoplasmic microtubule | 1.06E-02 | [CLASP1, HDAC6, KIF2C] |
| GO:1990752 | microtubule end | 9.07E-04 | [CAMSAP2, CLASP1, KIF2C] |
| GO:0030684 | preribosome | 1.29E-07 | [BMS1, NOB1, NOP14, RRP1, RRP9, UTP18, UTP20, WDR37] |
| GO:0030686 | 90S preribosome | 8.65E-06 | [BMS1, NOP14, UTP18, UTP20, WDR37] |
| GO:0030688 | preribosome, small subunit precursor | 1.08E-06 | [NOB1, NOP14, RRP1, UTP20] |
| GO:0032040 | small-subunit processome | 1.09E-04 | [NOP14, RRP9, UTP18, UTP20] |

**Supplementary Table 2. GO CC Enrichment of Proteins Unique to Nva Treatment.**

| GO-ID | Description | Term p-value | Associated Proteins Found |
|-------|-------------|--------------|----------------------------|
| GO:0071203 | WASH complex | 6.74E-04 | [CAPZB, SNX27, WASHC3] |
| GO:0097427 | microtubule bundle | 3.21E-05 | [ATAT1, NUMA1, TPPP3] |
| GO:0019897 | extrinsic component of plasma membrane | 1.68E-04 | [AAK1, ABL2, AKAP9, ESYT2, GNAQ, GNG2, KPNA1, LGALS7B, LYN, NUMA1] |
| GO:0044448 | cell cortex part | 1.65E-05 | [ACTB, BCAP31, CALD1, CAP2, CAPZB, EXOC8, GPSM2, GSN, NUMA1, PCLO, SERPINB6] |
| GO:0030863 | cortical cytoskeleton | 1.96E-05 | [ACTB, BCAP31, CALD1, CAP2, CAPZB, GSN, NUMA1, PCLO, SERPINB6] |
| GO:0030478 | actin cap | 1.86E-04 | [BCAP31, CALD1, GSN] |
| GO:0000313 | organellar ribosome | 1.92E-06 | [MRPL13, MRPL27, MRPL40, MRPS10, MRPS15, MRPS17, MRPS26, MRPS28, MRPS5] |
| GO:0005840 | ribosome | 2.28E-04 | [EIF4A2, MRPL13, MRPL27, MRPL40, MRPS10, MRPS15, MRPS17, MRPS25, MRPS26, MRPS28, MRPS5, RPS10-NUDT3] |
| GO:0044391 | ribosomal subunit | 8.81E-05 | [EIF4A2, MRPL13, MRPL27, MRPL40, MRPS10, MRPS15, MRPS17, MRPS26, MRPS28, MRPS5, RPS10-NUDT3] |
| GO:0098798 | mitochondrial protein complex | 1.13E-05 | [ATP5F1B, BAX, CYC1, MRPL13, MRPL27, MRPL40, MRPS10, MRPS15, MRPS17, MRPS26, MRPS28, MRPS5, NDUFB3, NDUFV3] |
| GO:0000314 | organellar small ribosomal subunit | 1.22E-06 | [MRPS10, MRPS15, MRPS17, MRPS26, MRPS28, MRPS5] |
| GO:0005761 | mitochondrial ribosome | 1.92E-06 | [MRPL13, MRPL27, MRPL40, MRPS10, MRPS15, MRPS17, MRPS26, MRPS28, MRPS5] |
| GO:0015935 | small ribosomal subunit | 1.37E-05 | [EIF4A2, MRPS10, MRPS15, MRPS17, MRPS26, MRPS28, MRPS5, RPS10-NUDT3] |
| GO:0005763 | mitochondrial small ribosomal subunit | 1.22E-06 | [MRPS10, MRPS15, MRPS17, MRPS26, MRPS28, MRPS5] |

**Supplementary Table 3. GO BP Enrichment of Proteins Unique to Control.**

| GO-ID | Description | Term p-value | Associated Proteins Found |
|---|---|---|---|
| GO:0031952 | regulation of protein autophosphorylation | 1.18E-02 | [MVP, RAP2A, RAP2C] |
| GO:0007029 | endoplasmic reticulum organization | 6.73E-04 | [LNPK, RTN4, SEC61A1, VAPB] |
| GO:0016239 | positive regulation of macroautophagy | 1.57E-03 | [GPSM1, HDAC6, PRKAA1, SPTLC1] |
| GO:0035510 | DNA dealkylation | 2.46E-03 | [ALKBH2, ALKBH5, CCDC88A] |
| GO:0051568 | histone H3-K4 methylation | 1.42E-02 | [EHMT2, HIST1H1C, NELFA] |
| GO:0099072 | regulation of postsynaptic membrane neurotransmitter receptor levels | 1.37E-02 | [DLG4, HRAS, TMPO] |
| GO:1901992 | positive regulation of mitotic cell cycle phase transition | 3.48E-03 | [CCDC88A, CDCA5, CDK4, ZMYM2] |
| GO:0051310 | metaphase plate congression | 9.65E-03 | [CDCA5, KIF2C, NDC80] |
| GO:0007080 | mitotic metaphase plate congression | 4.66E-03 | [CDCA5, KIF2C, NDC80] |
| GO:0051647 | nucleus localization | 1.29E-03 | [FHOD1, PTK2, TMEM201] |
| GO:0007097 | nuclear migration | 7.78E-04 | [FHOD1, PTK2, TMEM201] |
| GO:0097009 | energy homeostasis | 4.15E-03 | [ACACB, CHN1, PRKAA1] |
| GO:0050994 | regulation of lipid catabolic process | 1.27E-02 | [ACACB, CDK4, PRKAA1] |
| GO:0071398 | cellular response to fatty acid | 1.27E-02 | [CDK4, CREB1, PRKAA1] |
| GO:0000479 | endonucleolytic cleavage of tricistronic rRNA transcript (SSU-rRNA, 5.8S rRNA, LSU-rRNA) | 1.28E-04 | [BMS1, NOP14, UTP20] |
| GO:0042274 | ribosomal small subunit biogenesis | 3.39E-04 | [BMS1, NOB1, NOP14, UTP18, UTP20] |

| GO:0030490 | maturation of SSU-rRNA | 7.68E-05 | [BMS1, NOB1, NOP14, UTP18, UTP20] |
|---|---|---|---|
| GO:0090502 | RNA phosphodiester bond hydrolysis, endonucleolytic | 5.05E-04 | [BMS1, CCDC88A, NOB1, NOP14, UTP20] |
| GO:0000469 | cleavage involved in rRNA processing | 3.06E-05 | [BMS1, NOB1, NOP14, UTP20] |
| GO:0000460 | maturation of 5.8S rRNA | 1.97E-03 | [NOP14, UTP20, WDR37] |
| GO:0000462 | maturation of SSU-rRNA from tricistronic rRNA transcript (SSU-rRNA, 5.8S rRNA, LSU-rRNA) | 1.35E-04 | [BMS1, NOP14, UTP18, UTP20] |
| GO:0000478 | endonucleolytic cleavage involved in rRNA processing | 1.57E-04 | [BMS1, NOP14, UTP20] |
| GO:0043242 | negative regulation of protein complex disassembly | 1.57E-03 | [CLASP1, HDAC6, PLEKHH2, SPTAN1] |
| GO:1902904 | negative regulation of supramolecular fiber organization | 4.67E-04 | [CLASP1, DYRK1A, HDAC6, NAE1, PLEKHH2, SPTAN1] |
| GO:0007019 | microtubule depolymerization | 2.84E-03 | [CLASP1, HDAC6, KIF2C] |
| GO:0051261 | protein depolymerization | 1.18E-03 | [CLASP1, HDAC6, KIF2C, PLEKHH2, SPTAN1] |
| GO:1901879 | regulation of protein depolymerization | 3.48E-03 | [CLASP1, HDAC6, PLEKHH2, SPTAN1] |
| GO:0031110 | regulation of microtubule polymerization or depolymerization | 2.62E-03 | [CAMSAP2, CLASP1, DYRK1A, HDAC6] |
| GO:1901880 | negative regulation of protein depolymerization | 1.09E-03 | [CLASP1, HDAC6, PLEKHH2, SPTAN1] |
| GO:0031111 | negative regulation of microtubule polymerization or depolymerization | 2.84E-03 | [CLASP1, DYRK1A, HDAC6] |
| GO:0031113 | regulation of microtubule polymerization | 6.40E-03 | [CAMSAP2, CLASP1, DYRK1A] |

**Supplementary Table 4. GO BP Enrichment of Proteins Unique to Nva Treatment.**

| GO-ID | Description | Term p-value | Associated Proteins Found |
|---|---|---|---|
| GO:0006338 | chromatin remodeling | 2.13E-04 | [ABL2, ACTB, BAZ2A, CDK2, CHD2, GATA3, HDAC1, HNRNPC, SMARCD2, TPM1] |
| GO:0071731 | response to nitric oxide | 2.95E-04 | [CDK2, DNM2, EGLN1, NELFE] |
| GO:0017062 | respiratory chain complex III assembly | 2.22E-04 | [LYRM7, UQCC1, UQCC2] |
| GO:0034551 | mitochondrial respiratory chain complex III assembly | 2.22E-04 | [LYRM7, UQCC1, UQCC2] |
| GO:0010001 | glial cell differentiation | 1.02E-04 | [ATG5, GFAP, GSN, HDAC1, HMGCL, LGALS7B, LRP1, LYN, MAPK3, METTL3, MTOR, NFIB] |
| GO:0014013 | regulation of gliogenesis | 3.00E-04 | [ATG5, EZH2, GFAP, HDAC1, HMGCL, LGALS7B, LYN, MTOR] |
| GO:0014015 | positive regulation of gliogenesis | 5.67E-05 | [ATG5, GFAP, HDAC1, HMGCL, LGALS7B, LYN, MTOR] |
| GO:0022411 | cellular component disassembly | 7.93E-08 | [ATG3, ATG5, BAX, CAPZB, CDK2, CHMP3, ENDOG, EXOC8, GSN, GSPT2, HSPA8, KPNA1, LRP1, MRPL13, MRPL27, MRPL40, MRPS10, MRPS15, MRPS17, MRPS25, MRPS26, MRPS28, MRPS5, SMARCD2, STMN2, TMOD3] |
| GO:0032984 | protein-containing complex disassembly | 7.57E-07 | [CAPZB, CHMP3, GSN, GSPT2, HSPA8, MRPL13, MRPL27, MRPL40, MRPS10, MRPS15, MRPS17, MRPS25, MRPS26, MRPS28, MRPS5, SMARCD2, STMN2, TMOD3] |
| GO:0043624 | cellular protein complex disassembly | 3.27E-07 | [CAPZB, GSN, GSPT2, MRPL13, MRPL27, MRPL40, MRPS10, MRPS15, MRPS17, MRPS25, MRPS26, MRPS28, MRPS5, STMN2, TMOD3] |
| GO:0140053 | mitochondrial gene expression | 4.47E-08 | [MRPL13, MRPL27, MRPL40, MRPS10, MRPS15, MRPS17, MRPS25, MRPS26, MRPS28, MRPS5, PUS1, TFB2M, UQCC1, UQCC2] |

| GO:0006414 | translational elongation | 4.67E-06 | [EEFSEC, MRPL13, MRPL27, MRPL40, MRPS10, MRPS15, MRPS17, MRPS25, MRPS26, MRPS28, MRPS5] |
|---|---|---|---|
| GO:0006415 | translational termination | 1.71E-07 | [GSPT2, MRPL13, MRPL27, MRPL40, MRPS10, MRPS15, MRPS17, MRPS25, MRPS26, MRPS28, MRPS5] |
| GO:0032543 | mitochondrial translation | 2.66E-07 | [MRPL13, MRPL27, MRPL40, MRPS10, MRPS15, MRPS17, MRPS25, MRPS26, MRPS28, MRPS5, UQCC1, UQCC2] |
| GO:0070125 | mitochondrial translational elongation | 3.27E-07 | [MRPL13, MRPL27, MRPL40, MRPS10, MRPS15, MRPS17, MRPS25, MRPS26, MRPS28, MRPS5] |
| GO:0070126 | mitochondrial translational termination | 3.99E-07 | [MRPL13, MRPL27, MRPL40, MRPS10, MRPS15, MRPS17, MRPS25, MRPS26, MRPS28, MRPS5] |
| GO:0032886 | regulation of microtubule-based process | 2.21E-04 | [AKAP9, ATAT1, BICD2, CAPZB, CHMP3, CLIP1, GPSM2, LAMP1, NUMA1, STMN2, TUBB3, TUBB4A] |
| GO:1902903 | regulation of supramolecular fiber organization | 2.83E-05 | [AKAP9, ARHGAP35, CAPZB, CLIP1, GSN, HSPA8, MTOR, NUMA1, PAK3, PFN2, PXN, SMAD3, STMN2, TMOD3, TPM1, TUBB3, TUBB4A] |
| GO:0031109 | microtubule polymerization or depolymerization | 4.26E-05 | [AKAP9, CAPZB, CLIP1, NUMA1, STMN2, TPPP3, TUBB3, TUBB4A, TUBGCP3] |
| GO:0046785 | microtubule polymerization | 3.42E-06 | [AKAP9, CAPZB, CLIP1, NUMA1, STMN2, TPPP3, TUBB3, TUBB4A, TUBGCP3] |
| GO:0032271 | regulation of protein polymerization | 7.01E-05 | [AKAP9, CAPZB, CLIP1, GSN, MTOR, NUMA1, PAK3, PFN2, STMN2, TMOD3, TUBB3, TUBB4A] |
| GO:0070507 | regulation of microtubule cytoskeleton organization | 2.50E-04 | [AKAP9, ATAT1, BICD2, CAPZB, CHMP3, CLIP1, GPSM2, NUMA1, STMN2, TUBB3, TUBB4A] |
| GO:0051258 | protein polymerization | 6.37E-06 | [AKAP9, CAPZB, CHMP3, CLIP1, DNM2, GSN, MTOR, NUMA1, PAK3, PFN2, STMN2, TMOD3, TPPP3, TUBB3, TUBB4A, TUBGCP3] |
| GO:0031110 | regulation of microtubule polymerization or depolymerization | 9.84E-05 | [AKAP9, CAPZB, CLIP1, NUMA1, STMN2, TUBB3, TUBB4A] |

| GO-ID | Description | p-value | Proteins in test set |
|---|---|---|---|
| GO:0032272 | negative regulation of protein polymerization | 3.37E-05 | [CAPZB, GSN, PFN2, STMN2, TMOD3, TUBB3, TUBB4A] |
| GO:0031113 | regulation of microtubule polymerization | 6.30E-06 | [AKAP9, CAPZB, CLIP1, NUMA1, STMN2, TUBB3, TUBB4A] |
| GO:0031115 | negative regulation of microtubule polymerization | 6.53E-05 | [CAPZB, STMN2, TUBB3, TUBB4A] |

**Supplementary Table 5. GO BP Enrichment of Significant Cluster Unique to Control.**

| GO-ID | Description | p-value | corr p-value | Proteins in test set |
|---|---|---|---|---|
| 51301 | cell division | 5.46E-08 | 2.63E-05 | TPX2,PRC1,CDK4,CDCA5,KIF23,KIF2C,CLASP1,NDC80 |
| 42254 | ribosome biogenesis | 9.95E-08 | 2.63E-05 | NOP14,BMS1,RRP1,UTP20,UTP18,RRP9 |
| 6996 | organelle organization | 1.89E-07 | 3.13E-05 | EHMT2,CDCA5,KIF23,HDAC6,NDC80,HIST2H2AC,TPX2,PRC1,DLG4,BMS1,KIF2C,HRAS,CLASP1 |
| 278 | mitotic cell cycle | 2.37E-07 | 3.13E-05 | TPX2,PRC1,CDK4,CDCA5,KIF23,KIF2C,CLASP1,NDC80 |
| 22402 | cell cycle process | 4.83E-07 | 4.91E-05 | TPX2,PRC1,CDK4,CDCA5,KIF23,KIF2C,HRAS,CLASP1,NDC80 |
| 22403 | cell cycle phase | 6.62E-07 | 4.91E-05 | TPX2,PRC1,CDK4,CDCA5,KIF23,KIF2C,CLASP1,NDC80 |
| 6364 | rRNA processing | 7.21E-07 | 4.91E-05 | NOP14,RRP1,UTP20,UTP18,RRP9 |
| 44085 | cellular component biogenesis | 7.44E-07 | 4.91E-05 | NOP14,DLG4,BMS1,RRP1,UTP20,HRAS,UTP18,HDAC6,TUBA4A,RRP9,HIST2H2AC |
| 16072 | rRNA metabolic process | 8.84E-07 | 5.19E-05 | NOP14,RRP1,UTP20,UTP18,RRP9 |
| 22613 | ribonucleoprotein complex biogenesis | 1.06E-06 | 5.59E-05 | NOP14,BMS1,RRP1,UTP20,UTP18,RRP9 |
| 0000279 | M phase | 2.22E-06 | 6.71E-05 | TPX2,PRC1,CDCA5,KIF23,KIF2C,CLASP1,NDC80 |
| 7052 | mitotic spindle organization | 2.94E-06 | 6.71E-05 | PRC1,KIF23,NDC80 |

| | | | | |
|---|---|---|---|---|
| 280 | nuclear division | 2.99E-06 | 6.71E-05 | TPX2,CDCA5,KIF23,KIF2C,CLASP1,NDC80 |
| 7067 | mitosis | 2.99E-06 | 6.71E-05 | TPX2,CDCA5,KIF23,KIF2C,CLASP1,NDC80 |
| 22 | mitotic spindle elongation | 3.18E-06 | 6.71E-05 | PRC1,KIF23 |
| 51231 | spindle elongation | 3.18E-06 | 6.71E-05 | PRC1,KIF23 |
| 447 | endonucleolytic cleavage in ITS1 to separate SSU-rRNA from 5.8S rRNA and LSU-rRNA from tricistronic rRNA transcript (SSU-rRNA, 5.8S rRNA, LSU-rRNA) | 3.18E-06 | 6.71E-05 | NOP14,UTP20 |
| 462 | maturation of SSU-rRNA from tricistronic rRNA transcript (SSU-rRNA, 5.8S rRNA, LSU-rRNA) | 3.18E-06 | 6.71E-05 | NOP14,UTP20 |
| 469 | cleavage involved in rRNA processing | 3.18E-06 | 6.71E-05 | NOP14,UTP20 |
| 472 | endonucleolytic cleavage to generate mature 5'-end of SSU-rRNA from (SSU-rRNA, 5.8S rRNA, LSU-rRNA) | 3.18E-06 | 6.71E-05 | NOP14,UTP20 |
| 478 | endonucleolytic cleavage involved in rRNA processing | 3.18E-06 | 6.71E-05 | NOP14,UTP20 |
| 479 | endonucleolytic cleavage of tricistronic rRNA transcript (SSU-rRNA, 5.8S rRNA, LSU-rRNA) | 3.18E-06 | 6.71E-05 | NOP14,UTP20 |
| 480 | endonucleolytic cleavage in 5'-ETS of tricistronic rRNA transcript (SSU-rRNA, 5.8S rRNA, LSU-rRNA) | 3.18E-06 | 6.71E-05 | NOP14,UTP20 |
| 34471 | ncRNA 5'-end processing | 3.18E-06 | 6.71E-05 | NOP14,UTP20 |
| 967 | rRNA 5'-end processing | 3.18E-06 | 6.71E-05 | NOP14,UTP20 |

| 87 | M phase of mitotic cell cycle | 3.56E-06 | 7.22E-05 | TPX2,CDCA5,KIF23,KIF2C,CLASP1,NDC80 |
|---|---|---|---|---|
| 48285 | organelle fission | 3.73E-06 | 7.30E-05 | TPX2,CDCA5,KIF23,KIF2C,CLASP1,NDC80 |
| 7017 | microtubule-based process | 4.30E-06 | 8.11E-05 | PRC1,KIF23,KIF2C,CLASP1,NDC80,TUBA4A |
| 226 | microtubule cytoskeleton organization | 5.53E-06 | 1.01E-04 | PRC1,KIF23,KIF2C,CLASP1,NDC80 |
| 16043 | cellular component organization | 6.31E-06 | 1.08E-04 | EHMT2,CDCA5,KIF23,HDAC6,NDC80,TUBA4A,HIST2H2AC,TPX2,CREB1,PRC1,DLG4,BMS1,KIF2C,HRAS,CLASP1 |
| 7049 | cell cycle | 6.35E-06 | 1.08E-04 | TPX2,PRC1,CDK4,CDCA5,KIF23,KIF2C,HRAS,CLASP1,NDC80 |
| 30490 | maturation of SSU-rRNA | 9.52E-06 | 1.52E-04 | NOP14,UTP20 |
| 966 | RNA 5'-end processing | 9.52E-06 | 1.52E-04 | NOP14,UTP20 |
| 7010 | cytoskeleton organization | 1.11E-05 | 1.72E-04 | PRC1,DLG4,KIF23,KIF2C,HRAS,CLASP1,NDC80 |
| 460 | maturation of 5.8S rRNA | 1.90E-05 | 2.79E-04 | NOP14,UTP20 |
| 466 | maturation of 5.8S rRNA from tricistronic rRNA transcript (SSU-rRNA, 5.8S rRNA, LSU-rRNA) | 1.90E-05 | 2.79E-04 | NOP14,UTP20 |
| 34470 | ncRNA processing | 2.16E-05 | 3.09E-04 | NOP14,RRP1,UTP20,UTP18,RRP9 |
| 34660 | ncRNA metabolic process | 5.69E-05 | 7.91E-04 | NOP14,RRP1,UTP20,UTP18,RRP9 |
| 43242 | negative regulation of protein complex disassembly | 5.84E-05 | 7.91E-04 | SPTAN1,HDAC6,CLASP1 |
| 7051 | spindle organization | 9.29E-05 | 1.23E-03 | PRC1,KIF23,NDC80 |
| 32886 | regulation of microtubule-based process | 9.87E-05 | 1.27E-03 | TPX2,HDAC6,CLASP1 |
| 43244 | regulation of protein complex disassembly | 1.11E-04 | 1.36E-03 | SPTAN1,HDAC6,CLASP1 |
| 7163 | establishment or maintenance of cell polarity | 1.11E-04 | 1.36E-03 | DLG4,CLASP1,NDC80 |
| 6396 | RNA processing | 4.41E-04 | 5.30E-03 | NOP14,RRP1,DHX38,UTP20,UTP18,RRP9 |

| 51640 | organelle localization | 6.81E-04 | 7.99E-03 | CDCA5,HDAC6,NDC80 |
|---|---|---|---|---|
| 7018 | microtubule-based movement | 1.01E-03 | 1.16E-02 | KIF23,KIF2C,TUBA4A |
| 16070 | RNA metabolic process | 1.31E-03 | 1.48E-02 | NOP14,CREB1,RRP1,DHX38,UTP20,UTP18,RRP9 |
| 43933 | macromolecular complex subunit organization | 1.58E-03 | 1.73E-02 | DLG4,BMS1,KIF2C,HRAS,TUBA4A,HIST2H2AC |
| 70843 | misfolded protein transport | 1.82E-03 | 1.78E-02 | HDAC6 |
| 70845 | polyubiquitinated misfolded protein transport | 1.82E-03 | 1.78E-02 | HDAC6 |
| 70844 | polyubiquitinated protein transport | 1.82E-03 | 1.78E-02 | HDAC6 |
| 70846 | Hsp90 deacetylation | 1.82E-03 | 1.78E-02 | HDAC6 |
| 10727 | negative regulation of hydrogen peroxide metabolic process | 1.82E-03 | 1.78E-02 | HDAC6 |
| 90042 | tubulin deacetylation | 1.82E-03 | 1.78E-02 | HDAC6 |
| 70 | mitotic sister chromatid segregation | 1.93E-03 | 1.85E-02 | CDCA5,NDC80 |
| 819 | sister chromatid segregation | 2.03E-03 | 1.92E-02 | CDCA5,NDC80 |
| 51493 | regulation of cytoskeleton organization | 2.15E-03 | 1.99E-02 | TPX2,SPTAN1,CLASP1 |
| 51276 | chromosome organization | 2.27E-03 | 2.06E-02 | EHMT2,CDCA5,HDAC6,NDC80,HIST2H2AC |
| 90305 | nucleic acid phosphodiester bond hydrolysis | 2.38E-03 | 2.13E-02 | NOP14,UTP20 |
| 70507 | regulation of microtubule cytoskeleton organization | 2.62E-03 | 2.30E-02 | TPX2,CLASP1 |
| 32916 | positive regulation of transforming growth factor-beta3 production | 3.63E-03 | 2.88E-02 | CREB1 |
| 30951 | establishment or maintenance of microtubule cytoskeleton polarity | 3.63E-03 | 2.88E-02 | KIF2C |

| 35090 | maintenance of apical/basal cell polarity | 3.63E-03 | 2.88E-02 | DLG4 |
|---|---|---|---|---|
| 30011 | maintenance of cell polarity | 3.63E-03 | 2.88E-02 | DLG4 |
| 90035 | positive regulation of cellular chaperone-mediated protein complex assembly | 3.63E-03 | 2.88E-02 | HDAC6 |
| 90034 | regulation of cellular chaperone-mediated protein complex assembly | 3.63E-03 | 2.88E-02 | HDAC6 |
| 34621 | cellular macromolecular complex subunit organization | 3.66E-03 | 2.88E-02 | BMS1,KIF2C,TUBA4A,HIST2H2AC |
| 51129 | negative regulation of cellular component organization | 3.93E-03 | 3.05E-02 | SPTAN1,HDAC6,CLASP1 |
| 82 | G1/S transition of mitotic cell cycle | 3.98E-03 | 3.05E-02 | CDK4,CDCA5 |
| 7612 | learning | 4.45E-03 | 3.35E-02 | DLG4,HRAS |
| 22607 | cellular component assembly | 5.05E-03 | 3.76E-02 | DLG4,BMS1,HRAS,HDAC6,TUBA4A,HIST2H2AC |
| 32910 | regulation of transforming growth factor-beta3 production | 5.44E-03 | 3.83E-02 | CREB1 |
| 30952 | establishment or maintenance of cytoskeleton polarity | 5.44E-03 | 3.83E-02 | KIF2C |
| 6515 | misfolded or incompletely synthesized protein catabolic process | 5.44E-03 | 3.83E-02 | HDAC6 |
| 32418 | lysosome localization | 5.44E-03 | 3.83E-02 | HDAC6 |
| 51494 | negative regulation of cytoskeleton organization | 5.62E-03 | 3.90E-02 | SPTAN1,CLASP1 |
| 10467 | gene expression | 6.00E-03 | 4.11E-02 | NOP14,CREB1,RRP1,DHX38,UTP20,UTP18,RRP9 |
| 65003 | macromolecular complex assembly | 6.64E-03 | 4.50E-02 | DLG4,BMS1,HRAS,TUBA4A,HIST2H2AC |

| 34983 | peptidyl-lysine deacetylation | 7.25E-03 | 4.54E-02 | HDAC6 |
|---|---|---|---|---|
| 70841 | inclusion body assembly | 7.25E-03 | 4.54E-02 | HDAC6 |
| 70842 | aggresome assembly | 7.25E-03 | 4.54E-02 | HDAC6 |
| 35022 | positive regulation of Rac protein signal transduction | 7.25E-03 | 4.54E-02 | HRAS |
| 10671 | negative regulation of oxygen and reactive oxygen species metabolic process | 7.25E-03 | 4.54E-02 | HDAC6 |
| 7019 | microtubule depolymerization | 7.25E-03 | 4.54E-02 | KIF2C |
| 51656 | establishment of organelle localization | 7.31E-03 | 4.54E-02 | CDCA5,NDC80 |
| 6275 | regulation of DNA replication | 7.92E-03 | 4.85E-02 | GMNN,HRAS |
| 9987 | cellular process | 8.03E-03 | 4.85E-02 | NOP14,MAP2K2,EHMT2,CDCA5,RRP1,KIF23,UTP18,HDAC6,NDC80,TUBA4A,RRP9,HIST2H2AC,TPX2,CREB1,PRC1,CDK4,DLG4,BMS1,DHX38,UTP20,KIF2C,HRAS,CLASP1 |
| 51726 | regulation of cell cycle | 8.09E-03 | 4.85E-02 | TPX2,CDK4,GMNN,HRAS |
| 51261 | protein depolymerization | 9.06E-03 | 4.98E-02 | KIF2C |
| 51313 | attachment of spindle microtubules to chromosome | 9.06E-03 | 4.98E-02 | NDC80 |
| 60632 | regulation of microtubule-based movement | 9.06E-03 | 4.98E-02 | HDAC6 |
| 10458 | exit from mitosis | 9.06E-03 | 4.98E-02 | CLASP1 |
| 8608 | attachment of spindle microtubules to kinetochore | 9.06E-03 | 4.98E-02 | NDC80 |
| 51788 | response to misfolded protein | 9.06E-03 | 4.98E-02 | HDAC6 |
| 10870 | positive regulation of receptor biosynthetic process | 9.06E-03 | 4.98E-02 | HDAC6 |

| GO-ID | Description | p-value | corr p-value | Proteins in test set |
|---|---|---|---|---|
| 60236 | regulation of mitotic spindle organization | 9.06E-03 | 4.98E-02 | TPX2 |

**Supplementary Table 6. GO BP Enrichment of Significant Cluster Unique to Nva Treatment.**

| GO-ID | Description | p-value | corr p-value | Proteins in test set |
|---|---|---|---|---|
| 6412 | translation | 1.57E-09 | 2.30E-07 | MRPS17, MRPS15, MRPS25, MRPL27, MRPS10, MRPL15, MRPL13, MRPS5 |
| 10467 | gene expression | 5.84E-09 | 4.26E-07 | MRPS17, BTF3, PPIL1, MRPS15, MRPS25, MRPL27, MRPS10, SNRPB2, MRPL15, TFB2M, MRPL13, MRPS5 |
| 44237 | cellular metabolic process | 7.28E-08 | 3.54E-06 | MRPS28, MRPS17, BTF3,MRPS26,PPIL1,MRPS15,MDH1,MRPS25,NDUFB3,MRPL27,MRPS10,MRPL15,TFB2M,MRPL13,MRPS5,UQCRFS1,SNRPB2,CYC1 |
| 44249 | cellular biosynthetic process | 1.57E-07 | 5.37E-06 | MRPS28,MRPS17,BTF3,MRPS26,MRPS15,MRPS25,MRPL27,MRPS10,MRPL15,TFB2M,MRPL13,MRPS5 |
| 34645 | cellular macromolecule biosynthetic process | 1.84E-07 | 5.37E-06 | MRPS17,BTF3,MRPS15,MRPS25,MRPL27,MRPS10,MRPL15,TFB2M,MRPL13,MRPS5 |
| 9059 | macromolecule biosynthetic process | 2.22E-07 | 5.41E-06 | MRPS17,BTF3,MRPS15,MRPS25,MRPL27,MRPS10,MRPL15,TFB2M,MRPL13,MRPS5 |

| 9058 | biosynthetic process | 3.17E-07 | 6.61E-06 | MRPS28,MRPS17,BTF3,MRPS26,MRPS15,MRPS25,MRPL27,MRPS10,MRPL15,TFB2M,MRPL13,MRPS5 |
|---|---|---|---|---|
| 8152 | metabolic process | 1.61E-06 | 2.95E-05 | MRPS28,MRPS17,BTF3,MRPS26,PPIL1,MRPS15,MDH1,MRPS25,NDUFB3,MRPL27,MRPS10,MRPL15,TFB2M,MRPL13,MRPS5,UQCRFS1,SNRPB2,CYC1 |
| 42769 | DNA damage response, detection of DNA damage | 2.50E-05 | 4.06E-04 | MRPS28,MRPS26 |
| 43043 | peptide biosynthetic process | 2.82E-04 | 4.12E-03 | MRPS28,MRPS26 |
| 44260 | cellular macromolecule metabolic process | 3.95E-04 | 5.24E-03 | MRPS17,BTF3,PPIL1,MRPS15,MRPS25,MRPL27,MRPS10,SNRPB2,MRPL15,TFB2M,MRPL13,MRPS5 |
| 22900 | electron transport chain | 4.47E-04 | 5.44E-03 | NDUFB3,UQCRFS1,CYC1 |
| 6091 | generation of precursor metabolites and energy | 6.65E-04 | 7.46E-03 | MDH1,NDUFB3,UQCRFS1,CYC1 |
| 44267 | cellular protein metabolic process | 8.52E-04 | 8.88E-03 | MRPS17,PPIL1,MRPS15,MRPS25,MRPL27,MRPS10,MRPL15,MRPL13,MRPS5 |
| 43170 | macromolecule metabolic process | 1.49E-03 | 1.45E-02 | MRPS17,BTF3,PPIL1,MRPS15,MRPS25,MRPL27,MRPS10,SNRPB2,MRPL15,TFB2M,MRPL13,MRPS5 |
| 6518 | peptide metabolic process | 2.38E-03 | 2.17E-02 | MRPS28,MRPS26 |

| GO-ID | Description | p-value | corr p-value | Proteins in test set |
|---|---|---|---|---|
| 19538 | protein metabolic process | 3.48E-03 | 2.87E-02 | MRPS17,PPIL1,MRPS15,MRPS25,MRPL27,MRPS10,MRPL15,MRPL13,MRPS5 |
| 9987 | cellular process | 3.54E-03 | 2.87E-02 | MRPS28,MRPS17,BTF3,MRPS26,PPIL1,MRPS15,MDH1,MRPS25,NDUFB3,MRPL27,MRPS10,MRPL15,TFB2M,MRPL13,MRPS5,UQCRFS1,SNRPB2,CYC1 |
| 44238 | primary metabolic process | 5.32E-03 | 4.09E-02 | MRPS17,BTF3,PPIL1,MRPS15,MDH1,MRPS25,MRPL27,MRPS10,MRPL15,TFB2M,MRPL13,MRPS5,SNRPB2 |

**Supplementary Table 7. GO BP Enrichment of Proteins Significantly Downregulated Following Aze Treatment.**

| GO-ID | Description | p-value | corr p-value | Proteins in test set |
|---|---|---|---|---|
| 6334 | nucleosome assembly | 5.85E-06 | 7.25E-04 | Q9P0M6|Q5SSJ5|P16402|P16401 |
| 31497 | chromatin assembly | 7.06E-06 | 7.25E-04 | Q9P0M6|Q5SSJ5|P16402|P16401 |
| 65004 | protein-DNA complex assembly | 8.82E-06 | 7.25E-04 | Q9P0M6|Q5SSJ5|P16402|P16401 |
| 34728 | nucleosome organization | 9.20E-06 | 7.25E-04 | Q9P0M6|Q5SSJ5|P16402|P16401 |
| 6323 | DNA packaging | 2.36E-05 | 1.49E-03 | Q9P0M6|Q5SSJ5|P16402|P16401 |
| 6333 | chromatin assembly or disassembly | 3.15E-05 | 1.66E-03 | Q9P0M6|Q5SSJ5|P16402|P16401 |
| 71103 | DNA conformation change | 4.49E-05 | 2.02E-03 | Q9P0M6|Q5SSJ5|P16402|P16401 |
| 51276 | chromosome organization | 8.04E-05 | 3.17E-03 | Q9P0M6|Q5SSJ5|P35251|P16402|P26358|P16401 |
| 6325 | chromatin organization | 2.72E-04 | 9.51E-03 | Q9P0M6|Q5SSJ5|P16402|P26358|P16401 |
| 34622 | cellular macromolecular complex assembly | 1.04E-03 | 3.27E-02 | Q9P0M6|Q5SSJ5|P16402|P16401 |
| 21703 | locus ceruleus development | 1.47E-03 | 4.02E-02 | O14813 |

| | | | | |
|---|---|---|---|---|
| 34621 | cellular macromolecular complex subunit organization | 1.61E-03 | 4.02E-02 | Q9P0M6\|Q5SSJ5\|P16402\|P16401 |
| 9987 | cellular process | 1.66E-03 | 4.02E-02 | O15294\|Q9NWH9\|Q08380\|Q5SSJ5\|Q14966\|Q8N1G4\|Q86V81\|O95239\|Q8NC51\|Q9P0L0\|P16402\|P16401\|P42765\|Q9P0M6\|O14813\|Q8WTT2\|Q99453\|P35251\|P46013\|P26358 |

**Supplementary Table 8. GO BP Enrichment of Proteins Significantly Upregulated Following Aze Treatment.**

| GO-ID | Description | p-value | corr p-value | Proteins in test set |
|---|---|---|---|---|
| 6913 | nucleocytoplasmic transport | 1.43E-09 | 2.04E-07 | Q14974\|O43592\|Q8NI27\|Q9UIA9\|Q92621\|O00410\|O95373 |
| 51169 | nuclear transport | 1.50E-09 | 2.04E-07 | Q14974\|O43592\|Q8NI27\|Q9UIA9\|Q92621\|O00410\|O95373 |
| 46907 | intracellular transport | 1.71E-08 | 1.56E-06 | Q14974\|O43592\|Q8NI27\|O14980\|Q00610\|Q9UIA9\|Q92621\|Q96QK1\|O00410\|O95373 |
| 6886 | intracellular protein transport | 3.81E-08 | 2.60E-06 | Q14974\|O43592\|O14980\|Q00610\|Q9UIA9\|Q92621\|O00410\|O95373 |
| 34613 | cellular protein localization | 1.45E-07 | 6.98E-06 | Q14974\|O43592\|O14980\|Q00610\|Q9UIA9\|Q92621\|O00410\|O95373 |
| 70727 | cellular macromolecule localization | 1.53E-07 | 6.98E-06 | Q14974\|O43592\|O14980\|Q00610\|Q9UIA9\|Q92621\|O00410\|O95373 |
| 51649 | establishment of localization in cell | 2.06E-07 | 8.03E-06 | Q14974\|O43592\|Q8NI27\|O14980\|Q00610\|Q9UIA9\|Q92621\|Q96QK1\|O00410\|O95373 |
| 51236 | establishment of RNA localization | 3.80E-07 | 1.04E-05 | O43592\|Q8NI27\|O14980\|Q9UIA9\|Q92621 |
| 50657 | nucleic acid transport | 3.80E-07 | 1.04E-05 | O43592\|Q8NI27\|O14980\|Q9UIA9\|Q92621 |
| 50658 | RNA transport | 3.80E-07 | 1.04E-05 | O43592\|Q8NI27\|O14980\|Q9UIA9\|Q92621 |
| 6403 | RNA localization | 4.40E-07 | 1.09E-05 | O43592\|Q8NI27\|O14980\|Q9UIA9\|Q92621 |

| 51641 | cellular localization | 6.40E-07 | 1.46E-05 | Q14974\|O43592\|Q8NI27\|O14980\|Q00610\|Q9UIA9\|Q92621\|Q96QK1\|O00410\|O95373 |
|---|---|---|---|---|
| 15931 | nucleobase, nucleoside, nucleotide and nucleic acid transport | 7.58E-07 | 1.59E-05 | O43592\|Q8NI27\|O14980\|Q9UIA9\|Q92621 |
| 15031 | protein transport | 8.18E-07 | 1.60E-05 | Q14974\|O43592\|O14980\|Q00610\|Q9UIA9\|Q92621\|Q96QK1\|O00410\|O95373 |
| 45184 | establishment of protein localization | 9.24E-07 | 1.68E-05 | Q14974\|O43592\|O14980\|Q00610\|Q9UIA9\|Q92621\|Q96QK1\|O00410\|O95373 |
| 33036 | macromolecule localization | 2.09E-06 | 3.56E-05 | Q14974\|O43592\|Q8NI27\|O14980\|Q00610\|Q9UIA9\|Q92621\|Q96QK1\|O00410\|O95373 |
| 8104 | protein localization | 4.23E-06 | 6.80E-05 | Q14974\|O43592\|O14980\|Q00610\|Q9UIA9\|Q92621\|Q96QK1\|O00410\|O95373 |
| 6606 | protein import into nucleus | 4.50E-06 | 6.82E-05 | Q14974\|Q92621\|O00410\|O95373 |
| 51170 | nuclear import | 5.27E-06 | 7.57E-05 | Q14974\|Q92621\|O00410\|O95373 |
| 51028 | mRNA transport | 1.03E-05 | 1.40E-04 | Q8NI27\|O14980\|Q9UIA9\|Q92621 |
| 34504 | protein localization in nucleus | 1.12E-05 | 1.40E-04 | Q14974\|Q92621\|O00410\|O95373 |
| 6605 | protein targeting | 1.13E-05 | 1.40E-04 | Q14974\|Q9UIA9\|Q92621\|O00410\|O95373 |
| 17038 | protein import | 2.77E-05 | 3.29E-04 | Q14974\|Q92621\|O00410\|O95373 |
| 33365 | protein localization in organelle | 7.52E-05 | 8.56E-04 | Q14974\|Q92621\|O00410\|O95373 |
| 51168 | nuclear export | 9.22E-05 | 1.01E-03 | O43592\|Q8NI27\|Q9UIA9 |
| 44419 | interspecies interaction between organisms | 1.16E-04 | 1.21E-03 | Q14974\|Q8NI27\|O14980\|O00410\|O95373 |
| 6810 | transport | 1.22E-04 | 1.24E-03 | Q14974\|O75306\|O43592\|Q8NI27\|O14980\|Q00325\|Q00610\|Q9UIA9\|Q92621\|Q96QK1\|O00410\|O95373 |

| 51234 | establishment of localization | 1.39E-04 | 1.36E-03 | Q14974\|O75306\|O43592\|Q8NI27\|O14980\|Q00325\|Q00610\|Q9UIA9\|Q92621\|Q96QK1\|O00410\|O95373 |
|---|---|---|---|---|
| 6607 | NLS-bearing substrate import into nucleus | 1.74E-04 | 1.64E-03 | Q14974\|O00410 |
| 51179 | localization | 5.20E-04 | 4.73E-03 | Q14974\|O75306\|O43592\|Q8NI27\|O14980\|Q00325\|Q00610\|Q9UIA9\|Q92621\|Q96QK1\|O00410\|O95373 |
| 51704 | multi-organism process | 9.36E-04 | 8.24E-03 | Q14974\|P26641\|Q8NI27\|O14980\|O00410\|O95373 |
| 33342 | negative regulation of collagen binding | 1.54E-03 | 1.23E-02 | Q9BZE4 |
| 6409 | tRNA export from nucleus | 1.54E-03 | 1.23E-02 | O43592 |
| 51031 | tRNA transport | 1.54E-03 | 1.23E-02 | O43592 |
| 6405 | RNA export from nucleus | 1.87E-03 | 1.46E-02 | O43592\|Q8NI27 |
| 59 | protein import into nucleus, docking | 3.07E-03 | 2.15E-02 | Q92621 |
| 33341 | regulation of collagen binding | 3.07E-03 | 2.15E-02 | Q9BZE4 |
| 33572 | transferrin transport | 3.07E-03 | 2.15E-02 | Q00610 |
| 15682 | ferric iron transport | 3.07E-03 | 2.15E-02 | Q00610 |
| 6610 | ribosomal protein import into nucleus | 4.61E-03 | 3.14E-02 | Q14974 |

# REFERENCES

(Chapters one, two, five and six only)

1       Gitler, A. D., Dhillon, P. & Shorter, J. Neurodegenerative disease: models, mechanisms, and a new hope. *Disease models & mechanisms* **10**, 499-502, doi:10.1242/dmm.030205 (2017).

2       Heemels, M.-T. Neurodegenerative diseases. *Nature* **539**, 179, doi:10.1038/539179a (2016).

3       Skovronsky, D. M., Lee, V. M. Y. & Trojanowski, J. Q. Neurodegenerative Diseases: New Concepts of Pathogenesis and Their Therapeutic Implications. *Annual Review of Pathology: Mechanisms of Disease* **1**, 151-170, doi:10.1146/annurev.pathol.1.110304.100113 (2006).

4       Bertram, L. & Tanzi, R. E. The genetic epidemiology of neurodegenerative disease. *The Journal of Clinical Investigation* **115**, 1449-1457, doi:10.1172/JCI24761 (2005).

5       Migliore, L. & Coppedè, F. Genetics, environmental factors and the emerging role of epigenetics in neurodegenerative diseases. *Mutation Research/Fundamental and Molecular Mechanisms of Mutagenesis* **667**, 82-97, doi:http://dx.doi.org/10.1016/j.mrfmmm.2008.10.011 (2009).

6       Cannon, J. R. & Greenamyre, J. T. The role of environmental exposures in neurodegeneration and neurodegenerative diseases. *Toxicological Sciences : An Official Journal of the Society of Toxicology* **124**, 225-250, doi:10.1093/toxsci/kfr239 (2011).

7       Landrigan, P. J. *et al.* Early environmental origins of neurodegenerative disease in later life. *Environmental Health Perspectives* **113**, 1230-1233, doi:10.1289/ehp.7571 (2005).

8       Cox, P. A., Banack, S. A. & Murch, S. J. Biomagnification of cyanobacterial neurotoxins and neurodegenerative disease among the Chamorro people of Guam. *Proc Natl Acad Sci U S A* **100**, 13380-13383, doi:10.1073/pnas.2235808100 (2003).

9       Lafont, O. Vauquelin: Route from a thatched cottage to Institute of France. *Annales Pharmaceutiques Françaises* **72**, 221-228 (2014).

10      Bischoff, R. & Schluter, H. Amino acids: chemistry, functionality and selected non-enzymatic post-translational modifications. *Journal of Proteomics* **75**, 2275-2296, doi:10.1016/j.jprot.2012.01.041 (2012).

11      Vickery, H. B. & Schmidt, C. L. A. The History of the Discovery of the Amino Acids. *Chemical Reviews* **9**, 169-318, doi:10.1021/cr60033a001 (1931).

12      Berg, J., Tymoczko, J. & Stryer, L. in *Biochemistry 5th Edition* (2002).

13      Crick, F. H., Barnett, L., Brenner, S. & Watts-Tobin, R. J. General nature of the genetic code for proteins. *Nature* **192**, 1227-1232 (1961).

14      Lichtenthaler, F. W. Emil Fischer, His Personality, His Achievements, and His Scientific Progeny. *European Journal of Organic Chemistry* **2002**, 4095-4122 (2002).

15      Stretton, A. O. W. The First Sequence: Fred Sanger and Insulin. *Genetics* **162**, 527-532 (2002).

16    Thompson, J. F., Morris, C. J. & Smith, I. K. New naturally occurring amino acids. *Annu Rev Biochem* **38**, 137-158, doi:10.1146/annurev.bi.38.070169.001033 (1969).

17    Bell, E. A. Nonprotein amino acids of plants: significance in medicine, nutrition, and agriculture. *Journal of Agricultural and Food Chemistry* **51**, 2854-2865 (2003).

18    Häusler, R. E., Ludewig, F. & Krueger, S. Amino acids – A life between metabolism and signaling. *Plant Science* **229**, 225-237, doi:http://dx.doi.org/10.1016/j.plantsci.2014.09.011 (2014).

19    Cynober, L. in *Encyclopedia of Biological Chemistry* (ed William J. LennarzM Daniel Lane) 91-96 (Academic Press, 2013).

20    Hambræus, L. in *Reference Module in Biomedical Sciences* (Elsevier, 2014).

21    Wu, G. Amino acids: metabolism, functions, and nutrition. *Amino Acids* **37**, 1-17, doi:10.1007/s00726-009-0269-0 (2009).

22    Osowska, S., Moinard, C., Loï, C., Neveux, N. & Cynober, L. Citrulline increases arginine pools and restores nitrogen balance after massive intestinal resection. *Gut* **53**, 1781-1786 (2004).

23    Melamed, E., Hefti, F. & Wurtman, R. J. Nonaminergic striatal neurons convert exogenous l-dopa to dopamine in parkinsonism. *Annals of Neurology* **8**, 558-563, doi:10.1002/ana.410080603 (1980).

24    Chan, S. W., Dunlop, R. A., Rowe, A., Double, K. L. & Rodgers, K. J. L-DOPA is incorporated into brain proteins of patients treated for Parkinson's disease, inducing toxicity in human neuroblastoma cells in vitro. *Experimental Neurology* **238**, 29-37, doi:10.1016/j.expneurol.2011.09.029 (2012).

25    Bloomer, R. J. *et al.* Comparison of pre-workout nitric oxide stimulating dietary supplements on skeletal muscle oxygen saturation, blood nitrate/nitrite, lipid peroxidation, and upper body exercise performance in resistance trained men. *Journal of the International Society of Sports Nutrition* **7**, 1-15, doi:10.1186/1550-2783-7-16 (2010).

26    Allman, B. R., Kreipke, V. C. & Ormsbee, M. J. What Else Is in Your Supplement? A Review of the Effectiveness of the Supportive Ingredients in Multi-ingredient Performance Supplements to Improve Strength, Power, and Recovery. *Strength & Conditioning Journal* **37**, 54-69 (2015).

27    Huang, T., Jander, G. & de Vos, M. Non-protein amino acids in plant defense against insect herbivores: Representative cases and opportunities for further functional analysis. *Phytochemistry* **72**, 1531-1537, doi:http://dx.doi.org/10.1016/j.phytochem.2011.03.019 (2011).

28    Richmond, M. H. The effect of amino acid analogues on growth and protein synthesis in microorganisms. *Bacteriological Reviews* **26**, 398-420 (1962).

29    Merel, S. *et al.* State of knowledge and concerns on cyanobacterial blooms and cyanotoxins. *Environment International* **59**, 303-327, doi:http://dx.doi.org/10.1016/j.envint.2013.06.013 (2013).

30    Bertin, C. *et al.* Grass roots chemistry: meta-Tyrosine, an herbicidal nonprotein amino acid. *Proc Natl Acad Sci U S A* **104**, 16964-16969, doi:10.1073/pnas.0707198104 (2007).

31    Minakata, H. *et al.* Antimutagenic unusual amino acids from plants. *Experientia* **41**, 1622-1633 (1985).

32    Rubenstein, E. *et al.* Azetidine-2-carboxylic acid in the food chain. *Phytochemistry* **70**, 100-104, doi:10.1016/j.phytochem.2008.11.007 (2009).

33    Ravindranath, V. Neurolathyrism: mitochondrial dysfunction in excitotoxicity mediated by L-beta-oxalyl aminoalanine. *Neurochemistry International* **40**, 505-509 (2002).

34    Rosenthal, G. A. L-Canavanine: a higher plant insecticidal allelochemical. *Amino Acids* **21**, 319-330 (2001).

35    Krakauer, J., Long, Y., Kolbert, A., Thanedar, S. & Southard, J. Presence of L-Canavanine in Hedysarum alpinum Seeds and Its Potential Role in the Death of Chris McCandless. *Wilderness & Environmental Medicine* **26**, 36-42, doi:http://dx.doi.org/10.1016/j.wem.2014.08.014 (2015).

36    Matsumoto, H. The mechanisms of phytotoxic action and selectivity of non-protein aromatic amino acids L-DOPA and m-tyrosine. *Journal of Pesticide Science* **36**, 1-8, doi:10.1584/jpestics.R10-15 (2011).

37    Alvarez-Carreno, C., Becerra, A. & Lazcano, A. Norvaline and norleucine may have been more abundant protein components during early stages of cell evolution. *Orig Life Evol Biosph* **43**, 363-375, doi:10.1007/s11084-013-9344-3 (2013).

38    Fowden, L., Lewis, D. & Tristram, H. Toxic amino acids: their action as antimetabolites. *Advances in Enzymology and Related areas of Molecular Biology* **29**, 89-163 (1967).

39    Fowden, L. Amino-acid Analogues and the Growth of Seedlings. *Journal of Experimental Botany* **14**, 387-398, doi:10.1093/jxb/14.3.387 (1963).

40    Rosenthal, G. A., J.M., R. & Hoffmann, J. A. L-canavanine incorporation into vitellogenin and macromolecular conformation. *The Journal of Biological Chemistry* **264**, 13693-13696 (1989).

41    Woltz, S. S. Growth-Modifying & Antimetabolite Effects of Amino Acids on Chrysanthemum. *Plant physiology* **38**, 93-99, doi:10.1104/pp.38.1.93 (1963).

42    Cowie, D. B., Cohen, G. N., Bolton, E. T. & De Robichon-Szulmajster, H. Amino acid analog incorporation into bacterial proteins. *Biochimica et Biophysica Acta* **34**, 39-46, doi:10.1016/0006-3002(59)90230-6 (1959).

43    Fowden, L. & Richmond, M. H. Replacement of proline by azetidine-2-carboxylic acid during biosynthesis of protein. *Biochimica et Biophysica Acta* **71**, 459-461, doi:https://doi.org/10.1016/0006-3002(63)91104-1 (1963).

44    Bessonov, K., Fau, B. V. & Harauz, G. Misincorporation of the proline homologue Aze (azetidine-2-carboxylic acid) into recombinant myelin basic protein. *Phytochemistry* **71**, 502-507 (2010).

45    Nandi, P. & Sen, G. P. An Antifungal Substance from a Strain of B. subtilis. *Nature* **172**, 871, doi:10.1038/172871b0 (1953).

46    Kisumi, M., Sugiura, M., Kato, J. & Chibata, I. L-Norvaline and L-homoisoleucine formation by Serratia marcescens. *Journal of Biochemistry* **79** (1976).

47    Cvetesic, N., Palencia, A., Halasz, I., Cusack, S. & Gruic-Sovulj, I. The physiological target for LeuRS translational quality control is norvaline. *EMBO J* **33**, 1639-1653, doi:10.15252/embj.201488199 (2014).

48    Cvetesic, N., Akmacic, I. & Gruic-Sovulj, I. Lack of discrimination against non-proteinogenic amino acid norvaline by elongation factor Tu from. *Croat Chem Acta* **86**, 73-82, doi:10.5562/cca2173 (2013).

49    Apostol, I. *et al.* Incorporation of Norvaline at Leucine Positions in Recombinant Human Hemoglobin Expressed in *Escherichia coli*. *The Journal of Biological Chemistry* **272**, 28980-28988 (1997).

50    Johansson, M., Lovmar, M. & Ehrenberg, M. Rate and accuracy of bacterial protein synthesis revisited. *Current Opinions in Microbiology* **11**, 141-147, doi:10.1016/j.mib.2008.02.015 (2008).

51    Rizvi, S. J. H., Haque, H., Singh, V. K. & Rizvi, V. in *Allelopathy: Basic and applied aspects*  (eds S. J. H. Rizvi & V. Rizvi)  1-10 (Springer Netherlands, 1992).

52    Soares, A. R., de Cássia Siqueira-Soares, R., Salvador, V. H., de Lourdes Lucio Ferrarese, M. & Ferrarese-Filho, O. The effects of l-DOPA on root growth, lignification and enzyme activity in soybean seedlings. *Acta Physiologiae Plantarum* **34**, 1811-1817, doi:10.1007/s11738-012-0979-x (2012).

53    Mushtaq, M. N., Sunohara, Y. & Matsumoto, H. Allelochemical l-DOPA induces quinoprotein adducts and inhibits NADH dehydrogenase activity and root growth of cucumber. *Plant Physiology and Biochemistry* **70**, 374-378, doi:http://dx.doi.org/10.1016/j.plaphy.2013.06.003 (2013).

54    Hachinohe, M. & Matsumoto, H. Mechanism of selective phytotoxicity of L-3,4-dihydroxyphenylalanine (l-dopa) in barnyardgrass and lettuce. *Journal of Chemical Ecology* **33**, 1919-1926, doi:10.1007/s10886-007-9359-1 (2007).

55    Pitman, M. G., Wildes, R. A., Schaefer, N. & Wellfare, D. Effect of Azetidine 2-Carboxylic Acid on Ion Uptake and Ion Release to the Xylem of Excised Barley Roots. *Plant Physiology* **60**, 240-246, doi:10.1104/pp.60.2.240 (1977).

56    Bell, E. A. The non-protein amino acids of higher plants. *Endeavour* **4**, 102-107, doi:http://dx.doi.org/10.1016/0160-9327(80)90056-3 (1980).

57    Vaughan, D., Dekock, P. C. & Cusens, E. Effects of Hydroxyproline and other Amino Acid Analogues on the Growth of Pea Root Segments. *Physiologia Plantarum* **30**, 255-259, doi:10.1111/j.1399-3054.1974.tb03652.x (1974).

58    Lee, J. *et al.* Inhibition of Arabidopsis growth by the allelopathic compound azetidine-2-carboxylate is due to the low amino acid specificity of cytosolic prolyl-tRNA synthetase. *The Plant Journal* **88**, 236-246, doi:10.1111/tpj.13246 (2016).

59    Contardo-Jara, V., Schwanemann, T. & Pflugmacher, S. Uptake of a cyanotoxin, β-N-methylamino-l-alanine, by wheat (Triticum aestivum). *Ecotoxicology and Environmental Safety* **104**, 127-131, doi:http://dx.doi.org/10.1016/j.ecoenv.2014.01.039 (2014).

60    Kruse, P. F., White, P. B., Carter, H. A. & McCoy, T. A. Incorporation of canavanine into protein of Walker carcinosarcoma 256 cells cultured in vitro. *Cancer Research* **19**, 122-125, doi:D - CLML: 5935:48581:27:395:483 OTO - NLM (1959).

61    Dasuri, K. *et al.* in *The Journal of Neuroscience Research* Vol. 89   1471-1477 (Inc., 2011).

62    Knowles, S. E. & Ballard, F. J. Effects of amino acid analogues on protein synthesis and degradation in isolated cells. *British Journal of Nutrition* **40**, 275, doi:10.1079/bjn19780123 (1978).

63      Okle, O., Stemmer, K., Deschl, U. & Dietrich, D. R. L-BMAA induced ER stress and enhanced caspase 12 cleavage in human neuroblastoma SH-SY5Y cells at low nonexcitotocol concentrations. *Toxicol Sci* **131**, 217-224, doi:10.1093/toxsci/kfs291 (2013).

64      Main, B. J., Dunlop, R. A. & Rodgers, K. J. The use of l-serine to prevent β-methylamino-l-alanine (BMAA)-induced proteotoxic stress in vitro. *Toxicon* **109**, 7-12, doi:http://dx.doi.org/10.1016/j.toxicon.2015.11.003 (2016).

65      Main, B. J., Italiano, C. J. & Rodgers, K. J. Investigation of the interaction of β-methylamino-l-alanine with eukaryotic and prokaryotic proteins. *Amino Acids* **50**, 397-407, doi:10.1007/s00726-017-2525-z (2018).

66      Chiu, A. S. *et al.* Gliotoxicity of the cyanotoxin, beta-methyl-amino-L-alanine (BMAA). *Sci Rep* **3**, 1482, doi:10.1038/srep01482 (2013).

67      Chiu, A. S. *et al.* Excitotoxic potential of the cyanotoxin β-methyl-amino-l-alanine (BMAA) in primary human neurons. *Toxicon* **60**, 1159-1165 (2012).

68      Hunter, A. & Downs, C. E. The inhibition of arginase by amino acids. *The Journal of Biological Chemistry* **157** (1945).

69      Franek, F., Fismolova, I. & Eckschlager, T. Antiapoptotic and proapoptotic action of various amino acids and analogs in starving MOLT-4 cells. *Archives of Biochemistry and Biophysics* **398**, 141-146, doi:10.1006/abbi.2001.2698 (2002).

70      Yamazaki, M. & Chiba, K. Expression of Functional Nitric Oxide Synthase for Neuritogenesis in PC12h Cells. *Journal of Health Science* **52** (2006).

71      Ming, X. F., Rajapakse, A. G., Carvas, J. M., J, R. & Yang, Z. Inhibition of S6K1 accounts partially for the anti-inflammatory effects of the arginase inhibitor L-norvaline. *BMC Cardiovascular Disorders* **13** (2009).

72      Enneking, D. The nutritive value of grasspea (Lathyrus sativus) and allied species, their toxicity to animals and the role of malnutrition in neurolathyrism. *Food and Chemical Toxicology* **49**, 694-709, doi:http://dx.doi.org/10.1016/j.fct.2010.11.029 (2011).

73      Dunlop, R. A., Main, B. J. & Rodgers, K. J. The deleterious effects of non-protein amino acids from desert plants on human and animal health. *Journal of Arid Environments* **112, Part B**, 152-158, doi:http://dx.doi.org/10.1016/j.jaridenv.2014.05.005 (2015).

74      Rodgers, K. J., Samardzic, K. & Main, B. J. in *Plant Toxins*    1-20 (Springer, 2015).

75      Malinow, M. R., Bardana, E. J., Pirofsky, B., Craig, S. & McLaughlin, P. Systemic lupus erythematosus-like syndrome in monkeys fed alfalfa sprouts: role of a nonprotein amino acid. *Science* **216**, 415-417 (1982).

76      Affleck, H. Jack bean poisoning in cattle. *Rhodesian Agricultural Journal* **58**, 21 (1961).

77      Crawford, G. *et al.* Systemic effects of Leucaena leucocephala ingestion on ringtailed lemurs (Lemur catta) at Berenty Reserve, Madagascar. *American Journal of Primatology* **77**, 633-641, doi:10.1002/ajp.22386 (2015).

78      Dalzell, S. A., Burnett, D. J., Dowsett, J. E., Forbes, V. E. & Shelton, H. M. Prevalence of mimosine and DHP toxicity in cattle grazing Leucaena leucocephala pastures in Queensland, Australia. *Animal Production Science* **52**, 365-372 (2012).

79     Joneja, M. G. Teratogenic effects of proline analogue L-azetidine-2-carboxylic acid in hamster fetuses. *Teratology* **23**, 365-372, doi:10.1002/tera.1420230311 (1981).

80     Barbul, A. Proline Precursors to Sustain Mammalian Collagen Synthesis. *The Journal of Nutrition* **138**, 2021S-2024S, doi:10.1093/jn/138.10.2021S (2008).

81     Pokrovskiy, M. V. *et al.* Arginase inhibitor in the pharmacological correction of endothelial dysfunction. *International Journal of Hypertension* **2011**, 515047, doi:10.4061/2011/515047 (2011).

82     Alagiakrishnan, K., Jubry, A., Hanley, D., Tymchak, W. & Sclater, A. Role of vascular factors in osteoporosis. *Journal of Gerontology* **58A** (2003).

83     Sobolev, M. S. *et al.* Study of Endothelio- and Osteoprotective Effects of Combination of Rosuvastatin with L-Norvaline in Experiment. *Journal of Osteporosis* **2018**, 1585749, doi:10.1155/2018/1585749 (2018).

84     El-Bassossy, H. M., El-Fawal, R., Fahmy, A. & Watson, M. L. Arginase inhibition alleviates hypertension in the metabolic syndrome. *The British Journal of Pharmacology* **169**, 693-703, doi:10.1111/bph.12144 (2013).

85     Cuihua, Z., Travis W, H., Wei, W., Chiung-I, C. & Lih, K. U. O. Constitutive expression of arginase in microvascular endothelial cells counteracts nitric oxide-mediated vasodilatory function 1. *The FASEB Journal* **15**, 1264-1266 (2001).

86     De, A., Singh, M. F., Singh, V., Ram, V. & Bisht, S. Treatment effect of l-Norvaline on the sexual performance of male rats with streptozotocin induced diabetes. *The European Journal of Pharmacology* **771**, 247-254, doi:10.1016/j.ejphar.2015.12.008 (2016).

87     Sonntag, K. C. *et al.* Late-onset Alzheimer's disease is associated with inherent changes in bioenergetics profiles. *Sci Rep* **7**, 14038, doi:10.1038/s41598-017-14420-x (2017).

88     Polis, B., Srikanth, K. D., Elliott, E., Gil-Henn, H. & Samson, A. O. L-Norvaline Reverses Cognitive Decline and Synaptic Loss in a Murine Model of Alzheimer's Disease. *Neurotherapeutics*, doi:10.1007/s13311-018-0669-5 (2018).

89     Caller, T. A. *et al.* Spatial clustering of amyotrophic lateral sclerosis and the potential role of BMAA. *Amyotrophic Lateral Sclerosis* **13**, 25-32 (2012).

90     Banack, S. A. *et al.* Detection of cyanotoxins, beta-N-methylamino-L-alanine and microcystins, from a lake surrounded by cases of amyotrophic lateral sclerosis. *Toxins (Basel)* **7**, 322-336, doi:10.3390/toxins7020322 (2015).

91     Kanazawa, I. How do neurons die in neurodegenerative disease? *Trends in Molecular Medicine* **7**, 339-344 (2001).

92     Yan, Z.-Y. *et al.* Lathyrus sativus (grass pea) and its neurotoxin ODAP. *Phytochemistry* **67**, 107-121, doi:http://dx.doi.org/10.1016/j.phytochem.2005.10.022 (2006).

93     Woldeamanuel, Y. W., Hassan, A. & Zenebe, G. Neurolathyrism: two Ethiopian case reports and review of the literature. *Journal of Neurology* **259**, 1263-1268 (2012).

94     Cohn, D. F. & Streifler, M. Human neurolathyrism, a follow-up study of 200 patients. Part I: Clinical investigation. *Swiss Archives of Neurology, Psychiatry and Psychotherapy* **128**, 151-156 (1981).

95      Haimanot, R. T. *et al.* Lathyrism in Rural Northwestern Ethiopia: A Highly Prevalent Neurotoxic Disorder. *International Journal of Epidemiology* **19**, 664-672 (1990).

96      Mishra, V. N. *et al.* Lathyrism: has the scenario changed in 2013? *Neurological Research* **36**, 38-40, doi:10.1179/1743132813Y.0000000258 (2014).

97      Khandare, A. *et al.* Grass pea consumption & present scenario of neurolathyrism in Maharashtra State of India. *The Indian Journal of Medical Research* **140**, 96-101 (2014).

98      Yerra, S., Putta, S. & Kilari, E. K. Detoxification of ODAP in Lathyrus sativus by various food processing techniques. *Pharmaceutical and Biological Evaluations* **2**, 152-159 (2015).

99      Oyanagi, K. The nature of the parkinsonism-dementia complex and amyotrophic lateral sclerosis of Guam and magnesium deficiency. *Parkinsonism and Related Disorders* **11, Supplement 1**, S17-S23, doi:http://dx.doi.org/10.1016/j.parkreldis.2005.02.010 (2005).

100     Hof, P. R., Perl, D. P., Loerzel, A. J., Steele, J. C. & Morrison, J. H. Amyotrophic lateral sclerosis and parkinsonism-dementia from Guam: differences in neurofibrillary tangle distribution and density in the hippocampal formation and neocortex. *Brain Research* **650**, 107-116, doi:http://dx.doi.org/10.1016/0006-8993(94)90212-7 (1994).

101     Spencer, P. *et al.* Guam amyotrophic lateral sclerosis-parkinsonism-dementia linked to a plant excitant neurotoxin. *Science* **237**, 517-522, doi:10.1126/science.3603037 (1987).

102     Garruto, R. M., Gajdusek, C. & Chen, K. M. Amyotrophic lateral sclerosis among Chamorro migrants from Guam. *Annals of Neurology* **8**, 612-619 (1980).

103     Weiss, J. H., J.Y., K. & Choi, D. W. Neurotoxicity of beta-N-methylamino-L-alanine (BMAA) and beta-N-oxalylamino-L-alanine (BOAA) on cultured cortical neurons. *Brain Research* **497**, 64-71 (1989).

104     Muñoz-Sáez, E. *et al.* Analysis of β-N-methylamino-l-alanine (L-BMAA) neurotoxicity in rat cerebellum. *NeuroToxicology* **48**, 192-205, doi:http://dx.doi.org/10.1016/j.neuro.2015.04.001 (2015).

105     Al-Sammak, M. A., Rogers, D. G. & Hoagland, K. D. Acute beta-N-Methylamino-L-alanine Toxicity in a Mouse Model. *J Toxicol* **2015**, 739746, doi:10.1155/2015/739746 (2015).

106     Scott, L. L. & Downing, T. G. A Single Neonatal Exposure to BMAA in a Rat Model Produces Neuropathology Consistent with Neurodegenerative Diseases. *Toxins* **10**, 22, doi:10.3390/toxins10010022 (2018).

107     Karamyan, V. T. & Speth, R. C. Animal models of BMAA neurotoxicity: A critical review. *Life Sciences* **82**, 233-246, doi:http://dx.doi.org/10.1016/j.lfs.2007.11.020 (2008).

108     van Onselen, R., Downing, S., Kemp, G. & Downing, T. Investigating β-N-Methylamino-l-alanine Misincorporation in Human Cell Cultures: A Comparative Study with Known Amino Acid Analogues. *Toxins* **9**, 400, doi:10.3390/toxins9120400 (2017).

109     Murch, S. J., Cox, P. A., Banack, S. A., Steele, J. C. & Sacks, O. W. Occurrence of beta-methylamino-l-alanine (BMAA) in ALS/PDC patients from Guam. *Acta Neurol Scand* **110**, 267-269, doi:10.1111/j.1600-0404.2004.00320.x (2004).

110     Rubenstein, E. Misincorporation of the proline analog azetidine-2-carboxylic acid in the pathogenesis of multiple sclerosis: a hypothesis. *The Journal of Neuropathology & Experimental Neurology* **67**, 1035-1040, doi:10.1097/NEN.0b013e31818add4a (2008).

111     Bessonov, K., Bamm, V. V. & Harauz, G. Misincorporation of the proline homologue Aze (azetidine-2-carboxylic acid) into recombinant myelin basic protein. *Phytochemistry* **71**, 502-507, doi:10.1016/j.phytochem.2009.12.010 (2010).

112     Chalmers, G. A. Swayback (enzootic ataxia) in Alberta lambs. *Canadian journal of comparative medicine : Revue canadienne de medecine comparee* **38**, 111-117 (1974).

113     Lin, M. T. & Beal, M. F. Mitochondrial dysfunction and oxidative stress in neurodegenerative diseases. *Nature* **443**, 787-795 (2006).

114     Cozzolino, M. & Carrì, M. T. Mitochondrial dysfunction in ALS. *Progress in Neurobiology* **97**, 54-66, doi:http://dx.doi.org/10.1016/j.pneurobio.2011.06.003 (2012).

115     Yan, M. H., Wang, X. & Zhu, X. Mitochondrial defects and oxidative stress in Alzheimer disease and Parkinson disease. *Free Radical Biology and Medicine* **62**, 90-101, doi:http://dx.doi.org/10.1016/j.freeradbiomed.2012.11.014 (2013).

116     Jiang, Z., Wang, W., Perry, G., Zhu, X. & Wang, X. Mitochondrial dynamic abnormalities in amyotrophic lateral sclerosis. *Translational Neurodegeneration* **4**, 14, doi:10.1186/s40035-015-0037-x (2015).

117     Detmer, S. A. & Chan, D. C. Functions and dysfunctions of mitochondrial dynamics. *Nature Reviews Molecular Cell Biology* **8**, 870-879, doi:10.1038/nrm2275 (2007).

118     Parone, P. A. & Martinou, J.-C. Mitochondrial fission and apoptosis: An ongoing trial. *Biochimica et Biophysica Acta - Molecular Cell Research* **1763**, 522-530, doi:https://doi.org/10.1016/j.bbamcr.2006.04.005 (2006).

119     Skulachev, V. P. Bioenergetic aspects of apoptosis, necrosis and mitoptosis. *Apoptosis* **11**, 473-485, doi:10.1007/s10495-006-5881-9 (2006).

120     Chen, H. & Chan, D. C. Mitochondrial dynamics–fusion, fission, movement, and mitophagy–in neurodegenerative diseases. *Human Molecular Genetics* **18**, R169-R176, doi:10.1093/hmg/ddp326 (2009).

121     Konovalova, S. *et al.* Exposure to arginine analog canavanine induces aberrant mitochondrial translation products, mitoribosome stalling, and instability of the mitochondrial proteome. *The International Journal of Biochemistry & Cell Biology* **65**, 268-274, doi:http://dx.doi.org/10.1016/j.biocel.2015.06.018 (2015).

122     de Munck, E. *et al.* β-N-methylamino-l-alanine causes neurological and pathological phenotypes mimicking Amyotrophic Lateral Sclerosis (ALS): The first step towards an experimental model for sporadic ALS. *Environmental Toxicology and Pharmacology* **36**, 243-255, doi:http://dx.doi.org/10.1016/j.etap.2013.04.007 (2013).

123    Tian, K.-W., Jiang, H., Wang, B.-B., Zhang, F. & Han, S. Intravenous injection ofl-BMAA induces a rat model with comprehensive characteristics of amyotrophic lateral sclerosis/Parkinson–dementia complex. *Toxicolology Research* **5**, 79-96, doi:10.1039/c5tx00272a (2016).

124    Suzuki, T., Nagao, A. & Suzuki, T. Human Mitochondrial tRNAs: Biogenesis, Function, Structural Aspects, and Diseases. *Annual Review of Genetics* **45**, 299-329, doi:10.1146/annurev-genet-110410-132531 (2011).

125    Banack, S. A. *et al.* Detection of Cyanotoxins, β-N-methylamino-L-alanine and Microcystins, from a Lake Surrounded by Cases of Amyotrophic Lateral Sclerosis. *Toxins* **7**, 322-336 (2015).

126    Mondo, K. *et al.* Environmental neurotoxins β-N-methylamino-l-alanine (BMAA) and mercury in shark cartilage dietary supplements. *Food and Chemical Toxicology* **70**, 26-32, doi:http://dx.doi.org/10.1016/j.fct.2014.04.015 (2014).

127    Banack, S. A., Metcalf, J. S., Bradley, W. G. & Cox, P. A. Detection of cyanobacterial neurotoxin β-N-methylamino-l-alanine within shellfish in the diet of an ALS patient in Florida. *Toxicon* **90**, 167-173, doi:http://dx.doi.org/10.1016/j.toxicon.2014.07.018 (2014).

128    Hammerschlag, N. *et al.* Cyanobacterial Neurotoxin BMAA and Mercury in Sharks. *Toxins* **8**, pii: E238 (2016).

129    Reveillon, D. *et al.* Beta-N-methylamino-L-alanine: LC-MS/MS optimization, screening of cyanobacterial strains and occurrence in shellfish from Thau, a French Mediterranean lagoon. *Marine Drugs* **12**, 5441-5467, doi:10.3390/md12115441 (2014).

130    Reveillon, D., Sechet, V., Hess, P. & Amzil, Z. Systematic detection of BMAA (beta-N-methylamino-l-alanine) and DAB (2,4-diaminobutyric acid) in mollusks collected in shellfish production areas along the French coasts. *Toxicon* **110**, 35-46, doi:10.1016/j.toxicon.2015.11.011 (2016).

131    Davis, D. A. *et al.* Cyanobacterial neurotoxin BMAA and brain pathology in stranded dolphins. *PLOS ONE* **14**, e0213346, doi:10.1371/journal.pone.0213346 (2019).

132    Johnson, H. E. *et al.* Cyanobacteria (Nostoc commune) used as a dietary item in the Peruvian highlands produce the neurotoxic amino acid BMAA. *Journal of Ethnopharmacology* **118**, 159-165, doi:http://dx.doi.org/10.1016/j.jep.2008.04.008 (2008).

133    Bell, E. A. The discovery of BMAA, and examples of biomagnification and protein incorporation involving other non-protein amino acids. *Amyotroph Lateral Sclerosis* **10**, 21-25 (2009).

134    Rubenstein, E., Zhou, H., Krasinska, K. M., Chien, A. & Becker, C. H. Azetidine-2-carboxylic acid in garden beets (Beta vulgaris). *Phytochemistry* **67**, 898-903, doi:https://doi.org/10.1016/j.phytochem.2006.01.028 (2006).

135    Habeeb, A. A. M., Gad, A. E., El-Tarabany, A., Mustafa, M. M. & Atta, A. Using of Sugar Beet Pulp By-Product in Farm Animals Feeding. *International Journal of Scientific Research in Science and Technology* **3** (2017).

136    Kramer, R. & Nikolaidis, A.    (Google Patents, 2015).

137    Kramer, R. & Nikolaidis, A.    (Google Patents, 2013).

138    Kramer, R. & Nikolaidis, A.    (Google Patents, 2015).

139     Jeppesen, B. P. & Lavrsen, S.     (Google Patents, 2014).

140     iHerb.     *Now     Foods,     Dopa     Mucuna,     90     Veg     Capsules*,
        <https://au.iherb.com/pr/Now-Foods-Dopa-Mucuna-90-Veg-
        Capsules/8673?gclid=CjwKCAjwhbHlBRAMEiwAoDA345SeqN0O7--
        DYQBBQYMUPjfoA4C7HB6bvfzX-u-
        PTvnw9ql_BGlnaxoC71YQAvD_BwE&gclsrc=aw.ds> (2019).

141     iHerb.     *Life     Extension,     Dopa-Mind,     60     Vegetarian     Tablets*,
        <https://au.iherb.com/pr/Life-Extension-Dopa-Mind-60-Vegetarian-
        Tablets/67035?gclid=CjwKCAjwhbHlBRAMEiwAoDA34w7Gvfck8kBQoBDfqURiR
        FvglI3aK_U-p37M1-eSwmxI_iyZ6XhHSxoCEIUQAvD_BwE&gclsrc=aw.ds> (2019).

142     Biovea.     *MUCUNA     DOPA     250mg     60     Vegetarian     Capsules*,
        <https://www.biovea.net/au/product_detail.aspx?PID=3859&TI=GGLAU&C=N
        &gclid=CjwKCAjwhbHlBRAMEiwAoDA346AjNAkmSg6ON_j8oNcbBgIdBRmpSFaT
        F3Z9AK6dS0GXGzUmR5wvNhoCbMIQAvD_BwE> (2019).

143     iHerb.     *Solaray,     DopaBean,     Mucuna     Pruriens,     60     Veggie     Caps*,
        <https://au.iherb.com/pr/Solaray-DopaBean-Mucuna-Pruriens-60-Veggie-
        Caps/19249?gclid=CjwKCAjwhbHlBRAMEiwAoDA340dTd9H3cNDPwr57uPpNxR
        79NTdGD6wsT3ORxPckMkhScARXzhpG8xoCF8IQAvD_BwE&gclsrc=aw.ds>
        (2019).

144     Amazon.     *Sutherlandia     Frutescens     60     x     350mg     Capsules*,
        <https://www.amazon.com/SUTHERLANDIA-FRUTESCENS-60-350mg-
        Capsules/dp/B011AKS924> (2019).

145     Cyos.     *L-Norvaline     Powder*,     <https://cyos.online/product/powders/l-norvaline-
        powder/?attribute_pa_size=100-
        grams&adTribesID=83e90313db1726f3b9567271e3fff3ee%7Cadtribes%7C232
        &utm_source=Google%20Shopping&utm_campaign=Google%20Shopping%20A
        ds%20Feed&utm_medium=cpc&utm_term=232&utm_source=adwords&utm_c
        ampaign=Shopping+%7C+Powders&utm_term=&utm_medium=ppc&hsa_tgt=p
        la-
        297165437473&hsa_acc=1953337448&hsa_kw=&hsa_grp=68201699998&hsa_
        mt=&hsa_cam=1714031906&hsa_ad=333855185177&hsa_net=adwords&hsa_
        ver=3&hsa_src=g&gclid=CjwKCAjwhbHlBRAMEiwAoDA34_v8u1BaOO4EKJ4CH4
        uKia0u4Y6mga9Cq0IilUwphNcnvz5G_ijc0BoCACcQAvD_BwE> (2019).

146     Joes,     M.     *Primeval     Labs     Mega     Pre     Black*,
        <https://massivejoes.com/shop/primeval-labs-mega-pre-black> (2019).

147     Joes, M. *Ghost Pump*, <https://massivejoes.com/shop/ghost-pump> (2019).

148     Fruugo.     *Specialist     Supplements     Nat-Lax     90     Capsules*,
        <https://www.fruugoaustralia.com/specialist-supplements-natlax-tnt-90-
        capsules/p-15114909-
        32468230?language=en&ac=google&gclid=CjwKCAjwhbHlBRAMEiwAoDA342G
        1EatGqt8ze22XzVq0tEKa6eVCHfbMzThOte4mRo85krlpV20tWRoCY6AQAvD_Bw
        E> (2019).

149     Amazon.     *Belle     Dietary     Fibre     Blask-     High     Fibre     Tablets     pills*,
        <https://www.amazon.com/Belle%C2%AE-Dietary-Fibre-Blast-
        supplement/dp/B071G66T1R> (2019).

150 iHerb. *Nature's Answer, Whole Beets Powder*, <https://au.iherb.com/pr/Nature-s-Answer-Whole-Beets-Powder-6-34-oz-180-g/80094?gclid=CjwKCAjwhbHlBRAMEiwAoDA34_1ZCSHY_ReedagkKOWjxEf0saxlK59cylpxMWArFUvNBL_S02LEQhoCyEwQAvD_BwE&gclsrc=aw.ds> (2019).

151 Lodish, H., Berk, A. & Zipursky, S. L. in *Molecular Cell Biology 4th Edition* (W. H. Freeman, New York, 2000).

152 Ling, J., Reynolds, N. & Ibba, M. Aminoacyl-tRNA synthesis and translational quality control. *Annual Review of Microbiology* **63** (2009).

153 Hendrickson, T. L., de Crecy-Lagard, V. F. & Schimmel, P. Incorporation of nonnatural amino acids into proteins. *Annual Review of Biochemistry* **73**, 147-179 (2004).

154 Zaher, H. S. & Green, R. Fidelity at the molecular level: lessons from protein synthesis. *Cell* **136**, 746-762, doi:10.1016/j.cell.2009.01.036 (2009).

155 Moras, D. Proofreading in translation: dynamics of the double-sieve model. *Proceedings of the National Academy of Sciences of the United States of America* **107**, 21949-21950, doi:10.1073/pnas.1016083107 (2010).

156 Lue, S. W. & Kelley, S. O. An aminoacyl-tRNA synthetase with a defunct editing site. *Biochemistry* **44**, 3010-3016 (2005).

157 Haber, E. & Anfinsen, C. B. Regeneration of Enzyme Activity by Air Oxidation of Reduced Subtilisin-Modified Ribonuclease. *Journal of Biological Chemistry* **236**, 422-424 (1961).

158 Anfinsen, C. B. The formation and stabilization of protein structure. *The Biochemical journal* **128**, 737-749, doi:10.1042/bj1280737 (1972).

159 Reynaud, E. Protein Misfolding and Degenerative Diseases. *Nature Education* **3** (2010).

160 Rodgers, K. J. & Shiozawa, N. Misincorporation of amino acid analogues into proteins by biosynthesis. *The International Journal of Biochemistry & Cell Biology* **40**, 1452-1466, doi:http://dx.doi.org/10.1016/j.biocel.2008.01.009 (2008).

161 Berg, J. M., Tymoczko, J. L. & Stryer, L. in *Biochemistry. 5th edition.* (ed W.H Freeman) (New York, 2002).

162 Bence, A. K. & Crooks, P. A. The mechanism of L-canavanine cytotoxicity: arginyl tRNA synthetase as a novel target for anticancer drug discovery. *J Enzyme Inhib Med Chem* **18**, 383-394, doi:10.1080/1475636031000152277 (2003).

163 Dunlop, R. A., Cox, P. A., Banack, S. A. & Rodgers, K. J. The Non-Protein Amino Acid BMAA Is Misincorporated into Human Proteins in Place of l-Serine Causing Protein Misfolding and Aggregation. *PLoS ONE* **8**, 1-6, doi:10.1371/journal.pone.0075376 (2013).

164 Lane, J. M., Dehm, P. & Prockop, D. J. Effect of the Proline Analogue Azetidine-2-carboxylic Acid on Collagen Synthesis in vivo. *Biochimica et Biophysica Acta* **236**, 517- 527 (1970).

165 Hochstrasser, M. Ubiquitin and intracellular protein degradation. *Current Opinion in Cell Biology* **4**, 1024-1031, doi:http://dx.doi.org/10.1016/0955-0674(92)90135-Y (1992).

166 Munoz-Saez, E. *et al.* Neuroprotective role of sphingosine-1-phosphate in L-BMAA treated neuroblastoma cells (SH-SY5Y). *Neuroscience Letters* **593**, 83-89, doi:10.1016/j.neulet.2015.03.010 (2015).

167    Cvetesic, N., Perona, J. J. & Gruic-Sovulj, I. Kinetic Partitioning between Synthetic and Editing Pathways in Class I Aminoacyl-tRNA Synthetases Occurs at Both Pre-transfer and Post-transfer Hydrolytic Steps. *Journal of Biological Chemistry* **287**, 25381-25394 (2012).

168    Ozawa, K. *et al.* Translational incorporation of L-3,4-dihydroxyphenylalanine into proteins. *FEBS Journal* **272**, 3162-3171 (2005).

169    Cox, P. A., Davis, D. A., Mash, D. C., Metcalf, J. S. & Banack, S. A. Dietary exposure to an environmental toxin triggers neurofibrillary tangles and amyloid deposits in the brain. *Proc Biol Sci* **283**, doi:10.1098/rspb.2015.2397 (2016).

170    Shaw, C. A. & Wilson, J. M. B. Analysis of neurological disease in four dimensions: insight from ALS-PDC epidemiology and animal models. *Neuroscience & Biobehavioral Reviews* **27**, 493-505, doi:http://dx.doi.org/10.1016/j.neubiorev.2003.08.001 (2003).

171    Takada, L. T. & Geschwind, M. D. Prion diseases. *Semin Neurol* **33**, 348-356, doi:10.1055/s-0033-1359314 (2013).

172    Costanzo, M. & Zurzolo, C. The cell biology of prion-like spread of protein aggregates: mechanisms and implication in neurodegeneration. *Biochem J* **452**, 1-17, doi:10.1042/BJ20121898 (2013).

173    Kim, H. J. Alpha-Synuclein Expression in Patients with Parkinson's Disease: A Clinician's Perspective. *Experimental Neurology* **22**, 77-83, doi:D - NLM: PMC3699677 OTO - NOTNLM (2013).

174    Laferriere, F. & Polymenidou, M. Advances and challenges in understanding the multifaceted pathogenesis of amyotrophic lateral sclerosis. *Swiss Medicine Weekly* **145**, doi:10.4414/smw.2015.14054 (2015).

175    Galbiati, M. *et al.* ALS-related misfolded protein management in motor neurons and muscle cells. *Neurochemistry International* **79**, 70-78, doi:http://dx.doi.org/10.1016/j.neuint.2014.10.007 (2014).

176    Amani, S. & Naeem, A. Understanding protein folding from globular to amyloid state: Aggregation: Darker side of protein. *Process Biochemistry* **48**, 1651-1664, doi:http://dx.doi.org/10.1016/j.procbio.2013.08.011 (2013).

177    Naeem, A. & Fazili, N. A. Defective protein folding and aggregation as the basis of neurodegenerative diseases: the darker aspect of proteins. *Cell Biochemistry and Biophysics* **61**, 237-250 (2011).

178    Fulda, S., Gorman, A. M., Hori, O. & Samali, A. Cellular Stress Responses: Cell Survival and Cell Death %J International Journal of Cell Biology. *International Journal of Cell Biology* **2010**, 23, doi:10.1155/2010/214074 (2010).

179    Jackson, S. P. & Bartek, J. The DNA-damage response in human biology and disease. *Nature* **461**, 1071-1078, doi:10.1038/nature08467 (2009).

180    Morimoto, R. I., Kline, M. P., Bimston, D. N. & Cotto, J. J. The heat-shock response: regulation and function of heat-shock proteins and molecular chaperones. *Essays in biochemistry* **32**, 17-29 (1997).

181    Luo, B. & Lee, A. S. The critical roles of endoplasmic reticulum chaperones and unfolded protein response in tumorigenesis and anticancer therapies. *Oncogene* **32**, 805-818, doi:10.1038/onc.2012.130 (2013).

182    Garrido, C., Gurbuxani, S., Ravagnan, L. & Kroemer, G. Heat Shock Proteins: Endogenous Modulators of Apoptotic Cell Death. *Biochemical and Biophysical*

Research Communications **286**, 433-442, doi:https://doi.org/10.1006/bbrc.2001.5427 (2001).

183    Hetz, C. The unfolded protein response: controlling cell fate decisions under ER stress and beyond. *Nature Reviews Molecular Cell Biology* **13**, 89-102, doi:10.1038/nrm3270 (2012).

184    Jorgensen, I. & Miao, E. A. Pyroptotic cell death defends against intracellular pathogens. *Immunological Reviews* **265**, 130-142, doi:10.1111/imr.12287 (2015).

185    Kerr, J. F., Wyllie, A. H. & Currie, A. R. Apoptosis: a basic biological phenomenon with wide-ranging implications in tissue kinetics. *British Journal of Cancer* **26**, 239-257 (1972).

186    Arnoult, D. Mitochondrial fragmentation in apoptosis. *Trends in Cell Biology* **17**, 6-12, doi:https://doi.org/10.1016/j.tcb.2006.11.001 (2007).

187    Shamas-Din, A., Kale, J., Leber, B. & Andrews, D. W. Mechanisms of action of Bcl-2 family proteins. *Cold Spring Harbor perspectives in biology* **5**, a008714-a008714, doi:10.1101/cshperspect.a008714 (2013).

188    Hohn, A., Jung, T. & Grune, T. Pathophysiological importance of aggregated damaged proteins. *Free Radical Biology and Medicine* **71**, 70-89 (2014).

189    Aparicio, I. M. *et al.* Autophagy-related proteins are functionally active in human spermatozoa and may be involved in the regulation of cell survival and motility. *Scientific Reports* **6**, 33647, doi:10.1038/srep33647 (2016).

190    Vanden Berghe, T. *et al.* Necroptosis, necrosis and secondary necrosis converge on similar cellular disintegration features. *Cell Death & Differentiation* **17**, 922-930, doi:10.1038/cdd.2009.184 (2010).

191    Webster, K. A. Mitochondrial membrane permeabilization and cell death during myocardial infarction: roles of calcium and reactive oxygen species. *Future cardiology* **8**, 863-884, doi:10.2217/fca.12.58 (2012).

192    Festjens, N., Vanden Berghe, T., Cornelis, S. & Vandenabeele, P. RIP1, a kinase on the crossroads of a cell's decision to live or die. *Cell Death & Differentiation* **14**, 400-410 (2007).

193    Main, B. J. & Rodgers, K. J. Assessing the Combined Toxicity of BMAA and Its Isomers 2,4-DAB and AEG In Vitro Using Human Neuroblastoma Cells. *Neurotoxicity Research* **33**, 33-42, doi:10.1007/s12640-017-9763-4 (2018).

194    Beri, J., Nash, T., Martin, R. M. & Bereman, M. S. Exposure to BMAA mirrors molecular processes linked to neurodegenerative disease. *Proteomics* **17**, doi:10.1002/pmic.201700161 (2017).

195    Gu, F. *et al.* Protein-tyrosine phosphatase 1B potentiates IRE1 signaling during endoplasmic reticulum stress. *The Journal of Biological Chemistry* **279**, 49689-49693, doi:10.1074/jbc.C400261200 (2004).

196    Li, G. & Laszlo, A. Amino Acid Analogs While Inducing Heat Shock Proteins Sensitize CHO cells to Thermal Damage. *Journal of Cellular Physiology* **122**, 91-97 (1985).

197    Jinn, T. L., Chiu, C. C., Song, W. W., Chen, Y. M. & Lin, C. Y. Azetidine-induced accumulation of class I small heat shock proteins in the soluble fraction provides thermotolerance in soybean seedlings. *Plant Cell Physiol* **45**, 1759-1767. Epub 2004 Nov 1722., doi:10.1093/pcp/pch193 (2004).

198  Chi, C.-W., Ye, Q., Ji, Q.-Q., Fang, Z.-P. & Wang, E.-D. Self-protective responses to norvaline-induced stress in a leucyl-tRNA synthetase editing-deficient yeast strain. *Nucleic Acids Research* **45**, 7367-7381, doi:10.1093/nar/gkx487 (2017).

199  Pedrosa, R. & Soares-da-Silva, P. Oxidative and non-oxidative mechanisms of neuronal cell death and apoptosis by L-3,4-dihydroxyphenylalanine (L-DOPA) and dopamine. *British Journal of Pharmacology* **137**, 1305-1313, doi:10.1038/sj.bjp.0704982 (2002).

200  Jin, C. M., Yang, Y. J., Huang, H. S., Kai, M. & Lee, M. K. Mechanisms of L-DOPA-induced cytotoxicity in rat adrenal pheochromocytoma cells: implication of oxidative stress-related kinases and cyclic AMP. *Neuroscience* **170**, 390-398, doi:10.1016/j.neuroscience.2010.07.039 (2010).

201  Hamid, R., Rotshteyn, Y., Rabadi, L., Parikh, R. & Bullock, P. Comparison of alamar blue and MTT assays for high through-put screening. *Toxicology in Vitro* **18**, 703-710, doi:https://doi.org/10.1016/j.tiv.2004.03.012 (2004).

202  Takser, L., Benachour, N., Husk, B., Cabana, H. & Gris, D. Cyanotoxins at low doses induce apoptosis and inflammatory effects in murine brain cells: Potential implications for neurodegenerative diseases. *Toxicology reports* **3**, 180-189, doi:10.1016/j.toxrep.2015.12.008 (2016).

203  White, M. J., DiCaprio, M. J. & Greenberg, D. A. Assessment of neuronal viability with Alamar blue in cortical and granule cell cultures. *Journal of Neuroscience Methods* **70**, 195-200, doi:https://doi.org/10.1016/S0165-0270(96)00118-5 (1996).

204  Giannopoulos, S., Samardzic, K., Raymond, B. B. A., Djordjevic, S. P. & Rodgers, K. J. L-DOPA causes mitochondrial dysfunction in vitro: a novel mechanism of L-DOPA toxicity uncovered. *The International Journal of Biochemistry & Cell Biology*, 105624, doi:https://doi.org/10.1016/j.biocel.2019.105624 (2019).

205  Atale, N., Gupta, S., Yadav, U. C. S. & Rani, V. Cell-death assessment by fluorescent and nonfluorescent cytosolic and nuclear staining techniques. *Journal of Microscopy* **255**, 7-19, doi:10.1111/jmi.12133 (2014).

206  Frigault, M. M., Lacoste, J., Swift, J. L. & Brown, C. M. Live-cell microscopy – tips and tools. *Journal of Cell Science* **122**, 753, doi:10.1242/jcs.033837 (2009).

207  Schindelin, J. *et al.* Fiji: an open-source platform for biological-image analysis. *Nature methods* **9**, 676-682, doi:10.1038/nmeth.2019 (2012).

208  Zhang, G., Gurtu, V., Kain, S. R. & Yan, G. Early Detection of Apoptosis Using a Fluorescent Conjugate of Annexin V. *BioTechniques* **23**, 525-531, doi:10.2144/97233pf01 (1997).

209  Nicoletti, I., Migliorati, G., Pagliacci, M. C., Grignani, F. & Riccardi, C. A rapid and simple method for measuring thymocyte apoptosis by propidium iodide staining and flow cytometry. *Journal of Immunological Methods* **139**, 271-279, doi:https://doi.org/10.1016/0022-1759(91)90198-O (1991).

210  Chazotte, B. Labeling Lysosomes in Live Cells with LysoTracker. *Cold Spring Harbor Protocols* **2011**, pdb.prot5571 (2011).

211  Brand, M. D. & Nicholls, D. G. Assessing mitochondrial dysfunction in cells. *The Biochemical journal* **435**, 297-312, doi:10.1042/BJ20110162 (2011).

212  de Moura, M. B. & Van Houten, B. Bioenergetic analysis of intact mammalian cells using the Seahorse XF24 Extracellular Flux analyzer and a luciferase ATP

assay. *Methods in molecular biology (Clifton, N.J.)* **1105**, 589-602, doi:10.1007/978-1-62703-739-6_40 (2014).

213 Anderson, N. L. & Anderson, N. G. Proteome and proteomics: New technologies, new concepts, and new words. *Electrophoresis* **19**, 1853-1861 (1998).

214 Wetmore, B. A. & Merrick, B. A. Invited Review: Toxicoproteomics: Proteomics Applied to Toxicology and Pathology. *Toxicologic Pathology* **32**, 619-642, doi:10.1080/01926230490518244 (2016).

215 de Hoffmann, E. Mass Spectrometry. *Kirk-Othmer Encyclopedia of Chemical Technology* (2005).

216 Borman, S., Russell, H. & Siuzdak, G. in *Today's Chemist at Work*  4-49 (American Chemical Society, 2003).

217 Riley, N. M. & Coon, J. J. The Role of Electron Transfer Dissociation in Modern Proteomics. *Anal Chem* **90**, 40-64, doi:10.1021/acs.analchem.7b04810 (2018).

218 Zubarev, R. A. Electron-capture dissociation tandem mass spectrometry. *Curr Opin Biotechnol* **15**, 12-16, doi:10.1016/j.copbio.2003.12.002 (2004).

219 Zhang, Y., Fonslow, B. R., Shan, B., Baek, M.-C. & Yates, J. R., 3rd. Protein analysis by shotgun/bottom-up proteomics. *Chemical reviews* **113**, 2343-2394, doi:10.1021/cr3003533 (2013).

220 Butterfield, D. A., Boyd-Kimball, D. & Castegna, A. Proteomics in Alzheimer's disease: insights into potential mechanisms of neurodegeneration. *Journal of Neurochemistry* **86**, 1313-1327, doi:10.1046/j.1471-4159.2003.01948.x (2003).

221 Tsuji, T., Shiozaki, A., Kohno, R., Yoshizato, K. & Shimohama, S. Proteomic Profiling and Neurodegeneration in Alzheimer's  Disease. *Neurochemical Research* **27**, 1245-1253 (2002).

222 Poon, H. F., Vaishnav, R. A., Getchell, T. V., Getchell, M. L. & Butterfield, D. A. Quantitative proteomics analysis of differential protein expression and oxidative modification of specific proteins in the brains of old mice. *Neurobiology of Aging* **27**, 1010-1019, doi:10.1016/j.neurobiolaging.2005.05.006 (2006).

223 Licker, V., Kövari, E., Hochstrasser, D. F. & Burkhard, P. R. Proteomics in human Parkinson's disease research. *Journal of Proteomics* **73**, 10-29, doi:https://doi.org/10.1016/j.jprot.2009.07.007 (2009).

224 Basso, M. *et al.* Proteome analysis of human substantia nigra in Parkinson's disease. *Proteomics* **4**, 3943-3952, doi:10.1002/pmic.200400848 (2004).

225 Fuvesi, J. *et al.* Proteomic analysis of cerebrospinal fluid in a fulminant case of multiple sclerosis. *International Journal of Molecular Sciences* **13**, 7676-7693, doi:10.3390/ijms13067676 (2012).

226 Farias, A. S., Pradella, F., Schmitt, A., Santos, L. M. & Martins-de-Souza, D. Ten years of proteomics in multiple sclerosis. *Proteomics* **14**, 467-480, doi:10.1002/pmic.201300268 (2014).

227 Glover, W. B., Mash, D. C. & Murch, S. J. The natural non-protein amino acid N-beta-methylamino-L-alanine (BMAA) is incorporated into protein during synthesis. *Amino Acids* **46**, 2553-2559, doi:10.1007/s00726-014-1812-1 (2014).

228 Cvetesic, N. *et al.* Proteome-wide measurement of non-canonical bacterial mistranslation by quantitative mass spectrometry of protein modifications. *Sci Rep* **6**, 28631, doi:10.1038/srep28631 (2016).

229    Bilus, M. *et al.* On the Mechanism and Origin of Isoleucyl-tRNA Synthetase Editing against Norvaline. *Journal of Molecular Biology* **431**, 1284-1297, doi:https://doi.org/10.1016/j.jmb.2019.01.029 (2019).

230    Karlsson, O., Bergquist, J. & Andersson, M. Quality Measures of Imaging Mass Spectrometry Aids in Revealing Long-term Striatal Protein Changes Induced by Neonatal Exposure to the Cyanobacterial Toxin β-N-methylamino-L-alanine (BMAA). *Molecular & Cellular Proteomics* **13**, 93, doi:10.1074/mcp.M113.031435 (2014).

231    Frøyset, A. K., Khan, E. A. & Fladmark, K. E. Quantitative proteomics analysis of zebrafish exposed to sub-lethal dosages of β-methyl-amino-L-alanine (BMAA). *Scientific Reports* **6**, doi:10.1038/srep29631 (2016).

232    Schmidt, A., Forne, I. & Imhof, A. Bioinformatic analysis of proteomics data. *BMC Systems Biology* **8**, S3, doi:10.1186/1752-0509-8-S2-S3 (2014).

233    Ashburner, M. *et al.* Gene Ontology: tool for the unification of biology. *Nature Genetics* **25**, 25-29, doi:10.1038/75556 (2000).

234    Yon Rhee, S., Wood, V., Dolinski, K. & Draghici, S. Use and misuse of the gene ontology annotations. *Nature Reviews Genetics* **9**, 509-515, doi:10.1038/nrg2363 (2008).

235    Maere, S., Heymans, K. & Kuiper, M. BiNGO: a Cytoscape plugin to assess overrepresentation of gene ontology categories in biological networks. *Bioinformatics* **21** (2005).

236    Bindea, G. *et al.* ClueGO: a Cytoscape plug-in to decipher functionally grouped gene ontology and pathway annotation networks. *Bioinformatics (Oxford, England)* **25**, 1091-1093, doi:10.1093/bioinformatics/btp101 (2009).

237    Lee, S.-G., Yang, J.-S., Chung, I.-K. & Kim, Y.-S. BINGO: Biological Interpretation Through Statistically and Graph-theoretically Navigating Gene Ontology. *Molecular and Cellular Toxicology* **1** (2005).

238    Smith, P. K. *et al.* Measurement of protein using bicinchoninic acid. *Analytical Biochemistry* **150**, 76-85, doi:https://doi.org/10.1016/0003-2697(85)90442-7 (1985).

239    Rappsilber, J., Mann, M. & Ishihama, Y. Protocol for micro-purification, enrichment, pre-fractionation and storage of peptides for proteomics using StageTips. *Nature Protcols* **2**, 1896-1906, doi:10.1038/nprot.2007.261 (2007).

240    Cox, J. & Mann, M. MaxQuant enables high peptide identification rates, individualized p.p.b.-range mass accuracies and proteome-wide protein quantification. *Nature Biotechnology* **26** (2008).

241    Cox, J. *et al.* Accurate Proteome-wide Label-free Quantification by Delayed Normalization and Maximal Peptide Ratio Extraction, Termed MaxLFQ. *Molecular Cellular Proteomics* **13**, 2513, doi:10.1074/mcp.M113.031591 (2014).

242    Tyanova, S. *et al.* The Perseus computational platform for comprehensive analysis of (prote)omics data. *Nature Methods* **13**, 731, doi:10.1038/nmeth.3901 (2016).

243    Shannon, P. *et al.* Cytoscape: a software environment for integrated models of biomolecular interaction networks. *Genome Research* **13** (2003).

244    Nepusz, T., Yu, H. & Paccanaro, A. Detecting overlapping protein complexes in protein-protein interaction networks. *Nature methods* **9**, 471-472, doi:10.1038/nmeth.1938 (2012).

245    Szklarczyk, D. *et al.* STRING v10: protein-protein interaction networks, integrated over the tree of life. *Nucleic acids research* **43**, D447-D452, doi:10.1093/nar/gku1003 (2015).

246    Lopez, M. F. *et al.* Depletion of nuclear histone H2A variants is associated with chronic DNA damage signaling upon drug-evoked senescence of human somatic cells. *Aging* **4**, 823-842, doi:10.18632/aging.100507 (2012).

247    Bassett, A., Cooper, S., Wu, C. & Travers, A. The folding and unfolding of eukaryotic chromatin. *Current Opinion in Genetics & Development* **19**, 159-165, doi:https://doi.org/10.1016/j.gde.2009.02.010 (2009).

248    Groth, A. *et al.* Regulation of Replication Fork Progression Through Histone Supply and Demand. *Science* **318**, 1928, doi:10.1126/science.1148992 (2007).

249    Joo, H. Y. *et al.* Regulation of cell cycle progression and gene expression by H2A deubiquitination. *Nature* **449**, 1068-1072, doi:10.1038/nature06256 (2007).

250    Staley, J. P. & Woolford, J. L. Assembly of ribosomes and spliceosomes: complex ribonucleoprotein machines. *Current opinion in cell biology* **21**, 109-118, doi:10.1016/j.ceb.2009.01.003 (2009).

251    Fabian G.R. & Hopper, A. K. RRP1, a Saccharomyces cerevisiae gene affecting rRNA processing and production of mature ribosomal subunits. *J Bacteriol* **169** (1987).

252    Bernstein, K. A., Gallagher, J. E., Mitchell, B. M., Granneman, S. & Baserga, S. J. The small-subunit processome is a ribosome assembly intermediate. *Eukaryotic Cell* **3**, 1619-1626, doi:10.1128/EC.3.6.1619-1626.2004 (2004).

253    Rabl, J., Leibundgut, M., Ataide, S. F., Haag, A. & Ban, N. Crystal Structure of the Eukaryotic 40S Ribosomal Subunit in Complex with Initiation Factor 1. *Science* **331**, 730 (2011).

254    Jankowsky, E. RNA Helicases at work: binding and rearranging. *Trends in biochemical sciences* **36**, 19-29, doi:10.1016/j.tibs.2010.07.008 (2011).

255    Zybura-Broda, K. *et al.* HuR (Elavl1) and HuB (Elavl2) Stabilize Matrix Metalloproteinase-9 mRNA During Seizure-Induced Mmp-9 Expression in Neurons. *Frontiers in Neuroscience* **12**, 224 (2018).

256    Ahn, E.-Y. *et al.* SON Controls Cell-Cycle Progression by Coordinated Regulation of RNA Splicing. *Molecular Cell* **42**, 185-198, doi:https://doi.org/10.1016/j.molcel.2011.03.014 (2011).

257    Lu, X., Ng, H.-H. & Bubulya, P. A. The Role of SON in Splicing, Development and Disease. *Wiley interdisciplinary reviews: RNA* **5**, 637-646, doi:10.1002/wrna.1235 (2014).

258    Yang, F., Yi, F., Han, X., Du, Q. & Liang, Z. MALAT-1 interacts with hnRNP C in cell cycle regulation. *FEBS Letters* **587**, 3175-3181, doi:10.1016/j.febslet.2013.07.048 (2013).

259    Buée, L., Bussière, T., Buée-Scherrer, V., Delacourte, A. & Hof, P. R. Tau protein isoforms, phosphorylation and role in neurodegenerative disorders11These authors contributed equally to this work. *Brain Research Reviews* **33**, 95-130, doi:https://doi.org/10.1016/S0165-0173(00)00019-9 (2000).

260    Faustino, N. A. & Cooper, T. A. Pre-mRNA splicing and human disease. *Genes & Development* **17** (2003).

261    Schmitz, J., Watrin, E., Lénárt, P., Mechtler, K. & Peters, J.-M. Sororin Is Required for Stable Binding of Cohesin to Chromatin and for Sister Chromatid Cohesion in Interphase. *Current Biology* **17**, 630-636, doi:https://doi.org/10.1016/j.cub.2007.02.029 (2007).

262    Nishiyama, T. *et al.* Sororin Mediates Sister Chromatid Cohesion by Antagonizing Wapl. *Cell* **143**, 737-749, doi:https://doi.org/10.1016/j.cell.2010.10.031 (2010).

263    Valcárcel, J. & Malumbres, M. Splicing together sister chromatids. *The EMBO Journal* **33**, 2601-2603, doi:10.15252/embj.201489988 (2014).

264    Kato, J.-Y., Matsuoka, M., Polyak, K., Massague, J. & Sherr, C. J. Cyclic AMP-induced G1 phase arrest mediated by an inhibitor (p27Kip1) of cyclin-dependent kinase 4 activation. *Cell* **79**, 487-496, doi:https://doi.org/10.1016/0092-8674(94)90257-7 (1994).

265    Hendershott, M. C. & Vale, R. D. Regulation of microtubule minus-end dynamics by CAMSAPs and Patronin. *Proc Natl Acad Sci U S A* **22** (2014).

266    Maiato, H. *et al.* Human CLASP1 Is an Outer Kinetochore Component that Regulates Spindle Microtubule Dynamics. *Cell* **113**, 891-904, doi:https://doi.org/10.1016/S0092-8674(03)00465-3 (2003).

267    Bakhoum, S. F., Thompson, S. L., Manning, A. L. & Compton, D. A. Genome stability is ensured by temporal control of kinetochore-microtubule dynamics. *Nature Cell Biology* **11**, 27-35, doi:10.1038/ncb1809 (2009).

268    Hubbert, C. *et al.* HDAC6 is a microtubule-associated deacetylase. *Nature* **417**, 455-458, doi:10.1038/417455a (2002).

269    Jiang, W. *et al.* PRC1: a human mitotic spindle-associated CDK substrate protein required for cytokinesis. *Molecular cell* **2**, 877-885, doi:10.1016/s1097-2765(00)80302-0 (1998).

270    Zhu, C., Bossy-Wetzel, E. & Jiang, W. Recruitment of MKLP1 to the spindle midzone/midbody by INCENP is essential for midbody formation and completion of cytokinesis in human cells. *Biochemical Journal* **389**, 373, doi:10.1042/BJ20050097 (2005).

271    Chen, Y., Riley, D. J., Chen, P. L. & Lee, W. H. HEC, a novel nuclear protein rich in leucine heptad repeats specifically involved in mitosis. *Mol Biol Cell* **17** (1997).

272    Tateishi, K., Omata, M., Tanaka, K. & Chiba, T. The NEDD8 system is essential for cell cycle progression and morphogenetic pathway in mice. *The Journal of Cell Biology* **155**, 571, doi:10.1083/jcb.200104035 (2001).

273    Takahashi, S. *et al.* Downregulation of KIF23 suppresses glioma proliferation. *Journal of Neuro - Oncology* **106**, 519-529, doi:http://dx.doi.org/10.1007/s11060-011-0706-2 (2012).

274    Englmeier, R., Pfeffer, S. & Forster, F. Structure of the Human Mitochondrial Ribosome Studied In Situ by Cryoelectron Tomography. *Structure* **25**, 1574-1581 e1572, doi:10.1016/j.str.2017.07.011 (2017).

275    Amunts, A., Brown, A., Toots, J., Scheres, S. H. W. & Ramakrishnan, V. The structure of the human mitochondrial ribosome. *Science* **348**, 95-98 (2015).

276    Brown, A. *et al.* Structure of the large ribosomal subunit from human mitochondria. *Science* **346**, 718-722 (2015).

277    Posse, V. & Gustafsson, C. M. Human Mitochondrial Transcription Factor B2 Is Required for Promoter Melting during Initiation of Transcription. *Journal of Biological Chemistry* **292**, 2637-2645, doi:10.1074/jbc.M116.751008 (2017).

278    Smits, P., Smeitink, J. & van den Heuvel, L. Mitochondrial translation and beyond: processes implicated in combined oxidative phosphorylation deficiencies. *Journal of Biomedicine and Biotechnology* **2010**, 737385, doi:10.1155/2010/737385 (2010).

279    Ndi, M., Marin-Buera, L., Salvatori, R., Singh, A. P. & Ott, M. Biogenesis of the bc1 Complex of the Mitochondrial Respiratory Chain. *Journal of Molecular Biology* **430**, 3892-3905, doi:https://doi.org/10.1016/j.jmb.2018.04.036 (2018).

280    van Loo, G. *et al.* Endonuclease G: a mitochondrial protein released in apoptosis and involved in caspase-independent DNA degradation. *Cell Death & Differentiation* **8**, 1136-1142, doi:10.1038/sj.cdd.4400944 (2001).

281    Su, J. H., Deng, G. & Cotman, C. W. Bax Protein Expression Is Increased in Alzheimer's Brain: Correlations with DNA Damage, Bcl-2 Expression, and Brain Pathology. *Journal of Neuropathology & Experimental Neurology* **56**, 86-93, doi:10.1097/00005072-199701000-00009 (1997).

282    Samardzic, K. & Rodgers, K. J. Cytotoxicity and mitochondrial dysfunction caused by the dietary supplement l-norvaline. *Toxicology in Vitro* **56**, 163-171, doi:https://doi.org/10.1016/j.tiv.2019.01.020 (2019).

283    Suzuki, Y. *et al.* Relationships of diverse apoptotic death process patterns to mitochondrial membrane potential ($\Delta\psi m$) evaluated by three-parameter flow cytometric analysis. *Cytotechnology* **65**, 59-70, doi:10.1007/s10616-012-9455-0 (2013).

284    Bossy-Wetzel, E., Barsoum, M. J., Godzik, A., Schwarzenbacher, R. & Lipton, S. A. Mitochondrial fission in apoptosis, neurodegeneration and aging. *Current Opinion in Cell Biology* **15**, 706-716, doi:https://doi.org/10.1016/j.ceb.2003.10.015 (2003).

285    Naughton, B. J. *et al.* Blood genome-wide transcriptional profiles reflect broad molecular impairments and strong blood-brain links in Alzheimer's disease. *Journal of Alzheimer's disease : JAD* **43**, 93-108, doi:10.3233/JAD-140606 (2015).

286    Zhang, L. *et al.* Potential hippocampal genes and pathways involved in Alzheimer's disease: a bioinformatic analysis. *Genet Mol Res* **14**, 7218-7232, doi:10.4238/2015.June.29.15 (2015).

287    Lunnon, K. *et al.* Mitochondrial genes are altered in blood early in Alzheimer's disease. *Neurobiology of Aging* **53**, 36-47, doi:https://doi.org/10.1016/j.neurobiolaging.2016.12.029 (2017).

288    Do Carmo, S. *et al.* Hippocampal Proteomic Analysis Reveals Distinct Pathway Deregulation Profiles at Early and Late Stages in a Rat Model of Alzheimer's-Like Amyloid Pathology. *Molecular Neurobiology* **55**, 3451-3476, doi:10.1007/s12035-017-0580-9 (2018).

289    Chou, J. L. *et al.* Early dysregulation of the mitochondrial proteome in a mouse model of Alzheimer's disease. *Journal of Proteomics* **74**, 466-479, doi:https://doi.org/10.1016/j.jprot.2010.12.012 (2011).

290    Donahue, J. E. *et al.* RAGE, LRP-1, and amyloid-beta protein in Alzheimer's disease. *Acta Neuropathologica* **112**, 405-415, doi:10.1007/s00401-006-0115-3 (2006).

291    Chadwick, W., Brenneman, R., Martin, B. & Maudsley, S. Complex and multidimensional lipid raft alterations in a murine model of Alzheimer's disease. *Int J Alzheimers Dis* **2010**, 604792, doi:10.4061/2010/604792 (2010).

292    Brehme, M. *et al.* A Chaperone Subnetwork Safeguards Proteostasis in Aging and Neurodegenerative Disease. *Cell Reports* **9**, 1135-1150, doi:https://doi.org/10.1016/j.celrep.2014.09.042 (2014).

293    Quintá, H. R. *et al.* Management of cytoskeleton architecture by molecular chaperones and immunophilins. *Cellular signalling* **23**, 1907-1920, doi:10.1016/j.cellsig.2011.07.023 (2011).

294    Desai, A. & Mitchison, T. J. Microtubule Polymerization Dynamics. *Annual Review of Cell & Developmental Biology* **13**, 83, doi:10.1146/annurev.cellbio.13.1.83 (1997).

295    Chakraborti, S., Natarajan, K., Curiel, J., Janke, C. & Liu, J. The emerging role of the tubulin code: From the tubulin molecule to neuronal function and disease. *Cytoskeleton* **73**, 521-550, doi:10.1002/cm.21290 (2016).

296    The UniProt, C. UniProt: a worldwide hub of protein knowledge. *Nucleic Acids Research* **47**, D506-D515, doi:10.1093/nar/gky1049 (2018).

297    Xie, X. *et al.* β-Actin–dependent global chromatin organization and gene expression programs control cellular identity. *The FASEB Journal* **32**, 1296-1314, doi:10.1096/fj.201700753R (2018).

298    Cuylen, S. *et al.* Ki-67 acts as a biological surfactant to disperse mitotic chromosomes. *Nature* **535**, 308, doi:10.1038/nature18610

https://www.nature.com/articles/nature18610#supplementary-information (2016).

299    Podust, L. M., Podust, V. N., Sogo, J. M. & Hübscher, U. Mammalian DNA polymerase auxiliary proteins: analysis of replication factor C-catalyzed proliferating cell nuclear antigen loading onto circular double-stranded DNA. *Molecular and Cellular Biology* **15**, 3072, doi:10.1128/MCB.15.6.3072 (1995).

300    Pennaneach, V. *et al.* The Large Subunit of Replication Factor C Promotes Cell Survival after DNA Damage in an LxCxE Motif&#x2013; and Rb-Dependent Manner. *Molecular Cell* **7**, 715-727, doi:10.1016/S1097-2765(01)00217-9 (2001).

301    McAlear, M. A., Tuffo, K. M. & Holm, C. The Large Subunit of Replication Factor C (Rfclp/Cdc44p) Is Required for DNA Replication and DNA Repair in Saccharomyces cerevisiae. *Genetics* **142**, 65 (1996).

302    Inagaki, H. *et al.* A large DNA-binding nuclear protein with RNA recognition motif and serine/arginine-rich domain. *J Biol Chem* **271** (1996).

303    O'Leary, N. A. *et al.* Reference sequence (RefSeq) database at NCBI: current status, taxonomic expansion, and functional annotation. *Nucleic acids research* **44**, D733-D745, doi:10.1093/nar/gkv1189 (2016).

304    Razin, S. V., Borunova, V. V., Maksimenko, O. G. & Kantidze, O. L. Cys2His2 zinc finger protein family: Classification, functions, and major members. *Biochemistry (Moscow)* **77**, 217-226, doi:10.1134/S0006297912030017 (2012).

305     Tyler, J. K. Chromatin assembly. *European Journal of Biochemistry* **269**, 2268-2274, doi:10.1046/j.1432-1033.2002.02890.x (2002).

306     Su, C. *et al.* DNA damage induces downregulation of histone gene expression through the G1 checkpoint pathway. *EMBO J* **23** (2004).

307     Dutta, B. *et al.* Profiling of the Chromatin-associated Proteome Identifies HP1BP3 as a Novel Regulator of Cell Cycle Progression. *Mol Cell Proteomics* **13** (2014).

308     Peters, R. Introduction to nucleocytoplasmic transport: molecules and mechanisms. *Methods Mol Biol* (2006).

309     Mühlhäusser, P., Müller, E. C., Otto, A. & Kutay, U. Multiple pathways contribute to nuclear import of core histones. *EMBO reports* **2**, 690-696, doi:10.1093/embo-reports/kve168 (2001).

310     Galy, V., Mattaj, I. W. & Askjaer, P. Caenorhabditis elegans nucleoporins Nup93 and Nup205 determine the limit of nuclear pore complex size exclusion in vivo. *Molecular biology of the cell* **14**, 5104-5115, doi:10.1091/mbc.e03-04-0237 (2003).

311     Shen, Z. *et al.* Dynamic association of ORCA with prereplicative complex components regulates DNA replication initiation. *Mol Biol Cell* **32** (2012).

312     Heaton, J. H., Dlakic, W. M., Dlakic, M. & Gelehrter, T. D. Identification and cDNA cloning of a novel RNA-binding protein that interacts with the cyclic nucleotide-responsive sequence in the Type-1 plasminogen activator inhibitor mRNA. *J Biol Chem* **276** (2001).

313     Yamaguchi, A. & Takanashi, K. FUS interacts with nuclear matrix-associated protein SAFB1 as well as Matrin3 to regulate splicing and ligand-mediated transcription. *Sci Rep* **6** (2016).

314     Luo, M. L. *et al.* Pre-mRNA splicing and mRNA export linked by direct interactions between UAP56 and Aly. *Nature* **413** (2001).

315     Maeder, C. I. *et al.* The THO Complex Coordinates Transcripts for Synapse Development and Dopamine Neuron Survival. *Cell* **174**, 1436-1449 e1420, doi:10.1016/j.cell.2018.07.046 (2018).

316     Chen, S., Lu, F., Seeman, P. & Liu, F. Quantitative proteomic analysis of human substantia nigra in Alzheimer's disease, Huntington's disease and Multiple sclerosis. *Neurohem Research* **37** (2012).

317     Hauser, M. A. *et al.* Expression profiling of substantia nigra in Parkinson disease, progressive supranuclear palsy, and frontotemporal dementia with parkinsonism. *Arch Neurol* **62** (2005).

318     Messaritou, G., East, L., Roghi, C., Isacke, C. M. & Yarwood, H. Membrane type-1 matrix metalloproteinase activity is regulated by the endocytic collagen receptor Endo180. *Journal of cell science* **122**, 4042-4048, doi:10.1242/jcs.044305 (2009).

319     Laskowska, E., Kuczyńska-Wiśnik, D. & Lipińska, B. Proteomic analysis of protein homeostasis and aggregation. *Journal of Proteomics* **198**, 98-112, doi:https://doi.org/10.1016/j.jprot.2018.12.003 (2019).

320     Figueroa-González, G. & Pérez-Plasencia, C. Strategies for the evaluation of DNA damage and repair mechanisms in cancer. *Oncology letters* **13**, 3982-3988, doi:10.3892/ol.2017.6002 (2017).

321     Karamysheva, Z., Diaz-Martinez, L. A., Warrington, R. & Yu, H. Graded requirement for the spliceosome in cell cycle progression. *Cell Cycle* **14** (2015).

322     Chabot, B. & Shkreta, L. Defective control of pre–messenger RNA splicing in human disease. *The Journal of Cell Biology* **212**, 13, doi:10.1083/jcb.201510032 (2016).

323     Wang, Z., Gerstein, M. & Snyder, M. RNA-Seq: a revolutionary tool for transcriptomics. *Nature reviews. Genetics* **10**, 57-63, doi:10.1038/nrg2484 (2009).

324     Mohler, K. *et al.* MS-READ: Quantitative measurement of amino acid incorporation. *Biochimica et biophysica acta. General subjects* **1861**, 3081-3088, doi:10.1016/j.bbagen.2017.01.025 (2017).

325     Song, Y. *et al.* Double mimicry evades tRNA synthetase editing by toxic vegetable-sourced non-proteinogenic amino acid. *Nature Communications* **8**, 2281, doi:10.1038/s41467-017-02201-z (2017).

326     Paulo, J. A. *et al.* Subcellular fractionation enhances proteome coverage of pancreatic duct cells. *Biochimica et biophysica acta* **1834**, 791-797, doi:10.1016/j.bbapap.2013.01.011 (2013).

327     Gordon, J., Amini, S. & White, M. in *Neuronal Cell Culture* Vol. 1078 *Methods in Molecular Biology* (eds Shohreh Amini & Martyn K. White) Ch. 1, 1-8 (Humana Press, 2013).